University of Nebraska - Lincoln
DigitalCommons@University of Nebraska - Lincoln

Dissertations & Theses in Earth and Atmospheric Sciences

Earth and Atmospheric Sciences, Department of

4-2021

Case Studies of Alberta Clipper Systems and the Impacts on Winter Weather Road Maintenance

Cameron Wunderlin
University of Nebraska-Lincoln, cameron.wunderlin@huskers.unl.edu

Follow this and additional works at: https://digitalcommons.unl.edu/geoscidiss

 Part of the Earth Sciences Commons, and the Meteorology Commons

Wunderlin, Cameron, "Case Studies of Alberta Clipper Systems and the Impacts on Winter Weather Road Maintenance" (2021). *Dissertations & Theses in Earth and Atmospheric Sciences*. 132.
https://digitalcommons.unl.edu/geoscidiss/132

This Article is brought to you for free and open access by the Earth and Atmospheric Sciences, Department of at DigitalCommons@University of Nebraska - Lincoln. It has been accepted for inclusion in Dissertations & Theses in Earth and Atmospheric Sciences by an authorized administrator of DigitalCommons@University of Nebraska - Lincoln.

CASE STUDIES OF ALBERTA CLIPPER SYSTEMS AND THE IMPACTS ON WINTER WEATHER ROAD MAINTENANCE

by

Cameron Wunderlin

A THESIS

Presented to the Faculty of

The Graduate College of the University of Nebraska

In Partial Fulfillment of Requirements

For the Degree of Master of Science

Major: Earth and Atmospheric Sciences

Under the Supervision of Professor Mark R. Anderson

Lincoln, Nebraska

April, 2021

CASE STUDIES OF ALBERTA CLIPPER SYSTEMS AND THE IMPACTS ON WINTER WEATHER ROAD MAINTENANCE

Cameron Wunderlin, M.S.

University of Nebraska, 2021

Advisor: Mark R. Anderson

Winter weather can cause profound impacts to a variety of economic sectors in the mid-latitudes. In the Great Plains of North America, one sector that is highly impacted by winter weather is road transportation. The burdens to road transportation caused by winter weather have led to the adoption of a Maintenance Decision Support System (MDSS) by the Nebraska Department of Transportation (NDOT). Using both observational and numerical weather model data, NDOT-MDSS generates both winter weather forecasts and winter road maintenance recommendations. Little is known about how well NDOT-MDSS is forecasting conditions for different winter weather events. Using a case study approach, NDOT-MDSS output for two different winter storms which impacted Nebraska during the 2018-2019 winter are analyzed. Both winter storms were brought on by Alberta clipper systems, one impacting the Omaha area and the other impacting the Lincoln area. Three objectives are undertaken while analyzing each case study. For the first objective, synoptic background conditions are analyzed to get a sense of the environment which produced each system. This is followed by an analysis and comparison of multiple NDOT-MDSS forecast parameters with meteorological variables recorded in both Omaha and Lincoln. For the second objective, parameters pertaining to snowfall are examined for both events to see how NDOT-MDSS handled the generation

and timeline of snow. Finally, the last objective includes a comparison of snowfall accumulations produced by NDOT-MDSS for each event to other numerical weather models and forecasts made by the National Weather Service (NWS). A comparison of observed synoptic conditions and the output of NDOT-MDSS between the two different events are then undertaken briefly. This analysis helped in aiding NDOT with insight on the limitations, benefits, and overall effectiveness of the NDOT-MDSS. In both case studies, NDOT-MDSS had a good handle on each event but did present some biases. NDOT-MDSS rarely made any major errors. NDOT-MDSS may be able to be relied on for future winter weather events similar to the two case studies analyzed.

ACKNOWLEDGEMENTS

I would like to thank my advisor and mentor, Dr. Mark Anderson, for his support, dedication, and patience during the last two years. He was always available whenever I needed to ask questions or needed advice throughout my navigation of graduate school. I would also like to thank Dr. Clinton Rowe and Dr. Matthew Van Den Broeke for both their mentorship as professors for several of my graduate level courses and for their contributions to this project as my committee members.

I would like to thank the NDOT-MDSS research team of Nancy Barnhardt, Dr. Curtis Walker, and Nathan Rick for their contributions and input throughout the last two years that led to the completion of this project.

I would like to thank the Nebraska Department of Transportation for funding this project. I would also like to thank the employees of NDOT who were always available to answer my questions and concerns while investigating NDOT-MDSS and being present on the research team.

I would like to thank the Department of Earth and Atmospheric Sciences as well as my colleagues within EAS at the University of Nebraska-Lincoln for their continuous support during this project and during my growth as a researcher. Lastly, thank you to all my friends from New York, SUNY Oswego, and UNL as well as my family for your continuous encouragement and support during my journey throughout graduate school.

TABLE OF CONTENTS

CHAPTER 1: INTRODUCTION

Weather has long impacted the realm of transportation adversely in society. While many different forms of meteorological phenomena (such as hurricanes, tornadoes, and blizzards) can and have impacted transportation adversely, winter weather and the associated conditions have had a notorious and notable impact in both the minds and lives of people. As relevant today as ever, winter weather can wreak havoc on the road transportation sector as it is often accompanied by economic damage to property and both injuries and fatalities among humans. As a result of this, mitigation of the adverse impacts caused by winter weather has long since been an objective within the realm of road transportation and continues today. In the state of Nebraska, the Nebraska Department of Transportation (NDOT) has adopted a Maintenance Decision Support System (MDSS), which will hence be identified as NDOT-MDSS. The NDOT-MDSS is a type of information system which aims to provide NDOT with a plethora of information to create decision making and winter weather maintenance practices which are more effective and safer for the traveling public. NDOT-MDSS can be thought as a numerical weather model, road weather model, and a road treatment and maintenance guide all in one. Though having the potential to induce meaningful change and provide numerous benefits to the agency, NDOT-MDSS utilization and adoption by the agency only stems back to the 2017-2018 winter season. Little is known about how well NDOT-MDSS is performing, if conditions are being accurately represented and forecasted for the different types of winter storms which sweep across Nebraska and the Great Plains, and if suggested treatments output by the system are proper. The aim of this study was to see how NDOT-MDSS is performing overall with certain winter storms and provide that

information back to NDOT with the hope that the provided feedback would be beneficial to the agency. This study has three primary objectives to reach this aim.

The first objective of the project is to examine two different winter storms that impacted NDOT during the 2018-2019 winter season and see how well NDOT-MDSS forecasted several meteorological conditions associated with each storm. For winter storm examination, the specific goal is to assess the synoptic scale meteorological conditions for these storms which impact two separate areas managed by NDOT. Both areas in Nebraska are near densely populated areas of the state where road weather maintenance and operations by NDOT are critically important. A synoptic "top-down" overview is provided preceding, during, and succeeding the impact of each winter storm. Surface conditions as well as 300, 500, 700, 850 hPa level observations are analyzed and discussed, followed by an examination of the meteorological variables or parameters forecasted by the NDOT-MDSS. This includes air temperatures, dewpoint temperatures, and wind speeds for different selected road segments or routes within the NDOT-MDSS model domain for each event. The first event occurred on 26 January 2019, during which the Omaha region was impacted. The second event occurred on 15 February 2019, during which the Lincoln region was impacted. Both these winter weather events and the impacts they caused were brought on by Alberta clipper systems. Alberta clipper systems are a specific type of low pressure system or extratropical cyclone which frequently brings winter weather and associated impacts across North America during the cool season. Alberta clipper systems themselves, through their formation location and mechanism, bring a set of specific types of conditions and hazards to regions which make their impacts different from other types of low pressure systems that transverse and bring

winter weather to these regions. These conditions and hazards are notably impactful to road transportation. It is of importance to understand how exactly MDSS-NDOT is interpreting, forecasting, and handling the conditions induced by the onset of this type of cyclone during the winter season.

One of the most important meteorological forecast elements needed by transportation personnel is snowfall, particularly snowfall timing and accumulation. The second objective of the study is to examine how well NDOT-MDSS forecasted various parameters in relation to snowfall for both of the events. This includes the time NDOT-MDSS thought snowfall would take place, the snowfall start and end times, and the total snowfall accumulations forecasted by the system for the two different regions for each of the events. Several analyses are carried out to see how NDOT-MDSS interprets and handles an event as it pertains to snow. The final objective of the study is to compare NDOT-MDSS snowfall accumulations to other numerical weather model forecasts and forecasts generated by the National Weather Service (NWS). Thereafter, a comparison of the two different events for the two different regions is undertaken to understand and address the forecasting ability of the NDOT-MDSS as it pertains to Alberta clipper systems. For the first part of this objective specifically, total snowfall accumulation is compared against the Rapid Refresh model version 4 (RAP), the 12 km North American Mesoscale model version 4 (NAM), the 4 km North American Mesoscale model (NAM 4km), the Global Forecast System version 14 (GFS), a model average of these four numerical models, as well as the forecasts made by NWS. For the second part of this final objective a comparison of both synoptic environments which

lead to each event as well as a comparison of what NDOT-MDSS produces and forecasts between the two different Alberta clipper systems is provided.

While the results of this study give insight to the accuracy of how NDOT-MDSS interpreted, forecasted, and handled these two winter weather events during the 2018-2019 winter, it is important to point out that the study had limitations and several handicaps. Verification of actual snowfall for each route was not possible due to sparseness of data, leading to reliance on nearest snowfall accumulation observations that occurred at the closest airport, which may not have been representative of each road segment chosen to be analyzed. NDOT-MDSS is proprietary software which presented a major challenged while carrying out this study; the inner workings of the system, including the theory of data generation and preservation, were not known. Data were limited particularly when it came to available data on Alberta clipper systems. Ultimately there was and is no way to completely understand how NDOT-MDSS was forecasting what it was and why it handles a winter weather event the way it does. However, despite these limitations, NDOT-MDSS did a good job overall, with the system interpreting, forecasting, and handling each Alberta clipper system event well with rarely any major errors occurring.

CHAPTER 2: BACKGROUND

2.1 Extratropical Cyclones and Winter Weather

Winter weather poses a hazard to life and property and can cause adverse conditions to the transportation sector. The Great Plains and Nebraska are no stranger to winter weather and its associated impacts. Winter weather is brought to these regions as the consequence of the lifecycle and movements of extratropical cyclones, synoptic-scale low pressure systems which frequently develop over and impact different regions year-round. Although the conditions coinciding with these lows may range from minor inconveniences to major impacts for people depending on a number of factors such as season, location, and moisture content, extratropical cyclones play a key role in the Earth's climate system and act to redistribute heat, momentum, and moisture. The cyclones also strongly affect many meteorological attributes such as the distribution of mid-latitude cool-season (October-April) precipitation (Lareau and Horel 2012). The occurrence and progression of extratropical cyclones across different locations can have a significant impact on a region's characteristics such as regional hydrologic cycles or the development of snow packs on mountain terrains (Changnon et al. 1993; Cayan 1996; Serreze et al. 1996; Lareau and Horel 2012). Not all extratropical cyclones exhibit the same characteristics and bring the same conditions to every location. Extratropical cyclones which traverse a region can form from several distinct atmospheric processes, undergo genesis in various locations, take a number of different tracks, and reach contrasting intensities. The result of these differences sometimes results in a naming convention or classification scheme of these cyclones which attempts to classify several of these different low pressure systems based on location of development, the winter

weather associated with the event, and the track that the low takes. Of all the types of low pressure systems, Nebraska and the Great Plains are primarily impacted by two different classified types, the Colorado low system and the Alberta clipper system (Figure 2.1). Both of these systems form from the same process and can bring snow during winter. However, the winter weather and conditions associated with the two can be radically different from each other in terms of intensity, duration, and impacts to regions based mainly on their formation location difference. This study focuses on the Alberta clipper system while others previously have focused on Colorado low systems (Barnhardt 2019; Rick 2020). The Alberta clipper system is one of the most significant synoptic-scale winter weather phenomena which affects central North America (Thomas and Martin 2007) with the track taken by these low pressure systems representing one of the major storm tracks for winter-season cyclones in the Northern Hemisphere (Petterssen 1956; Reitan 1974; Zishka and Smith 1980; Hoskins and Hodges 2002; Thomas and Martin 2007).

2.1.1 North America and Lee Cyclogenesis

Atmospheric waves generally move from west to east in the mid-latitudes. These atmospheric waves can take the form of mid- to upper-tropospheric waves or be associated with a surface extratropical cyclone which can a take a variety of tracks. Upper-tropospheric waves and extratropical cyclones are associated with vertical motion in the atmosphere. Synoptic scale upward vertical motion is the primary driver of the location and intensity of these waves and extratropical cyclones. This upward vertical motion represents a good sense of extratropical storm tracks and genesis in the mid-latitudes (Lareau and Horel 2012). Storm tracks are regions where the synoptic-scale

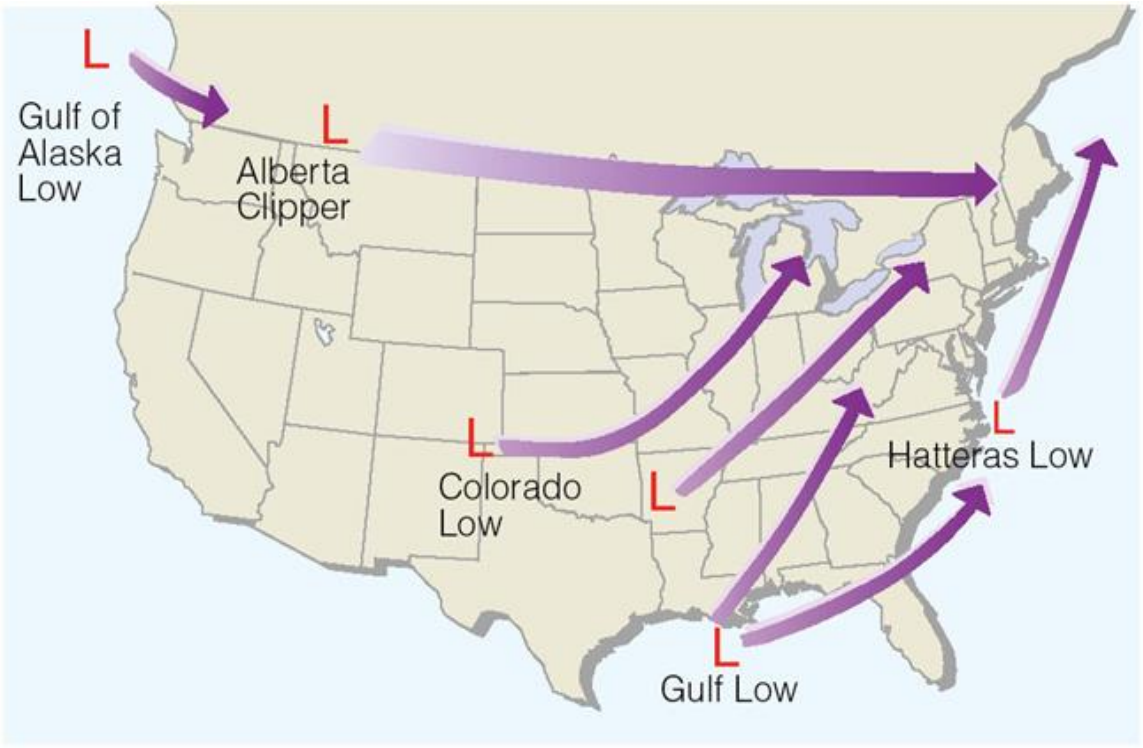

Figure 2.1: A general schematic of extratropical low formation and tracks. Image credit: Ahrens (2012)

transient eddy activity is locally most prevalent and intense (Glickman 2000; Lareau and Horel 2012). Lareau and Horel (2012) conducted a study which examined the climatology of synoptic-scale ascent over western North America using 21 cool seasons from 1989-2010. The results of their study showed that there is a climatological distribution of synoptic-scale ascent in an amplified sinusoidal pathway traversing North America where ascent tends to be greatest upstream of a climatological mean ridge over the Canadian Rockies and downstream of a mean trough over the southwestern United States (Figure 2.2). These locations of strong ascent translate downstream to a number of different storm tracks across North America that generally move from west to east (Figure 2.3). As disturbances approach North America from the west, resulting storm tracks tend to result in either (1) low-amplitude zonally progressive troughs impacting coastal British Columbia and southern Canada, (2) digging then lifting longwave troughs moving across the Intermountain West, or (3) cutoff lows forming over the southwestern United States (Lareau and Horel 2012). Seasonality has a major impact on the climatology of ascent which occurs to the west of North America, directly impacting wave and/or extratropical storm tracks and their location. For example, ascent increases from fall through early winter over coastal British Columbia and the Pacific Northwest as the prevailing southwesterly flow is enhanced. Year round, the latitude of the mean storm track over western North America varies from 30° to 55° N with spatial distributions of the tracks ranging from zonal to meridional (Lareau and Horel 2012). Alberta clipper system formation may be associated with pathway (1) while Colorado low system formation is associated with pathways (2) and (3).

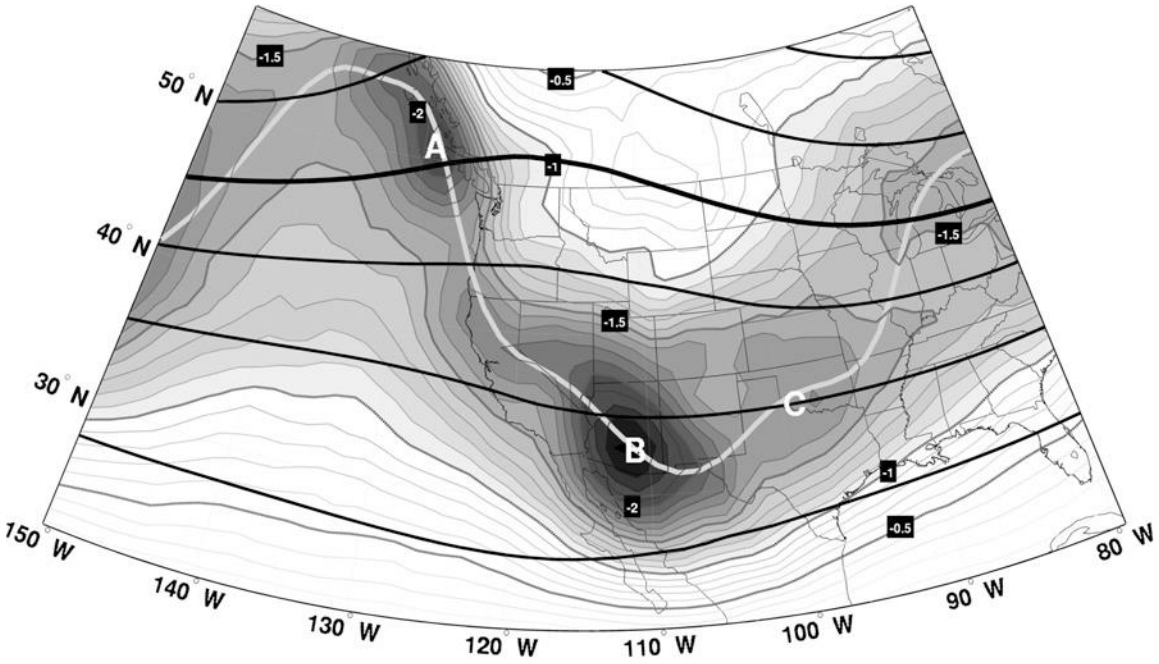

Figure 2.2: Climatological mean synoptic-scale ascent, $\overline{\omega}$ (labeled at intervals of 0.5 cPa s^{-1}, contoured every 0.1 cPa s^{-1}, and shading below 21 cPa s^{-1}) during 21 cool seasons (October–April) 1989-2010. Shaded regions denote locations within the primary storm track and the solid gray line depicts the storm track centroid. Letters A-C denote locations of local ascent maxima. The climatological mean 500 hPa geopotential height is shown by solid black contours at an interval of 100 m with the 5500 m contour emphasized for reference. Image credit: Lareau and Horel (2012).

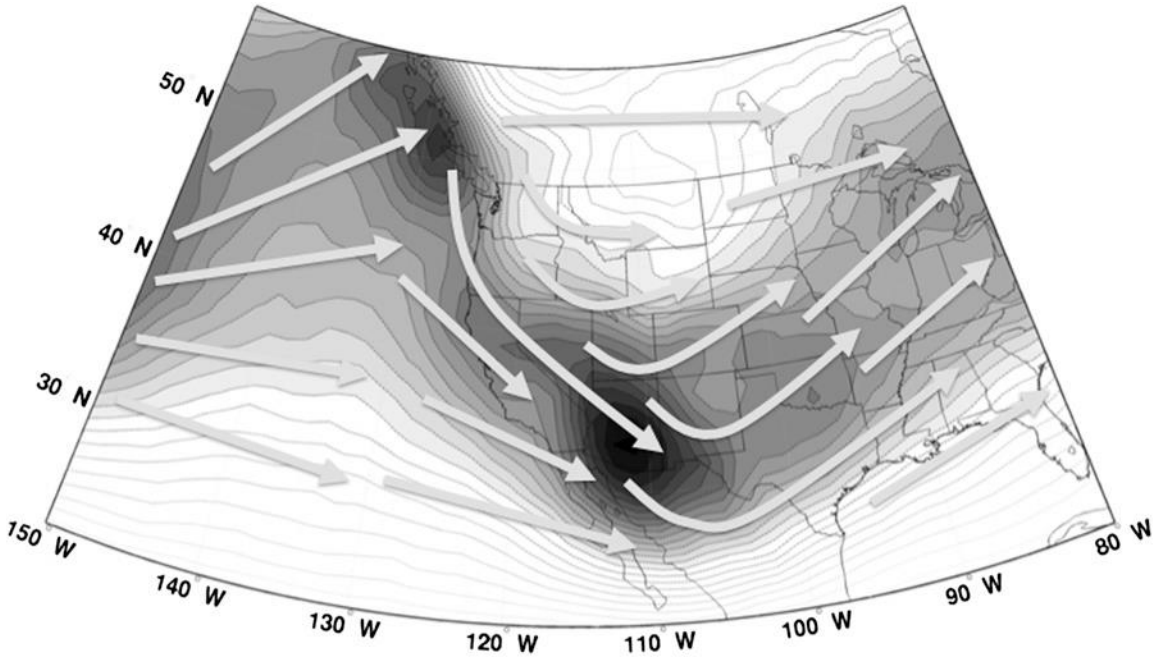

Figure 2.3: Climatological mean synoptic-scale ascent, $\overline{\omega}$ (contoured every 0.1 cPa s^{-1} and shading below 21 cPa s^{-1}) during 21 cool seasons (October–April) 1989-2010 with conceptual summary of composite storm trajectories overlayed (gray arrows). Image credit: Lareau and Horel (2012).

Disturbances (mid- to upper-tropospheric waves and/or surface extratropical cyclones) in the mid-latitudes which approach North America will encounter topography at some point as a consequence of their west to east movement and the physical geography. Virtually all eastward moving cyclones and waves must pass over the high terrain of the Rocky Mountains before they reach the central United States (Hobbs et al. 1996). It is this interaction with the Rocky Mountains which allows for the birth and subsequent evolution of several extratropical cyclones across North America including Alberta clipper and Colorado low systems. Both Alberta clipper and Colorado low systems are a result of the mechanics of lee cyclogenesis which occurs on the lee side of the Rocky Mountains. Lee cyclogenesis or the genesis of a cyclone on the lee side of a mountain barrier occurs mainly due to the column stretching phenomenon which is particularly known to occur on the lee side of the Rocky Mountains. This process begins with lower tropospheric wind flow across the Rocky Mountains. As a shortwave trough moves eastward, westerly downslope flow increases over the Rockies and this results in adiabatic warming and a pressure trough at the surface in the lee of the Rockies, called the lee trough (Hobbs et al. 1996; Thomas and Martin 2007). Although lee troughing commonly occurs in association with cross-mountain flow in the lower troposphere, additional conditions are necessary for the development of a surface cyclone within the lee trough (Thomas and Martin 2007). Lee troughing is not synonymous with lee cyclogenesis (Pierrehumbert 1986; Tibaldi et al. 1990; Thomas and Martin 2007). However, surface low pressure centers often form within the lee trough (Hobbs et al. 1996; Thomas and Martin 2007). Lee cyclogenesis takes place when a region of strong ascent in the middle and upper troposphere associated with differential cyclonic vorticity

advection is superimposed over a band of maximum descent in the lower troposphere (Newton 1956; Steenburgh and Mass 1994; Schultz and Doswell 2000; Thomas and Martin 2007) which acts to physically stretch the column of air. On the lee side of most of the Rocky Mountains, descent is often present from the westerly downslope flow that occurs from flow moving west to east. Strong ascent in the middle and upper troposphere is often present (Figure 2.2 and Figure 2.3) as shown by the climatology carried out by Lareau and Horel (2012). Due to this setup, the resulting differential vertical motion generates cyclonic vorticity via column stretching (Thomas and Martin 2007) which in return results in the genesis of a surface cyclone which then becomes an Alberta clipper system or a Colorado low system. The difference between the two types of systems is simply a matter of location rather than one of mechanical process, although after formation, characteristics of each of the systems and the winter weather associated with them are different as a consequence of this location difference.

2.1.2 Alberta Clipper Systems

The Alberta clipper (low pressure only), or Alberta clipper system (low pressure, associated fronts, and high pressure system behind the low) gets its name from the Canadian province it often forms over or near. The lee side of the Canadian Rockies essentially act as breeding grounds for Alberta clipper systems, where, as several authors (Zishka and Smith 1980; Whittaker and Horn 1981; Nielsen and Dole 1992) have shown there is a relative maximum in cyclogenesis (Hutchinson 1995). Hutchinson (1995) states "The Alberta clipper can be defined as cyclones that move southeast from regions of western Canada into south-central Canada or the north-central United States before moving eastward to the coast of North America." Glickman (2000) defines an Alberta

clipper as “a low pressure system that is often fast moving, has low moisture content, and originates in western Canada (in or near Alberta province).” Alberta clipper systems have a complex evolution and lifecycle which result in the systems bringing winter weather conditions and impacts to regions that are very different from other classified extratropical cyclones such as the Colorado low system. This is especially true for Nebraska and the Great Plains. The Alberta clipper system generally occurs between late fall and early spring (Hutchison 1995) with the systems occurring most frequently during December through February and substantially less frequently during the October and March timeframe (Thomas and Martin 2007). The larger number of cases observed during the middle of the cold season is a consequence of the more southerly position of the jet stream that provides a more favorable upper-level flow pattern for Alberta clipper system development (Thomas and Martin 2007). Thomas and Martin (2007) carried out a climatology of Alberta clipper systems in which they examined 177 Alberta clipper systems (Table 2.1) through surface and upper-air analyses using the ECMWF Tropical Ocean Global Atmosphere (TOGA) dataset over 15 boreal cold seasons from 1986/87 to 2000/01. The evolution of the Alberta clipper system can best be defined and explained following the outline made by Thomas and Martin (2007) where the evolution of the Alberta clipper system is divided up into two separate periods: the pre-departure period (36 hours leading up to the time of departure) followed by the post-departure period (60 hours after departure), where departure time is defined as the last analysis time before a sea level pressure (SLP) minimum (or rather the low pressure system) begins making appreciable movement away from the Canadian Rockies. Specifically, Thomas and Martin (2007) looked at synoptic conditions (SLP, 850 hPa potential temperatures,

Table 2.1: The number of Alberta clipper systems that developed during each individual month and year in Thomas and Martin's (2007) Climatology. Boldface numbers represent monthly totals. Numbers in parentheses indicate the number of Alberta clipper systems normalized to a 30-day month for each of the months.

Season	Oct	Nov	Dec	Jan	Feb	Mar	Total
1987/1988	2	0	1	2	2	0	7
1988/1989	1	0	3	4	1	0	9
1989/1990	0	7	3	6	3	0	19
1990/1991	3	1	2	3	1	2	12
1991/1992	1	2	3	5	3	0	14
1992/1993	2	1	2	1	0	3	9
1993/1994	3	2	4	1	2	2	14
1994/1995	0	1	3	0	3	1	8
1995/1996	1	3	1	2	3	2	12
1996/1997	1	1	2	4	5	5	18
1997/1998	1	0	4	1	0	0	6
1998/1999	1	3	3	0	3	1	11
1999/2000	3	2	3	3	2	0	13
2000/2001	0	2	3	3	2	0	10
Total	**20** (19.4)	**28** (28.0)	**43** (41.6)	**37** (35.8)	**32** (34.0)	**17** (16.5)	177

850 hPa height and vorticity, and 500 hPa height and vorticity) at T-36, T-12, T=0, T+12, T+24, T+36, T+48, T+60 hours (h) from the departure (T) of the Alberta clipper systems in order to understand Alberta clipper system formation and lifecycle. Their analysis is sharp and in depth with several important facts to point out and summarize to understand Alberta clipper systems and their evolution (Figure 2.4-2.11).

The pre-departure period for the Alberta clipper system is marked by three major features: a cyclone over the Gulf of Alaska, a tropospheric deep ridge over western North America, and a lee trough developing east of the Canadian Rockies in British Columbia and Alberta (Figure 2.4). The development of nearly every Alberta clipper system is preceded by the landfall of a cyclone along the southeastern coastline of Alaska or British Columbia. These cyclones over the Gulf of the Alaska typically move northeastward and begin to dissipate as they approach the coastal mountain ranges bordering the northeast Pacific Ocean (Figure 2.5). As the low center interacts with orography along the coast, the SLP of the cyclone dramatically weakens. As the cyclone approaches the Rockies, cross-mountain flow strengthens over the Rockies which results in adiabatic warming from downslope flow in the lee of the Canadian Rockies (Figure 2.6). This leads to the development of a lee-trough at the surface along with the development and amplification of a thermal ridge at 850 hPa (Thomas and Martin 2007). Eventually a sudden increase in vorticity occurs over the last 12 hours of the pre-departure period which is most likely the result of differential vertical motion (i.e., descent at low levels, ascent at upper levels) which in turn causes column stretching leading to a new surface cyclone. Continuing cross mountain flow increases 850-hPa potential temperature over southern Alberta which enhances the baroclinic zone between Alberta and Saskatchewan (Thomas and

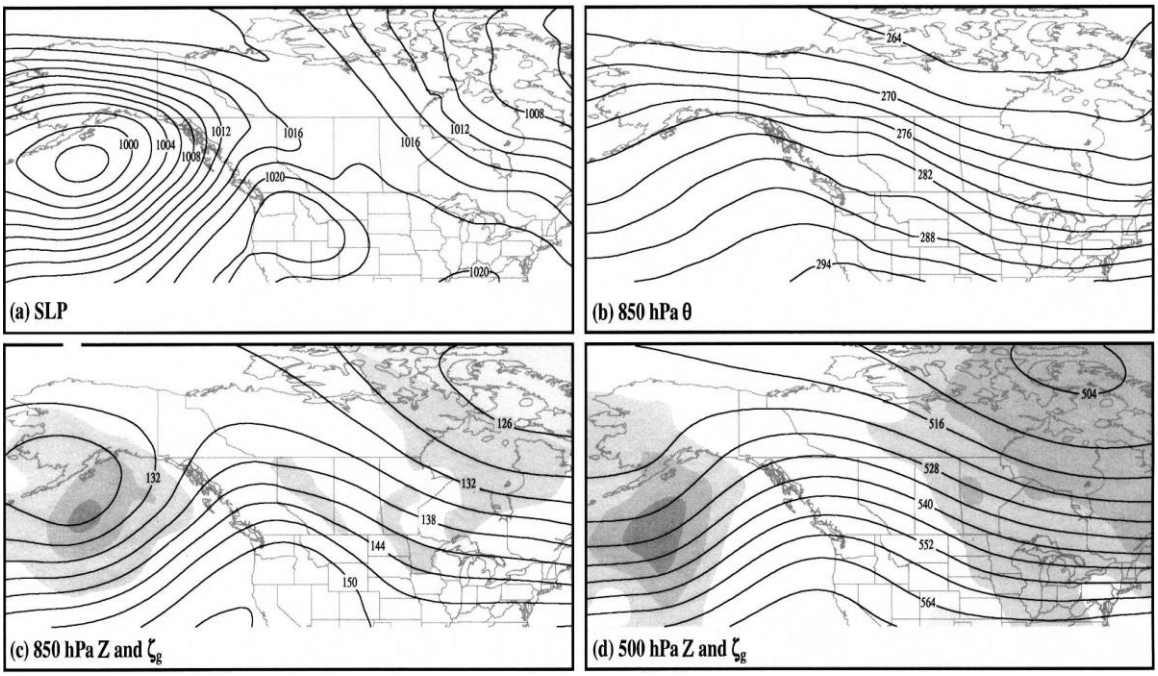

Figure. 2.4: Composite analyses for all Alberta clipper systems at T-36 h. (a) Composite SLP (hPa) contoured every 2 hPa. (b) Composite 850 hPa potential temperature (K) contoured every 3 K. (c) Composite 850 hPa geopotential height (dam; solid lines) contoured every 3 dam and 850 hPa geostrophic relative vorticity (shading). Shading for geostrophic relative vorticity begins at 5 x 10^{-6} s^{-1} with a shading interval of 10 x 10^{-6} s^{-1}. (d) Composite 500 hPa geopotential height (dam; solid lines) contoured every 6 dam and 500 hPa geostrophic relative vorticity (shading). Image credit: Thomas and Martin (2007)

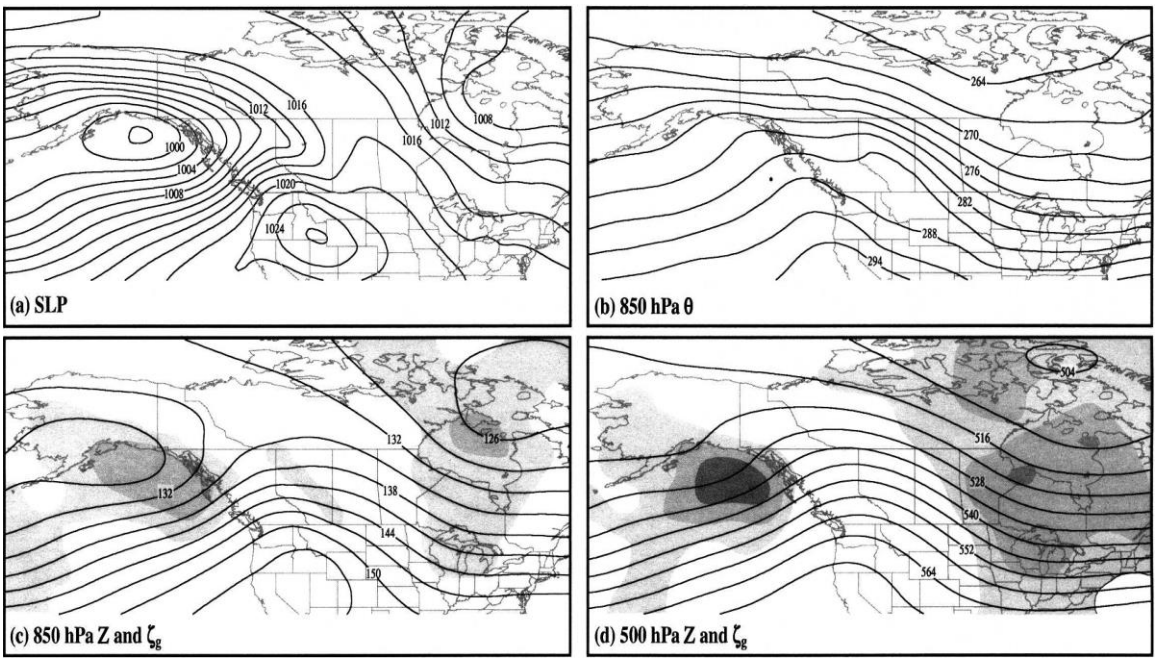

Figure 2.5: Composite analyses for all Alberta clipper systems at T-12 h. (a) Composite SLP (hPa) contoured every 2 hPa. (b) Composite 850 hPa potential temperature (K) contoured every 3 K. (c) Composite 850 hPa geopotential height (dam; solid lines) contoured every 3 dam and 850 hPa geostrophic relative vorticity (shading). Shading for geostrophic relative vorticity begins at 5 x 10^{-6} s^{-1} with a shading interval of 10 x 10^{-6} s^{-1}. (d) Composite 500 hPa geopotential height (dam; solid lines) contoured every 6 dam and 500 hPa geostrophic relative vorticity (shading). Image credit: Thomas and Martin (2007)

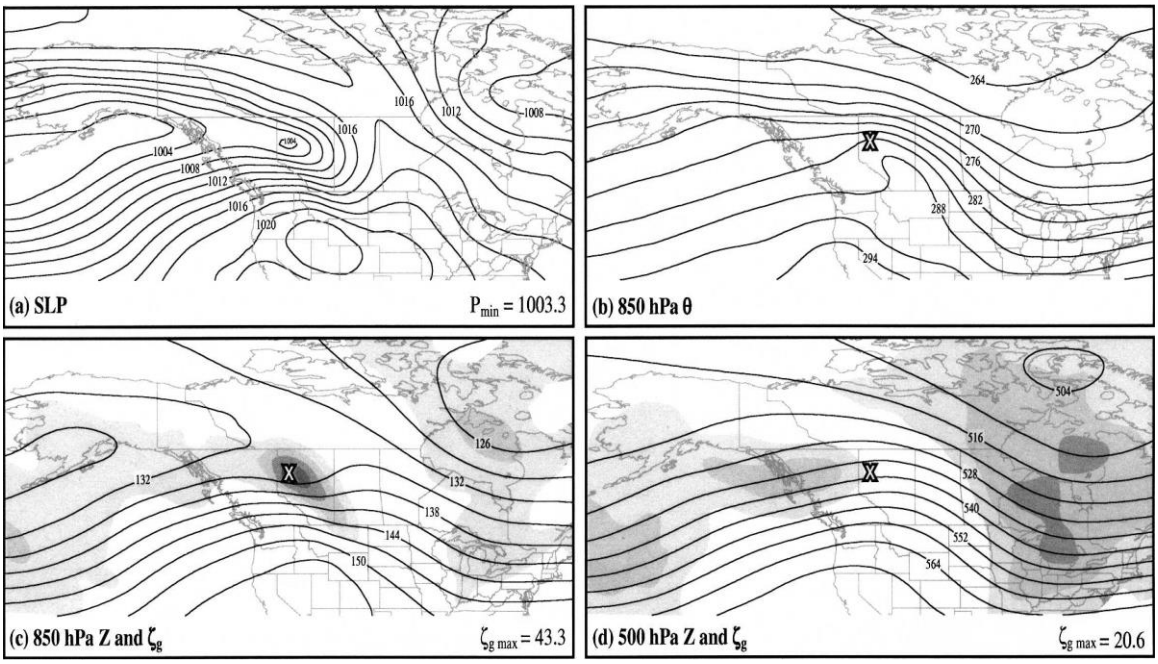

Figure 2.6: Composite analyses for all Alberta clipper systems at T=0 h. (a) Composite SLP (hPa) contoured every 2 hPa. (b) Composite 850 hPa potential temperature (K) contoured every 3 K. (c) Composite 850 hPa geopotential height (dam; solid lines) contoured every 3 dam and 850 hPa geostrophic relative vorticity (shading). Shading for geostrophic relative vorticity begins at 5 x 10^{-6} s^{-1} with a shading interval of 10 x 10^{-6} s^{-1}. (d) Composite 500 hPa geopotential height (dam; solid lines) contoured every 6 dam and 500 hPa geostrophic relative vorticity (shading). Values in the lower-right corner of (a), (c), and (d) are the minimum SLP (hPa), maximum 850 hPa geostrophic relative vorticity (x10^{-6} s^{-1}), and maximum 500 hPa geostrophic relative vorticity (x10^{-6} s^{-1}), respectively. The X symbol in (b)-(d) corresponds to the location of the SLP minima of the composite Alberta clipper system. Image credit: Thomas and Martin (2007)

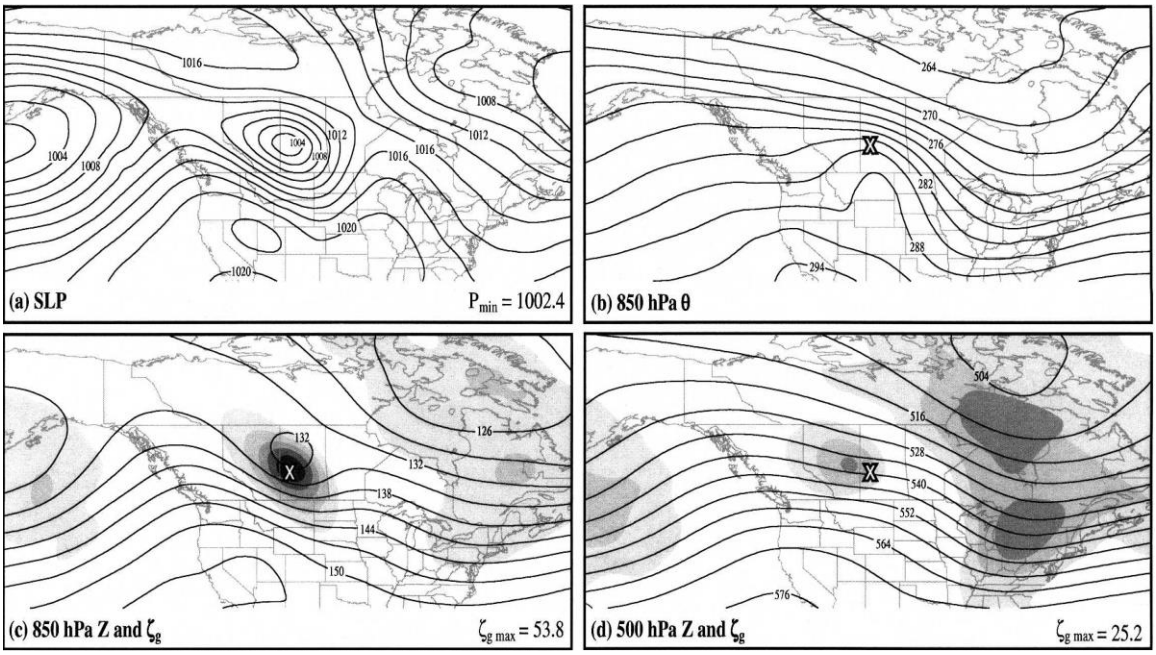

Figure 2.7: Composite analyses for all Alberta clipper systems at T+12 h. (a) Composite SLP (hPa) contoured every 2 hPa. (b) Composite 850 hPa potential temperature (K) contoured every 3 K. (c) Composite 850 hPa geopotential height (dam; solid lines) contoured every 3 dam and 850 hPa geostrophic relative vorticity (shading). Shading for geostrophic relative vorticity begins at 5 x 10^{-6} s^{-1} with a shading interval of 10 x 10^{-6} s^{-1}. (d) Composite 500 hPa geopotential height (dam; solid lines) contoured every 6 dam and 500 hPa geostrophic relative vorticity (shading). Values in the lower-right corner of (a), (c), and (d) are the minimum SLP (hPa), maximum 850 hPa geostrophic relative vorticity (x10^{-6} s^{-1}), and maximum 500 hPa geostrophic relative vorticity (x10^{-6} s^{-1}), respectively. The X symbol in (b)-(d) corresponds to the location of the SLP minima of the composite Alberta clipper system. Image credit: Thomas and Martin (2007)

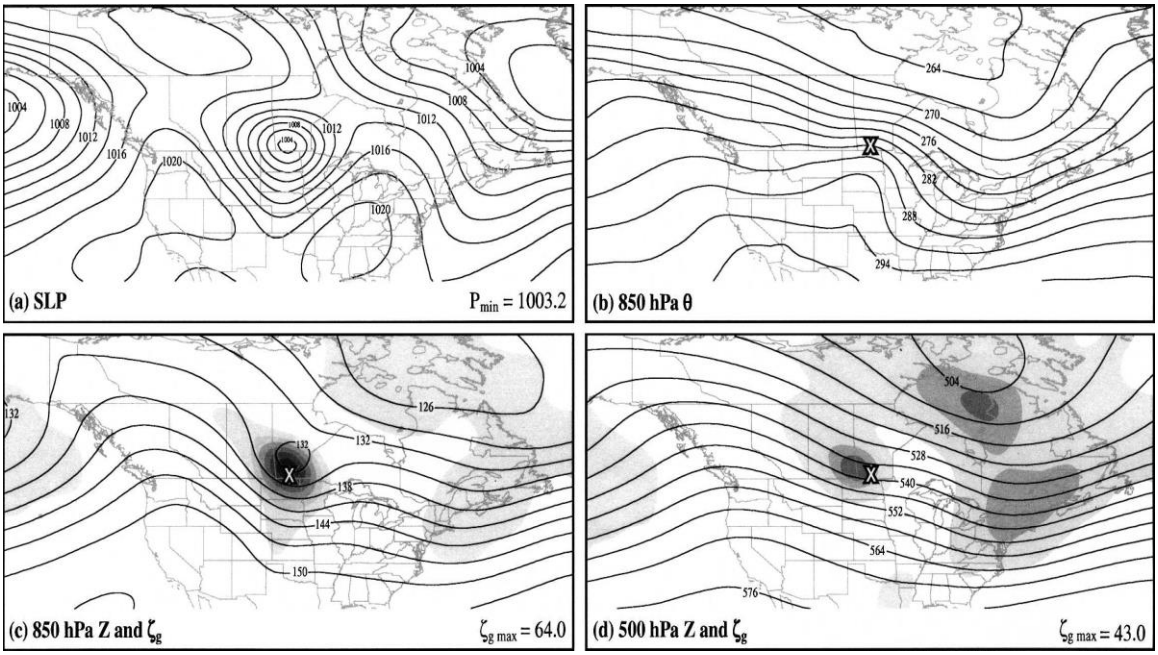

Figure 2.8: Composite analyses for all Alberta clipper systems at T+24 h. (a) Composite SLP (hPa) contoured every 2 hPa. (b) Composite 850 hPa potential temperature (K) contoured every 3 K. (c) Composite 850 hPa geopotential height (dam; solid lines) contoured every 3 dam and 850hPa geostrophic relative vorticity (shading). Shading for geostrophic relative vorticity begins at 5 x 10^{-6} s^{-1} with a shading interval of 10 x 10^{-6} s^{-1}. (d) Composite 500 hPa geopotential height (dam; solid lines) contoured every 6 dam and 500 hPa geostrophic relative vorticity (shading). Values in the lower-right corner of (a), (c), and (d) are the minimum SLP (hPa), maximum 850 hPa geostrophic relative vorticity (x10^{-6} s^{-1}), and maximum 500 hPa geostrophic relative vorticity (x10^{-6} s^{-1}), respectively. The X symbol in (b)-(d) corresponds to the location of the SLP minima of the composite Alberta clipper system. Image credit: Thomas and Martin (2007)

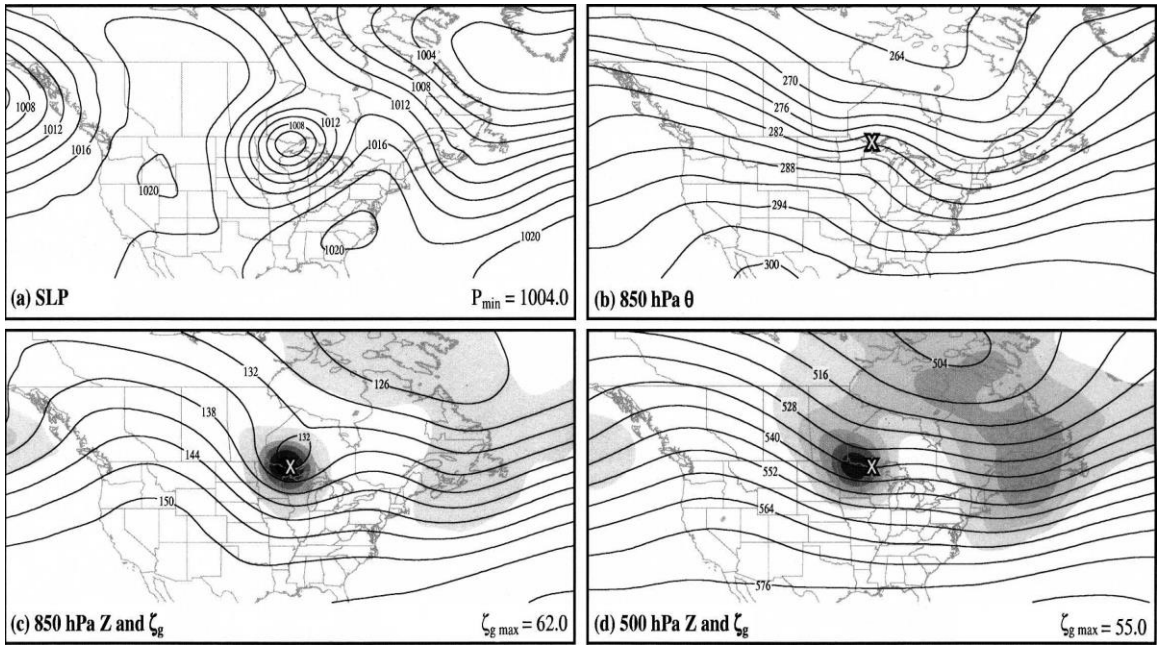

Figure 2.9: Composite analyses for all Alberta clipper systems at T+36 h. (a) Composite SLP (hPa) contoured every 2 hPa. (b) Composite 850 hPa potential temperature (K) contoured every 3 K. (c) Composite 850 hPa geopotential height (dam; solid lines) contoured every 3 dam and 850 hPa geostrophic relative vorticity (shading). Shading for geostrophic relative vorticity begins at 5 x 10^{-6} s^{-1} with a shading interval of 10 x 10^{-6} s^{-1}. (d) Composite 500 hPa geopotential height (dam; solid lines) contoured every 6 dam and 500 hPa geostrophic relative vorticity (shading). Values in the lower-right corner of (a), (c), and (d) are the minimum SLP (hPa), maximum 850 hPa geostrophic relative vorticity (x10^{-6} s^{-1}), and maximum 500 hPa geostrophic relative vorticity (x10^{-6} s^{-1}), respectively. The X symbol in (b)-(d) corresponds to the location of the SLP minima of the composite Alberta clipper system. Image credit: Thomas and Martin (2007)

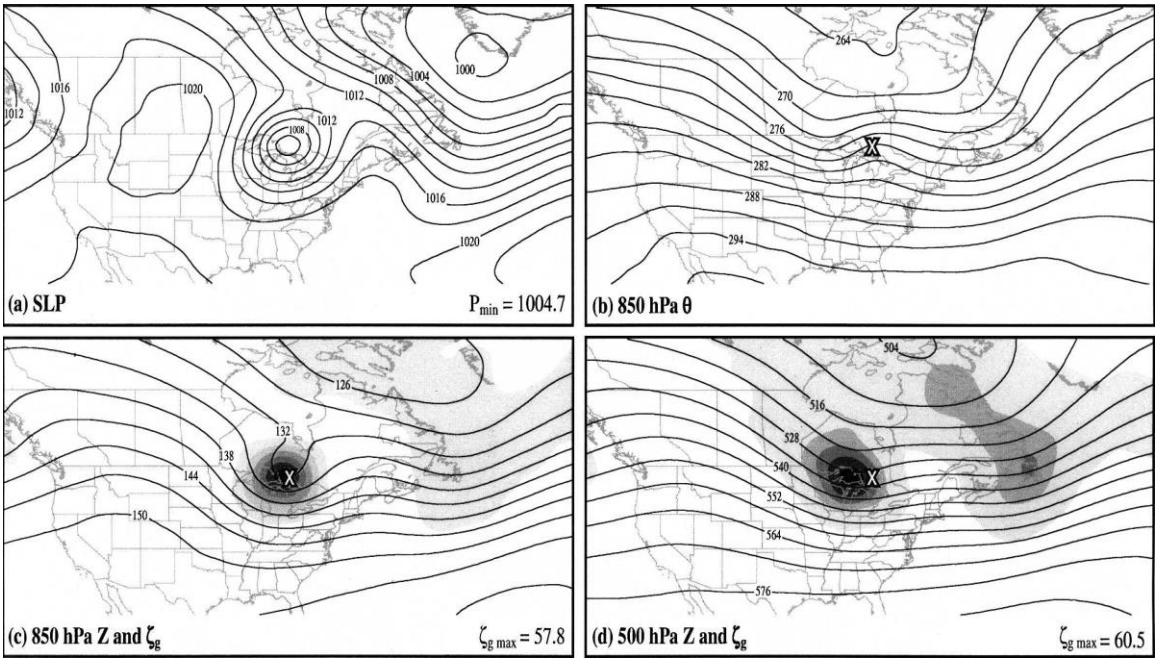

Figure 2.10: Composite analyses for all Alberta clipper systems at T+48 h. (a) Composite SLP (hPa) contoured every 2 hPa. (b) Composite 850 hPa potential temperature (K) contoured every 3 K. (c) Composite 850 hPa geopotential height (dam; solid lines) contoured every 3 dam and 850 hPa geostrophic relative vorticity (shading). Shading for geostrophic relative vorticity begins at 5 x 10^{-6} s^{-1} with a shading interval of 10 x 10^{-6} s^{-1}. (d) Composite 500 hPa geopotential height (dam; solid lines) contoured every 6 dam and 500 hPa geostrophic relative vorticity (shading). Values in the lower-right corner of (a), (c), and (d) are the minimum SLP (hPa), maximum 850 hPa geostrophic relative vorticity (x10^{-6} s^{-1}), and maximum 500 hPa geostrophic relative vorticity (x10^{-6} s^{-1}), respectively. The X symbol in (b)-(d) corresponds to the location of the SLP minima of the composite Alberta clipper system. Image credit: Thomas and Martin (2007)

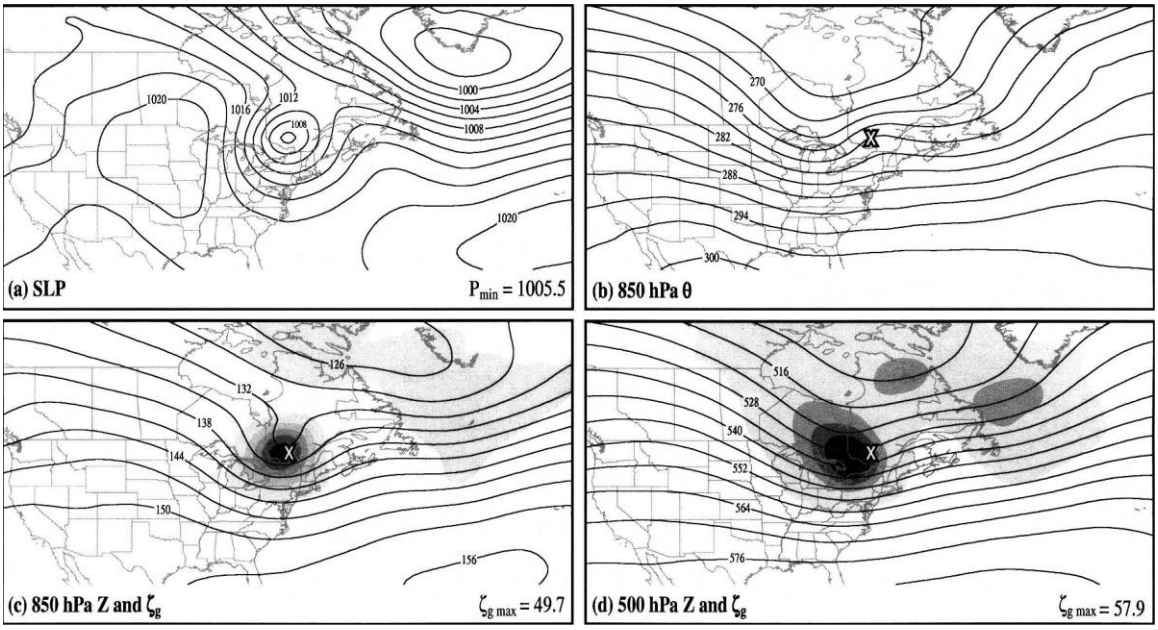

Figure 2.11: Composite analyses for all Alberta clipper systems at T+60 h. (a) Composite SLP (hPa) contoured every 2 hPa. (b) Composite 850 hPa potential temperature (K) contoured every 3 K. (c) Composite 850 hPa geopotential height (dam; solid lines) contoured every 3 dam and 850 hPa geostrophic relative vorticity (shading). Shading for geostrophic relative vorticity begins at 5 x 10^{-6} s^{-1} with a shading interval of 10 x 10^{-6} s^{-1}. (d) Composite 500 hPa geopotential height (dam; solid lines) contoured every 6 dam and 500 hPa geostrophic relative vorticity (shading). Values in the lower-right corner of (a), (c), and (d) are the minimum SLP (hPa), maximum 850 hPa geostrophic relative vorticity (x10^{-6} s^{-1}), and maximum 500 hPa geostrophic relative vorticity (x10^{-6} s^{-1}), respectively. The X symbol in (b)-(d) corresponds to the location of the SLP minima of the composite Alberta clipper system. Image credit: Thomas and Martin (2007)

Martin 2007). In addition, differential cyclonic vorticity advection over the established low-level baroclinic zone in the lee of the Rockies also promotes the development of the lee cyclone (Steenburgh and Mass 1994; Davis 1997; Thomas and Martin 2007). Following this pre-departure period, the Alberta clipper system usually moves into western Saskatchewan around 12 hours after departure and as a result of this movement the strong thermal ridge formed by adiabatic warming decreases in strength (Figure 2.7). The central SLP of the low pressure portion of the Alberta clipper system remains relatively high and does not usually drop any lower during its entire life cycle. At this point the system is flanked by anticyclones to its south and northwest that lead to relatively strong pressure gradients around the system. Another characteristic at this point is strong geostrophic frontogenesis located well east of the SLP minimum along the broad northwest-southeast-oriented baroclinic zone, while geostrophic frontolysis occurs to the northwest of the SLP minimum (Thomas and Martin 2007). By 24 hours after departure a surface anticyclone usually becomes evident to the northwest of the Alberta clipper low, and as usually seen by depressions in 850 hPa isentropes, colder air begins to move southward to the west-northwest of the SLP minimum (Figure 2.8). Previously blocked by the higher terrain, colder air to the northwest of the Alberta clipper low pressure center funnels southward as the system progresses away from the Rockies. By 36 hours after departure, the 850 hPa ridge rotates counterclockwise and is now east of the SLP minimum (Figure 2.9). The Alberta clipper low acquires more classic frontal features mainly as a consequence of rotation of the 850 hPa thermal ridge axis and the increasing westward tilt with the height of the system. Prior to this point, the cyclone had mainly a nonclassical thermal structure (Thomas and Martin 2007). Over the last

24 hours of the post-departure period (Figure 2.10), the baroclinic zones take on an orientation resembling that of the cold and warm fronts in a classical cyclone (Bjerknes and Solberg 1922; Thomas and Martin 2007). By 60 hours after departure the Alberta clipper system has generated a structure conducive for baroclinic development and approaches the east of the Continental United States (CONUS) (Figure 2.11). In summary, Alberta clipper systems tend to generally move southeastward from the lee of the Canadian Rockies toward or just north of Lake Superior before progressing eastward into southeastern Canada or the northeastern United States, with less than 10 percent of the cases in the climatology tracking south of the Great Lakes (Figure 2.12 and 2.13). Alberta clipper systems moving as far south as the latitude of Nebraska are rare.

Alberta clipper systems have some notable characteristics which make them different from other extratropical cyclones. Within the spectrum of all extratropical cyclones, Alberta clipper systems are generally regarded as weak, small-scale systems (Thomas and Martin 2007). Generally, Alberta clipper systems are often associated with light-to-moderate precipitation (Hutchinson 1995) with moderate precipitation generally occurring in areas up to a few hundred kilometers north of the system's track while lighter precipitation generally falls to the south of the track (Harms 1973; Beckman 1987; Hutchinson 1995; Thomas and Martin 2007). The systems usually lack moisture and have a rapid movement which combine to produce relatively low precipitation amounts over a narrow path. (Thomas and Martin 2007). However, these characteristics of the cyclones do not mean the winter weather they bring to different regions is not impactful. For instance, relatively little moisture is necessary for Alberta clipper systems to produce snow accumulations of 80-150 mm (3-6 in.) in 3-6 hours given the very cold air and

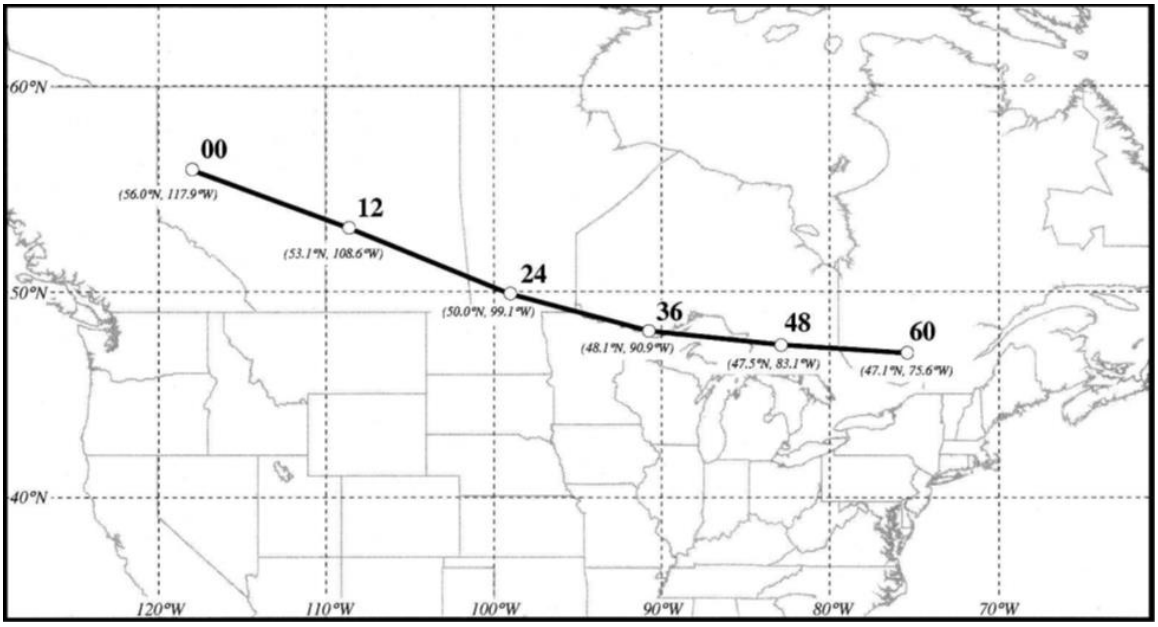

Figure 2.12: The average position of all Alberta clipper systems, represented by gray dots, in the climatology constructed by Thomas and Martin (2007) at the given time (h) after departure. The black line connecting the dots represents the average track of the Alberta clipper system in the climatology. Latitude and longitude of each average position are indicated. Image credit: Thomas and Martin (2007)

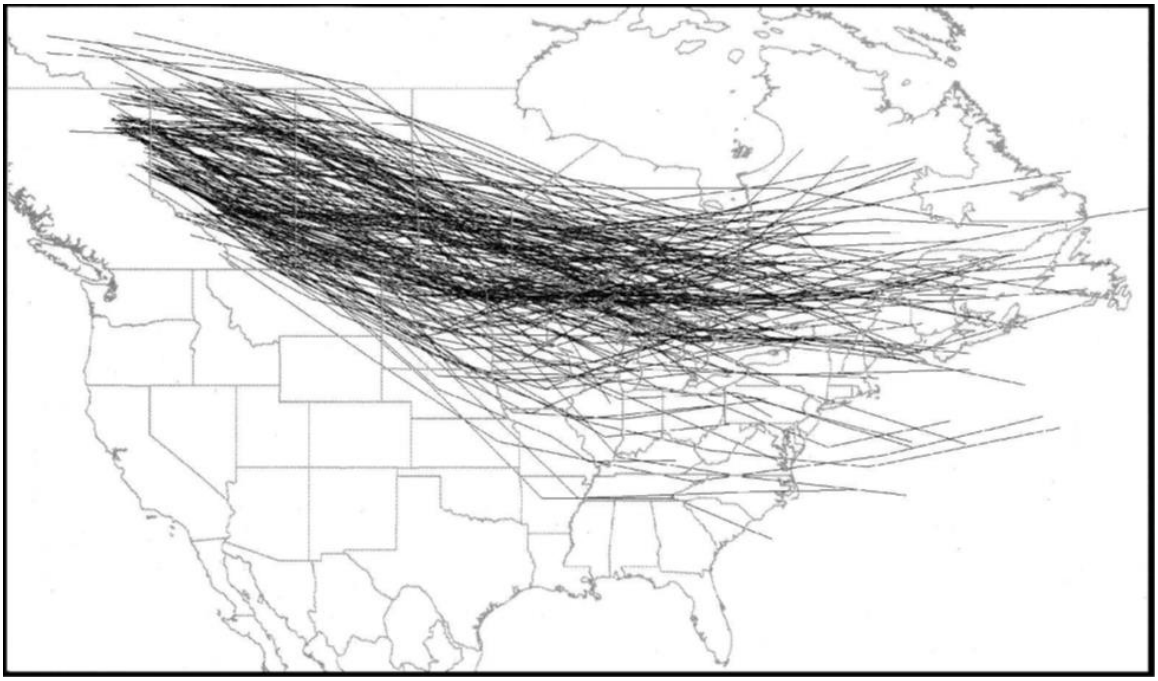

Figure 2.13: Storm tracks of all Alberta clipper systems used in the climatology constructed by Thomas and Martin (2007) out to 60 h after departure. Image credit: Thomas and Martin (2007)

correspondingly large snow-to-liquid equivalent ratios (generally 20 to 1 or greater) associated with these systems (Harms 1973; Thomas and Martin 2007). In addition, they can be more impactful depending on the region they are traversing. For example, snowfall amounts can be enhanced in the east through an influx of low-level moisture from the Great Lakes into the systems (Harms 1973; Vinzani and Changnon 1981; Silberberg 1990; Angel and Isard 1997; Thomas and Martin 2007) or as a result of locally intense upper-level forcing in the presence of low conditional stability (Smart and Carr 1986; Silberberg 1990; Gallus and Bresch 1997; Thomas and Martin 2007). When it comes to the Alberta clipper systems, often the most significant sensible weather element associated with the systems is strong wind. Areas in the lee of the Rocky Mountains and Alberta are susceptible to frontal chinooks as a Pacific cyclone approaches the British Columbia coast and the low pressure of the Alberta clipper system develops within the lee trough (Price 1971; Oard 1993; Schultz and Doswell 2000; Thomas and Martin 2007). Over central and eastern North America, the strongest winds are usually located on the western side of the Alberta clipper in the region between the surface cyclone and the often-intense anticyclone trailing the low pressure part of the Alberta clipper system. Strong winds with Alberta clipper systems can also arise from enhanced isallobaric winds associated with a substantial pressure rise-fall couplet, and a downward transport of high momentum air in regions of strong cold-air advection and low static stability (Kapela et al. 1995; Schultz and Doswell 2000; Thomas and Martin 2007). The strong winds that follow the passage of an Alberta clipper, coupled with preexisting or freshly fallen snow, can result in considerable blowing and drifting of snow and the creation of ground

blizzard conditions (Stewart et al. 1995; Schwartz and Schmidlin 2002; Thomas and Martin 2007).

In Nebraska, the Alberta clipper system is very different from the Colorado low system. The Colorado low system and Alberta clipper system are similar in that they both form due to lee cyclogenesis which is the product of differential vertical motion generating cyclonic vorticity via column stretching on the lee side of the Rocky Mountains, and that they are both extratropical cyclones. They may also be similar in cyclone structure. For example, lee cyclogenesis can sometimes result in a cyclone frontal structure known as a cold front aloft brought on by a lee cyclone having its baroclinic zone eroded at low levels from adiabatic warming associated with downslope flow. The result of this is a cyclone with exhibits a cold front feature associated with precipitation aloft with a weaker front at the surface that is behind the cold front aloft (Hobbs et al. 1996). In this case, precipitation usually occurs before the temperature decrease is noticed from the movement or passage of the surface cold front; similar to the known katafront nature in meteorology (Moore and Smith 1989). This can occur in both Colorado low systems and Alberta clipper systems (Hobbs et al. 1996). The main difference between the two is that they form in different locations and subsequently have different tracks, making the winter weather and conditions brought by them notably different. Alberta clipper systems will typically bring all snow to regions they cross while Colorado low systems may bring rain, snow, or a wintery mix to regions. In terms of amount of snowfall, the Alberta clipper system will generally bring light dry snows with less in accumulation then that of the Colorado low system, which has access to the Gulf of Mexico for moisture availability and may result in heavy rain or snow being brought to

a region. Alberta clipper systems are typically faster moving systems compared to Colorado low systems, resulting in snowfall impacts upon a region from Alberta clipper systems typically not lasting as long as those from a Colorado low system. The Alberta clipper system is more often associated with strong wind impacts as they are likely to bring strong winds with and after passage because of the surrounding pressure gradients while the Colorado low system may not always bring strong winds after the passage of the system. The overall impacts and tracks of the two different systems are very different despite the cyclone genesis and structure similarities (Figure 2.14 and 2.15). Based on these differences, the public and the road transportation sector need to prepare differently depending on the type of system that is expected to impact their roads, highways, and interstates. For example, when expecting an Alberta clipper system the main preparation may be for high winds and freezing temperatures to follow rather than heavy rain or flash flooding which may occur during the passage of a Colorado low system.

2.2 Road Weather

Winter weather and its impacts brought by the extratropical cyclone can be hazardous to several different industries within regions in the mid-latitudes. Impacts can be in the form of injuries and fatalities or large financial burdens from damage and loss of property. The impacts of winter weather are particularly hazardous within the realm of transportation. Adverse effects to transportation can be more substantial based on location and the frequency of observed winter weather in a given region. Overall, winter weather within the midwestern United States brings a variety of weather and precipitation types that are hazardous to travel (Carmichael et al. 2004). Hazards to road transportation do not just include snow on roadways, but they can also manifest from a variety of

Figure 2.14: Alberta clipper system typical storm track and impact. Image Credit: NWS (2020)

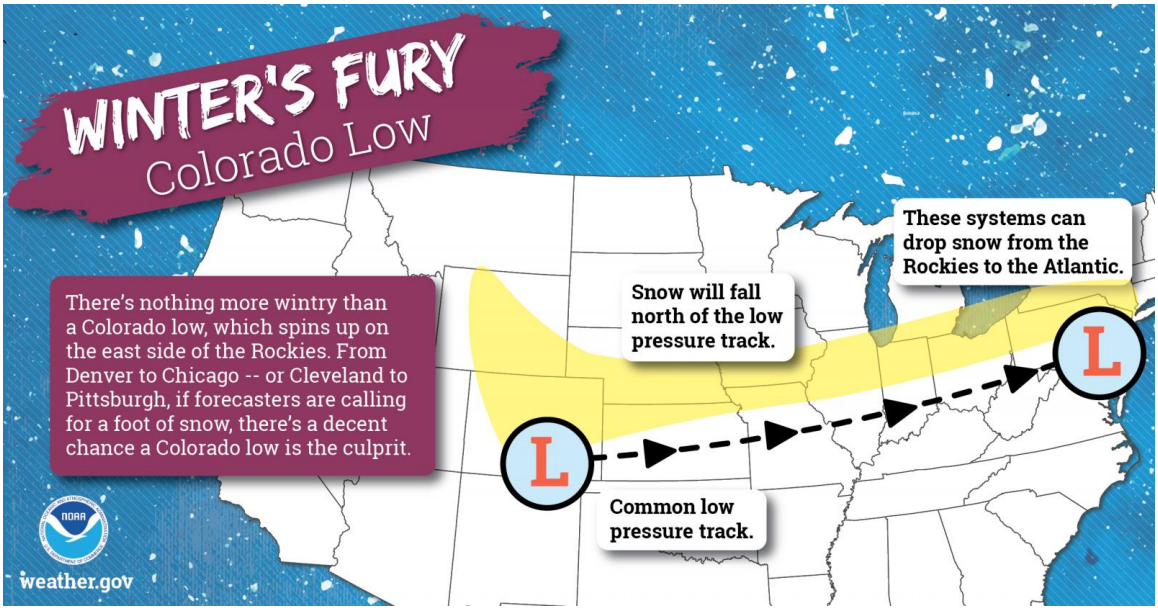

Figure 2.15: Colorado low system typical storm track and impact. Image Credit: NWS (2020)

conditions brought on by winter weather. These conditions include different types of winter precipitation (such as snow, sleet, freezing rain, and rain), pavement characteristics becoming altered (such as roads becoming slick or icy due to the precipitation), visibility being reduced, and freezing temperatures. Andrey et al. (2003) found that 16 percent of fatal collisions and 18.5 percent of personal injury collisions occur during adverse weather conditions (rain, snow, freezing rain, hail, sleet, fog, mist, smog, dust, smoke) when reviewing national summary of accident statistics for 1998 in Canada. On average, precipitation is associated with a 75 percent increase in traffic collisions and a 45 percent increase in related injuries, compared to "normal" seasonal conditions. Effects from snowfall were found to be more pronounced than those from rainfall with snow events being associated with disproportionately more single-vehicle crashes overall (Andrey et al. 2003). Eisenberg and Warner (2005) state that snowfall poses a substantial risk for drivers as snow makes driving more dangerous by causing hazards such as reducing tire adherence and impairing visibility. They find that both nonfatal injury crashes and property-damage-only crashes increase significantly when it snows, while finding a decline in fatal crashes overall. They estimate that snowfall in the United States each year leads to an additional 45,000 nonfatal-injury crashes and 150,000 property-damage-only crashes, relative to what would be expected if these days were dry. Not surprisingly, precipitation-related fatalities occur most often during the cool season (Tobin et al. 2019) with most fatalities occurring during the winter season, roughly October through April (Black and Mote 2015a). Black and Mote (2015a) conducted a study in which they looked at the characteristics of winter-precipitation-related transportation fatalities in the United States. Their study highlights just how impactful

winter weather is in the United States when accounting for indirect (fatalities that occur when the weather creates a situation that leads to a death) and direct deaths together. They find that between 1975 and 2011, winter precipitation was a factor in nearly 28,000 aviation and motor vehicle crashes that resulted in over 32,000 fatalities, which is an average of nearly 900 fatalities per year. Winter-precipitation-related vehicle crashes when taking into account indirect fatalities far eclipse fatality totals from other, more prominent weather hazards such as tornadoes, flooding, and hurricanes (Figure 2.16). In addition, 70 percent of fatal crashes occurred during meteorological winter (December through February) with January having the most fatalities and collisions (7805 fatalities and 6912 crashes), and December having the second-most fatalities and crashes (7664 fatalities and 6748 crashes). These months correspond with the height of Alberta clipper system occurrence as found by Thomas and Martin (2007). Another point found by Black and Mote (2015a) is that a large percentage of all winter-related crashes occur during the morning and daytime hours defined as 0600-1859 local time (Figure 2.17). Black and Mote (2015b) also found that winter precipitation leads to a 19 percent increase in crash risk and a 13 percent increase in injury risk, but no significant difference in the relative risk of fatality as compared to dry conditions. The snow and high winds brought by the passage of the Alberta clipper systems are hazardous to transportation and can cause crashes and subsequent impacts over the locations they cross. Alberta clipper systems represent a winter forecasting challenge as they are often difficult to predict more than 12 hours ahead of time in addition to the resulting impacts to road transportation produced (UCAR 2010). Alberta clipper systems can shut down highways with heavy blowing/drifting snow, cause severely restricted visibility, induce dangerously low wind

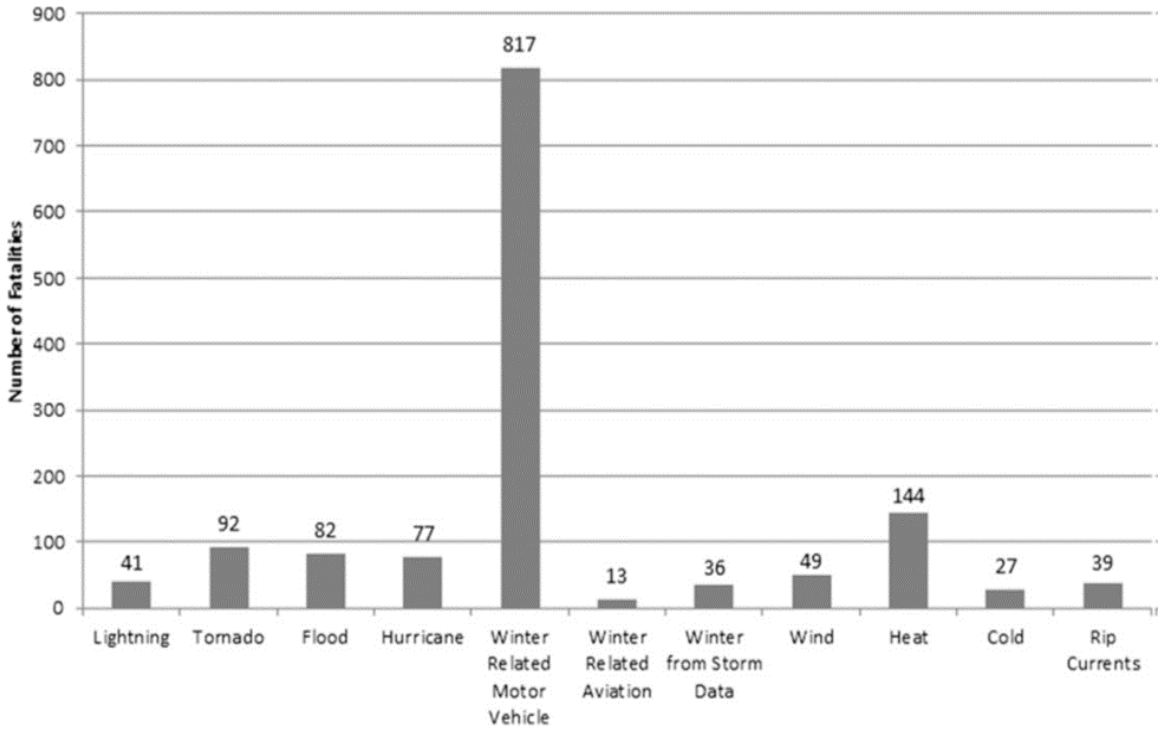

Figure 2.16: Average number of fatalities per year from various meteorological hazards for the period 1996-2011. Totals for all hazards except winter-related motor vehicle and winter-related aviation fatalities are from *Storm Data*. Image credit: Black and Mote (2015a)

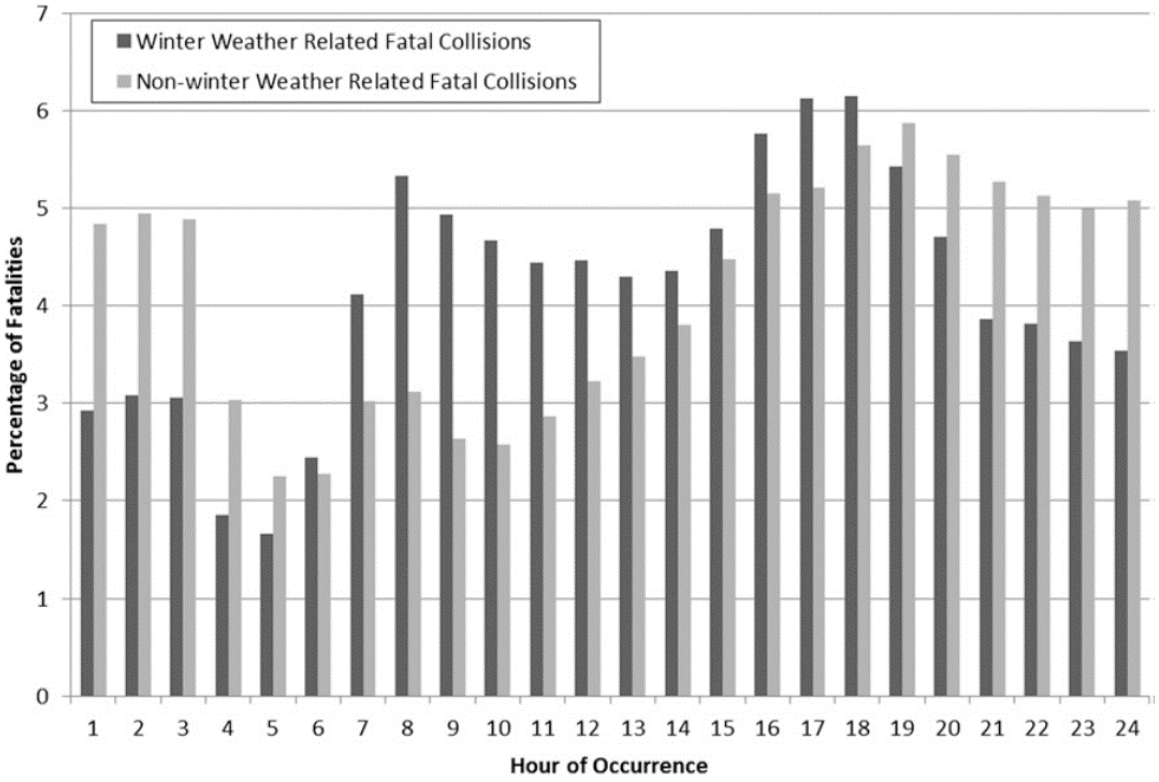

Figure 2.17: Percentage of winter-precipitation-related fatal motor vehicle accidents by hour (dark gray) and nonwinter-related fatal motor vehicle accidents by hour (light gray), 1975-2011. Image credit: Black and Mote (2015a)

chills, and cause slowdowns across all transportation systems (UCAR 2010). Alberta clipper system impacts likely contribute to some of the statistics cited in these studies.

2.3 MDSS and NDOT

Transportation has been adversely affected by weather for centuries. The range of impacts weather brings to various sectors of transportation has ultimately resulted in societal attempts to minimize these impacts. Some early mitigation efforts involving road transportation are well known such as the addition of windshield wipers to vehicles, the invention of mud and snow tires, and the introduction of four-wheel drive, while more recent improvements include concrete grooving for traction and reflective signage for raising visibility on roads (Mahoney and Myers 2003). Recent technological growth and development has allowed for the advancement and applicable use of information systems that integrate data and provide decision support guidance to a broad group of users. Some examples of these systems include the well-known message signs on many interstates and 511 service across many states which aim to inform travelers on weather and road conditions (Mahoney and Myers 2003). Information systems have had and continue to have the ability to address stakeholders and maintenance practitioners in transportation with nearly real time information to help make effective and efficient decisions. However, sometimes there is simply too much information brought to stakeholders and maintenance practitioners which can lead to confusion and difficulties in making effective decisions. For example, having to make a maintenance decision while having to keep in mind regulations concerning chemical applications, environmental impacts, and receiving multiple, weather forecasts can lead to information overload (Pisano et al. 2005). In the late 1990's, as part of its Road Weather Management (RWM) program, the

U.S. Department of Transportation Federal Highway Administration (FHWA) recognized this problem. There was an overall abundance of weather forecasts with several companies issuing road specific forecasts, however, there was a lack of linkage between the information available and the decisions made by winter maintenance managers (Pisano et al. 2005). It was this gap between meteorology and surface transportation which eventually led to the creation of the winter Maintenance Decision Support System (MDSS) (Mahoney and Myers 2003; Pisano et al. 2005).

The creation of MDSS stems back to 2000 when the U.S. FHWA Road Maintenance Management Program began an initiative to gather surface transportation weather decision support requirements from state Department of Transportation (DOT) personnel (Mahoney and Myers 2003). While doing so, it became clear that substantial benefits could be realized if weather forecasts were improved, and became more specific, timelier, and tailored for surface transportation decision makers who are not meteorologists. This resulted in the FHWA undertaking a project in 2001 to develop a conceptual prototype MDSS tailored for winter road maintenance decision makers (Mahoney and Myers 2003). With the program being extended into 2002, a functional prototype of MDSS was released in September of that year with the aid of five national research centers: the Army's Cold Regions Research band Engineering Laboratory (CRREL), the National Science Foundation's National Center for Atmospheric Research (NCAR), Massachusetts Institute of Technology-Lincoln Laboratory (MIT/LL), the National Oceanic and Atmospheric Administration's (NOAA) National Severe Storms Laboratory (NSSL), and the NOAA Forecast Systems Laboratory (FSL) (Mahoney and Myers 2003; Pisano et al. 2005). The development of this project (MDSS Functional

Prototype (FP)) from October 2001 to September 2002 was designed to be a template for future operational capabilities where it was envisioned that the private sector together with local DOTs would review the prototype and jointly develop operational versions of the system whether standalone or integrated with broader decision support systems (Mahoney and Myers 2003; Pisano et al. 2005). The MDSS FP also had a number of goals including demonstrating to the State DOTs that new technologies are available to assist maintenance managers with maintaining safety and mobility on roadways, provide for more efficient use of chemicals, equipment, and staff, and as well as show the private sector road weather providers that there is a market for these new technologies within the states (Pisano et al. 2005). While MDSS FP was made available to the public to aid the process of privatization, the FHWA provided the core MDSS modules to any company or organization using an aggressive technology transfer process with the expectation that MDSS technologies would be further improved and commercialized (Pisano et al. 2005). Following 2002 and the release of MDSS FP, several field demonstrations--2002-2003 and 2003-2004 winters in central Iowa as well as campaigns in Colorado from the winters of 2005-2008--took place to discover what could be improved with MDSS FP (Pisano et al. 2005; Petty and Mahoney 2008). Each field campaign contributed to a number of enhancements and modifications to system components in order to produce a better working MDSS. The key components of the system include: 1) an observation and numerical model data ingest module, 2) a road weather forecast and data fusion system, 3) a road condition and treatment module, and 4) a display system (Figure 2.18). Both MDSS FP and MDSS ingest data from several different numerical models along with real-time observation data. These data are then fed into the Road Weather Forecast

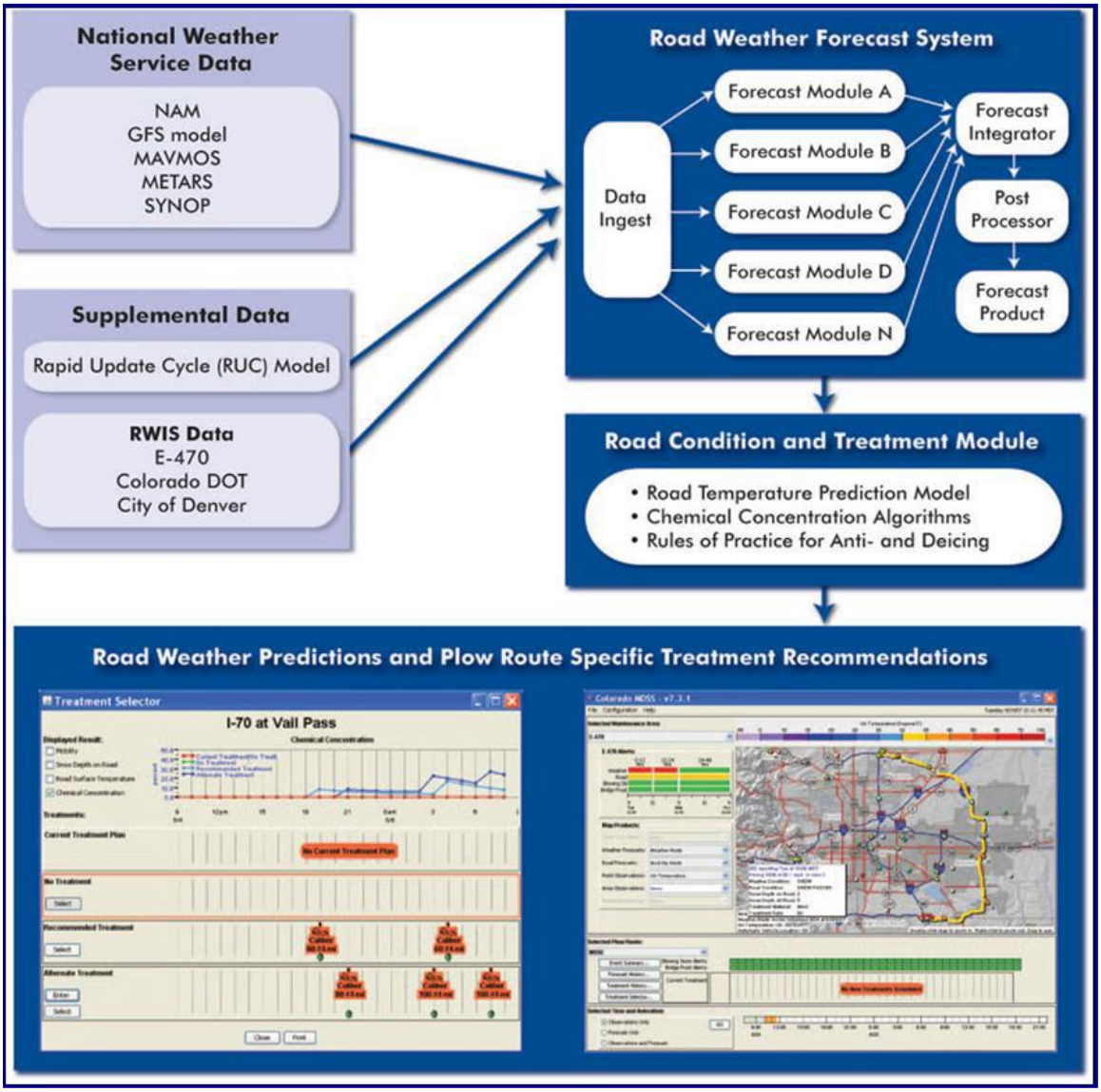

Figure 2.18: Illustration of the MDSS framework during Colorado demonstrations. Image credit: Mahoney and Myers (2008)

System Module (RWFS) module; a proprietary system run by NCAR to generate consensus forecasts (Petty and Mahoney 2008). These consensus forecasts are then passed to the Road Condition and Treatment Module (RCTM) where the forecasts are used to force a one-dimensional energy and mass-balance model to predict the evolution of road and bridge temperatures, as well as the state of roadways (such as dry, wet, snow depth). The condition information is used in conjunction with best practice rules for anti-icing and deicing to formulate treatment recommendations. Data and information are then supplied to users through a graphical user interface (display) and through this interface, maintenance practitioners can examine hourly predictions of road weather conditions out to 48 hours at user-specified locations (Petty and Mahoney 2008). A number of enhancements within these modules have also taken place such as the incorporation of the Model of the Environment and Temperature of Roads (METRo) as part of a sub-module in the RCTM. This is because METRo was found to be superior to two other models which had a warm bias during one of the Colorado field campaigns (Petty and Mahoney 2008). The Rules of Practice Module within the RCTM has also been changed to reflect feedback received from users and a module was added within MDSS to generate short-term weather and road condition alerts. MDSS now has the ability to display gridded products such as radar and satellite data, support dynamic base maps, and allow a user to look at historical forecasts produced by MDSS in the past and archive them (Petty and Mahoney 2008). The overall success of MDSS can be measured by the fact that several private sector companies have begun developing operational versions of the MDSS (Petty and Mahoney 2008). Several private sector companies are still developing operational versions to this day (DTN 2019). While MDSS has come a

long way, one of the drawbacks to its evolution is the privatization of source code and knowledge of the system's inner workings, due to enhancements carried out by private entities. Privatization of source code leads to a “black box” architecture in which users outside of the company are unaware of the inner workings of MDSS. A potential drawback of this is that users of MDSS at a transportation agency, such as NDOT, may not know if MDSS is producing accurate recommendations for the different types of extratropical cyclones which travel through and impact an overseen region.

CHAPTER 3: DATA AND METHODOLOGY PLUS LIMITATIONS

3.1 Data and Methodology

Two case studies involving different winter storm events for Nebraska were selected. NDOT-MDSS keeps a database of saved events for which data can be obtained from previous storms which have impacted Nebraska (DTN 2019). However, due to the proprietary nature of the NDOT-MDSS it is unknown how these events are saved and what the criteria are for saving them. During data obtainment, saved data for Alberta clipper systems were rare. This resulted in two winter weather storms being selected for this study that most resembled Alberta clipper systems. This study had three primary objectives. The first objective was to examine each winter storm that impacted Nebraska during the 2018-2019 winter season and see how well NDOT-MDSS forecasted several meteorological conditions associated with each storm. The second objective was to see how well NDOT-MDSS forecasted various parameters in relation to snowfall for both of the events. The final objective was to compare NDOT-MDSS snowfall accumulations to other numerical weather model forecasts and forecasts generated by the National Weather Service (NWS) and thereafter, compare the two different events.

For examination of both events, understanding the synoptic background environment which lead to the formation and evolution of each Alberta clipper system for each case was of major importance. A top-down analysis was undertaken to accomplish this in both case studies of this project. Upper air analysis at the 300, 500, 700, and 850 hPa levels was conducted along with surface analysis. Upper air maps were obtained from the NWS's Storm Prediction Center (SPC) surface and upper air maps page (SPC 2020) and surface maps were obtained from the NWS's Weather Prediction Center

(WPC) surface analysis archive page (WPC 2020). Analysis of the 300 hPa level reveals jet streak patterns aloft. These jet streaks ultimately lead to the generation of lift and cyclogenesis through upper-level divergence. Trough and ridge patterns at 500 hPa can indicate the movement of high and low pressure systems at the surface, including Alberta clipper systems. The 700 and 850 hPa levels can show if there is moisture available to the system to produce snowfall, show the magnitude and placement of temperature and pressure gradients, and indicate temperature advections. Of course, surface analysis shows the location of the low pressure systems, surface pressure gradients, and gives an idea of where fronts, strong winds, and precipitation are located. For the synoptic overview of the first objective, for each of the case studies, upper air and surface analyses were conducted 24 hours back from the closest set of available observations that occurred before the start of snowfall. This was followed by upper air and surface analyses being conducted during the time in which snowfall occurred and for the next closest observations available after snowfall stopped. Start of the event was defined as the earliest start of snowfall within a one-hour time frame upon just one selected road segment for each event. This earliest start of snowfall upon just one selected road segment was determined by looking at radar returns over segments in NDOT-MDSS. Examining 24 hours back from the closest set of available observations that occurred before snowfall started is consistent which the methodology given in Thomas and Martin (2007). Examining any observations that occurred during snowfall and the closest observations that occurred after the start of snowfall allows for the short impact of these Alberta clipper systems to be analyzed. This examination also shows the progression of cold air, strong wind fields, and further evolution of the Alberta clipper systems as the

low pressure portion of the systems approach the east of the CONUS. Upper air analyses for the 300, 500, 700, and 850 hPa levels were available every 12 hours and surface analyses was available every 3 hours.

In order to understand the forecast ability of NDOT-MDSS for both the remainder of the first objective and the second objective, numerous road segment numerical data were extracted from the NDOT-MDSS saved storm database and user interface display system (DTN 2019). NDOT divides the state of Nebraska into eight separate districts for management and maintenance purposes (Figure 3.1). Road segments were selected for two separate NDOT districts (District 1 and District 2) with a total of five segments selected for each of those districts (Figure 3.2 and Figure 3.3). The selection of the segments was determined by segment proximity to each other and proximity to highway cameras available in NDOT-MDSS. The first case study occurred on 26 January 2019 for the Omaha region which corresponds to NDOT District 2. The exact names of the five segments selected for this case study and what the segments will be referred to is shown by Table 3.1. The second case study occurred on 15 February 2019 for which the Lincoln area was examined which corresponds to NDOT District 1. The five segments selected for this case study and what the segments will be referred to is shown by Table 3.2. Both the Omaha and Lincoln regions encompass relatively populated areas compared to the rest of Nebraska. Analysis of Alberta clipper system impact within these regions for this study provided more useful information which could then be relayed to NDOT. Maintenance operations are of higher priority within these districts.

The NDOT-MDSS saved storm database is spotty and sometimes has incomplete data for each snowfall event. Data are represented with respect to time of day (Local

Figure 3.1: The eight NDOT maintenance districts within the state of Nebraska. Image credit: NDOT (2020)

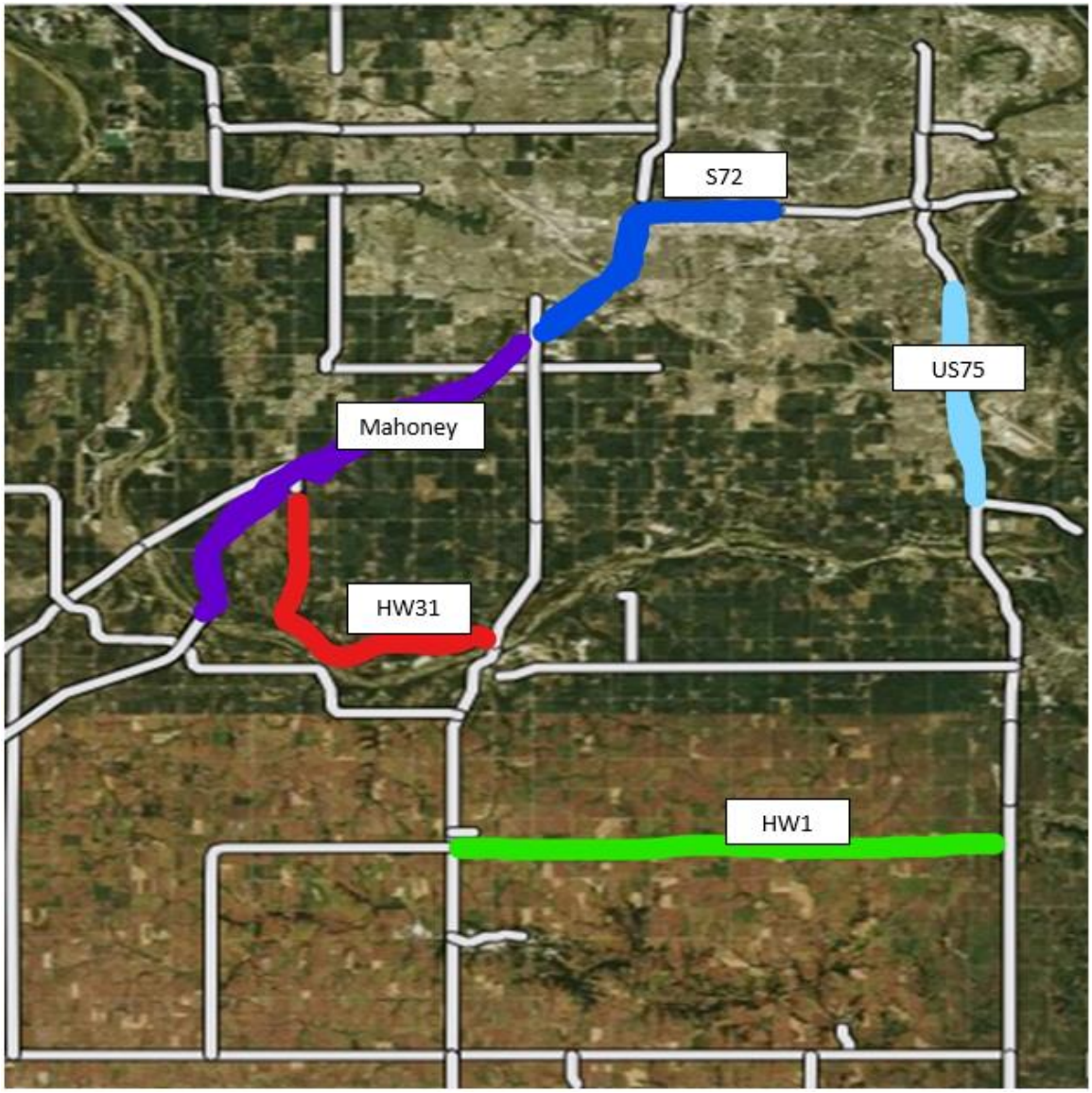

Figure 3.2: A section of NDOT District 2 taken from NDOT-MDSS. S72 is highlighted in blue, Mahoney in violet, HW31 in red, HW1 in green, and US75 in light blue. Image credit: DTN (2019)

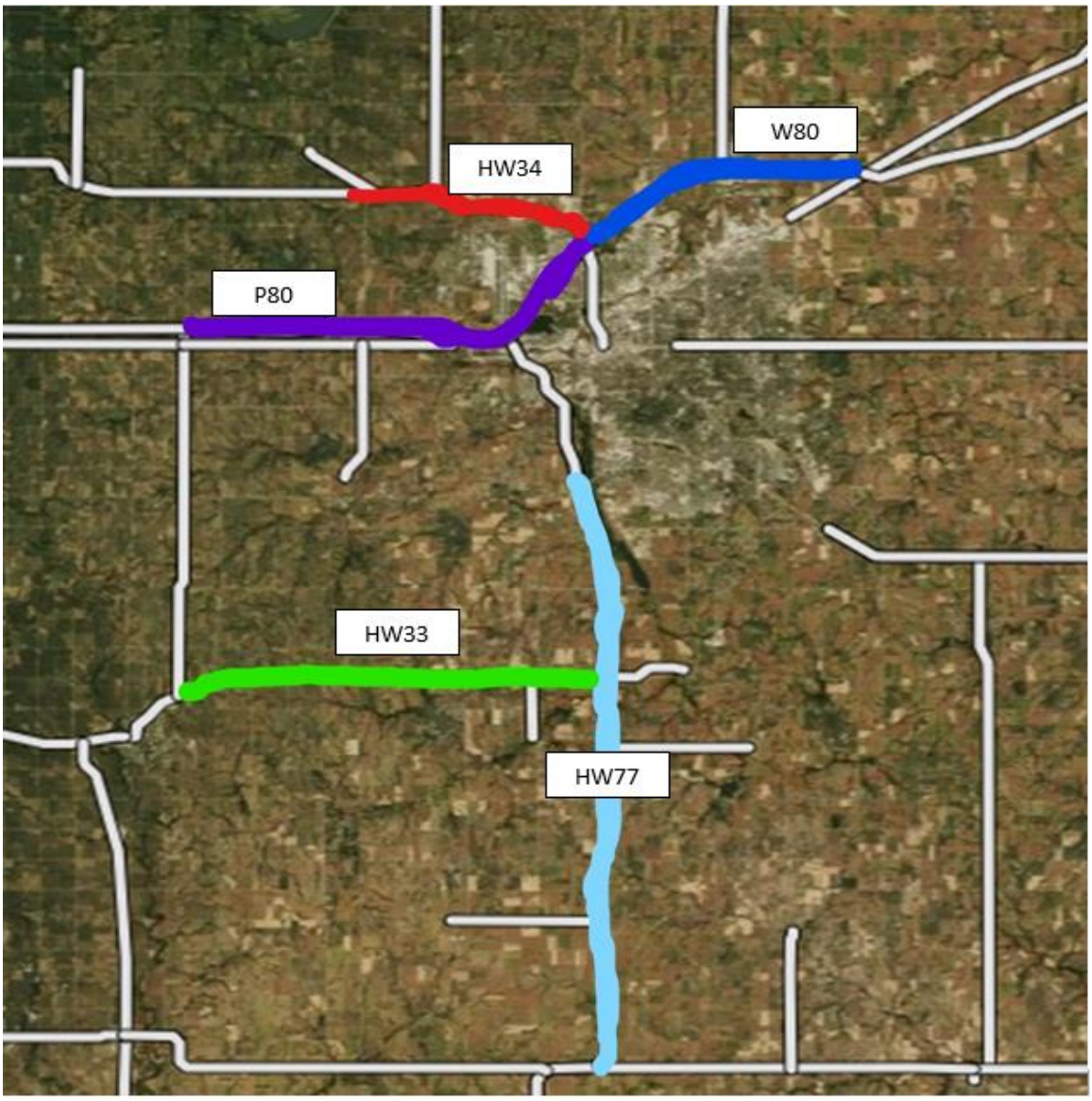

Figure 3.3: A section of NDOT District 1 taken from NDOT-MDSS. W80 is highlighted in blue, P80 in violet, HW34 in red, HW33 in green, and HW77 in light blue. Image credit: DTN (2019)

Table 3.1: The name of the selected road segments from NDOT-MDSS used for the first case study located in NDOT District 2, what the selected road segments will be referred to as, and the snowfall start and end times for each of those segments. MP in the NDOT-MDSS Segment Name column stands for Mile Post.

NDOT-MDSS Segment Name	Referred to as	Snowfall Start	Snowfall End
Hwy1, Jct. Hwy50 to Jct. Hwy34 (MP 12.98 to 26.88)	HW1	0700 UTC	1200 UTC
Hwy31, Hwy50 to I-80	HW31	0700 UTC	1200 UTC
I-80, Mahoney Interchange to Hwy50 (MP 426.26 - 440.66)	Mahoney	0700 UTC	1200 UTC
I-80, Hwy 50 to 72nd Street Interchange (MP 440.66 - 449.27)	S72	0700 UTC	1200 UTC
US75, Jct Hwy34 to Hwy US275	US75	0800 UTC	1200 UTC

Table 3.2: The name of the selected road segments from NDOT-MDSS used for the second case study located in NDOT District 1, what the selected road segments will be referred to as, and the snowfall start and end times for each of those segments.

NDOT-MDSS Segment Name	Referred to as	Snowfall Start	Snowfall End
I-80, Pleasant Dale Interchange to I-80 Interchange	P80	1300 UTC	2200 UTC
Hwy 34, Malcolm to Lincoln	HW34	1300 UTC	2200 UTC
Hwy 80, Lincoln to Waverly	W80	1300 UTC	2200 UTC
US77, Jct. 41 to 155w	HW77	1200 UTC	2100 UTC
33, Crete to #77 mp 13 to 25	HW33	1200 UTC	2100 UTC

Standard Time) and date in which the user can scroll to get model data for a specific hour within the saved timeframe. However, sometimes start and end times randomly occur during saved storm events. For the first case study, snowfall begins at 1:00 am LST 26 January 2019 for all routes except US75 which begins at 2:00 am LST 26 January 2019. Snowfall ends for all the routes by 6:00 am LST 26 February 2019 (Table 3.1). Saved storm data for this event were available from 4:30 pm LST 25 January (2230 UTC 25 January) until 5:50 pm LST 27 January 2019 (2350 UTC 27 January 2019). Since NDOT-MDSS data are represented in the timeframe of hours, data that were extracted from the web interface were only at complete hourly intervals of 5:00 pm LST 25 January (2300 UTC 25 January) until 5:00 pm LST 27 January 2019 (2300 UTC 27 January 2019). For the second case study snowfall begins at 6:00 am LST 15 February 2019 for HW33 and HW77 and 7:00 am LST 15 February 2019 for P80, W80, and HW34. Snowfall ends 3:00 pm LST 15 February 2019 for HW33 and HW77 and 4:00 pm LST 15 February 2019 for P80, W80, and HW34 (Table 3.2). Saved storm data for this event were available from 6:00 pm LST 14 February (0000 UTC 15 February) until 11:50 am LST 18 February 2019 (17:50 UTC 18 February 2019). For the second part of the first objective, from this interface, several forecasted meteorological variables were extracted. This included temperature, dewpoint temperature, and wind speed. For both case studies, 3, 6, 9, and 12 hourly forecast data containing these meteorological variables were extracted from the NDOT-MDSS saved storm dataset, if available. The data were compared with the nearest Automated Surface Observing System (ASOS) observations for the time of observed snowfall during the event. For the first case study ASOS data from the Eppley Airfield (KOMA) were used, while for the second case study

ASOS data from the Lincoln Municipal Airport (KLNK) were used. For the second objective parameters pertaining to snowfall, including snowfall start, snowfall end, snowfall event length, and snowfall accumulation were extracted. For a given route, snowfall start was defined as the first hour before snowfall rate increased above 0.0 inches/hr (0.0 cm/hr) within NDOT-MDSS, snowfall end was defined as the first hour snowfall rate fell to 0.0 inches/hr (0.0 cm/hr) within NDOT-MDSS, snowfall event length was defined as the difference between snowfall end and snowfall start time in NDOT-MDSS, and snowfall accumulation was defined as the amount of accumulated snowfall within NDOT-MDSS between the hour after snowfall rate increased above 0.0 inches/hr (0.0 cm/hr) and the hour after the snowfall rate fell to 0.0 inches/hr (0.0 cm/hr) for which snowfall accumulation did not increase further. Data were compared with snowfall observations recorded at KOMA for the first case study and KLNK for the second case study.

For the final objective, NDOT-MDSS model output snowfall accumulation data were compared to other numerical model snowfall accumulation output data and forecasts made by the NWS (Iowa State University (ISU) 2020b). Snowfall accumulation forecasts were compared with the Rapid Refresh version 4 (RAP), the 12 km North American Mesoscale model version 4 (NAM), the 4 km North American Mesoscale model (NAM 4km), the Global Forecast System version 14 (GFS), and a derived model average of these four numerical models. Hourly data obtained for these numerical models were retrieved from an archive maintained by ISU (ISU 2020a). Following this comparison, a brief discussion was undertaken that compares the differences between

these two case studies in terms of the synoptic environment associated with the formation of each Alberta clipper system and NDOT-MDSS model output for each event.

3.2 Limitations

Despite the history of MDSS stemming from an open source and multi-disciplinary collaboration, the current version of MDSS utilized for this study, NDOT-MDSS, is closed-source software and owned privately. Due to the proprietary nature of the system, several limitations occurred when completing this project. First, it was unknown what the criteria were for storm data being saved in the system and what the process was to save the data. Saved storm data within the system were not always available going back for an amount of time needed for a forecast or an overall analysis of an event. In some saved storm cases, data were available going back at least 12 hours before an event start time while in other cases this was not so. In addition, Alberta clipper system occurrence in Nebraska is rare compared with that of the Colorado low system; less than 10 percent of Alberta clipper systems track south of the Great Lakes (Thomas and Martin 2007). This made selection of Alberta clipper systems to conduct analysis on extremely limited due to an overall lack of saved storm data involving Alberta clipper systems. This limitation was likely only further enhanced by the fact that Alberta clipper systems tend to be less impactful than their Colorado low system counter parts regarding snowfall. If event data were saved based on snowfall impact, then it stands to reason why the number of Alberta clipper system saved events within NDOT-MDSS were lower. Another limitation was that it is unclear exactly how snowfall accumulations, maintenance recommendations, and other parameters are computed within the NDOT-MDSS since obtaining a copy of the system's source code was not possible.

Verification of the accuracy of what NDOT-MDSS was forecasting was extremely limited and relied solely on nearest meteorological observations recorded at the closest airports, which may have not been representative of each road segment chosen to be analyzed. This is because segments are different in length within NDOT-MDSS and each road segment is a different distance from the airport where observations are recorded. Observed conditions may not be representative for a road segment which is sometimes miles away or representative of a road segment which spans several miles, as the observation acts as a single point rather than the entirety of a domain.

CHAPTER 4: RESULTS

4.1 Case Study I: 26 January 2019

4.1.1 Synoptic Analysis:

The 26 January 2019 case study event is an Alberta clipper system that impacts the Omaha region with snow from approximately 1:00 am to 6:00 am LST 26 January 2019 (0700 to 1200 UTC 26 January 2019). This Alberta clipper system had light snowfall which largely impacted road transportation within District 2 (Figure 3.1 and Figure 3.2). Synoptic conditions from 6:00 pm LST 24 January 2019 (0000 UTC 25 January 2019) through 6:00 am LST 26 January 2019 (1200 UTC 26 January 2019) are analyzed. This timeframe of analysis was based on an event start time of 1:00 am LST 26 January 2019 (0700 UTC 26 January 2019) for most of the road segments chosen in District 2. An event start time was defined as the hour in which snowfall fell upon the segment. At 6:00 pm LST 24 January 2019 (0000 UTC 25 January 2019), 300 hPa analysis reveals a large portion of the jet stream over the CONUS (Figure 4.1). A split in the jet stream into two separate streaks is noted over the Great Plains, Northern Rocky Mountains region of the CONUS, and Canada. Another strong jet streak is noted over the Southeast and another over the Northeast. At 500 hPa the large portion of the jet stream noted corresponds to a longwave trough over the CONUS with a small embedded shortwave over the desert Southwest (Figure 4.1). The 700 and 850 hPa analysis reveals very cold and dry northwesterly flow from Canada over much of the Great Plains (Figure 4.1). By 6:00 am LST 25 January 2019 (1200 UTC 25 January 2019), the longwave trough pattern over the CONUS remains similar (Figure 4.2). Over the northeastern United States the jet streak has amplified and become stronger while dry northwesterly

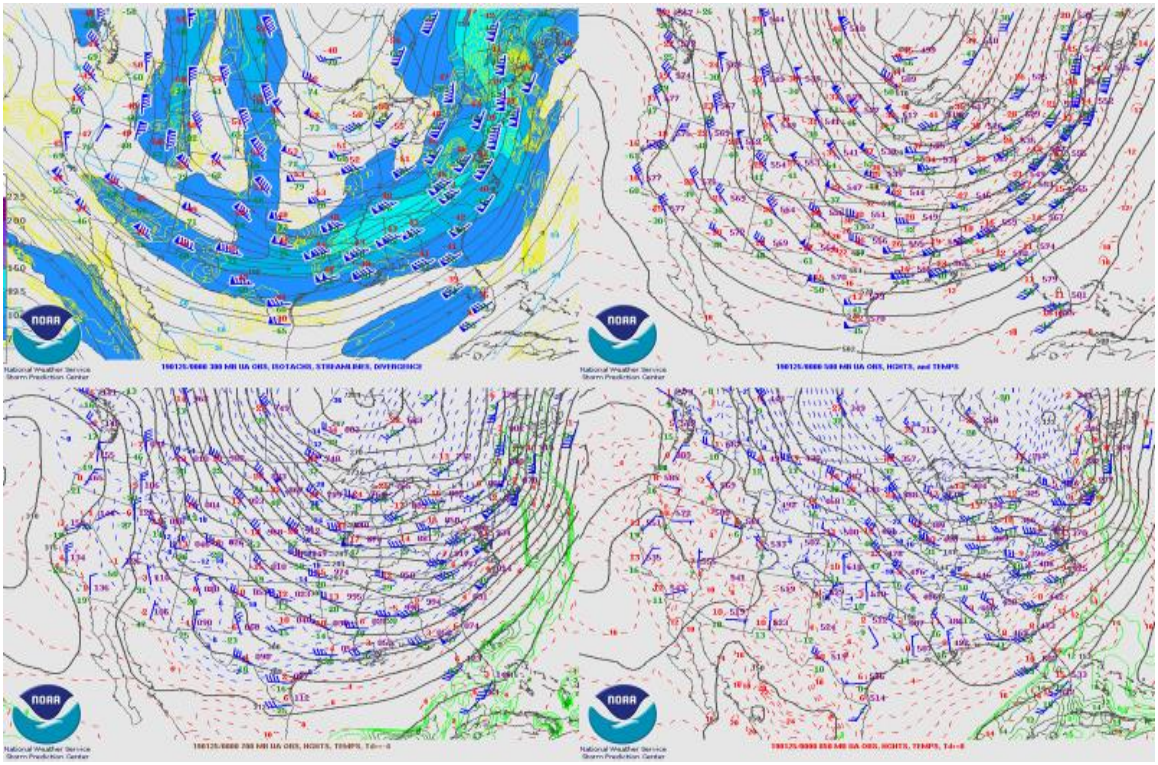

Figure 4.1: 300 hPa analysis (top left), 500 hPa analysis (top right), 700 hPa analysis (bottom left), 850 hPa analysis (bottom right) at 0000 UTC 25 January 2019. Image credits: SPC (2020)

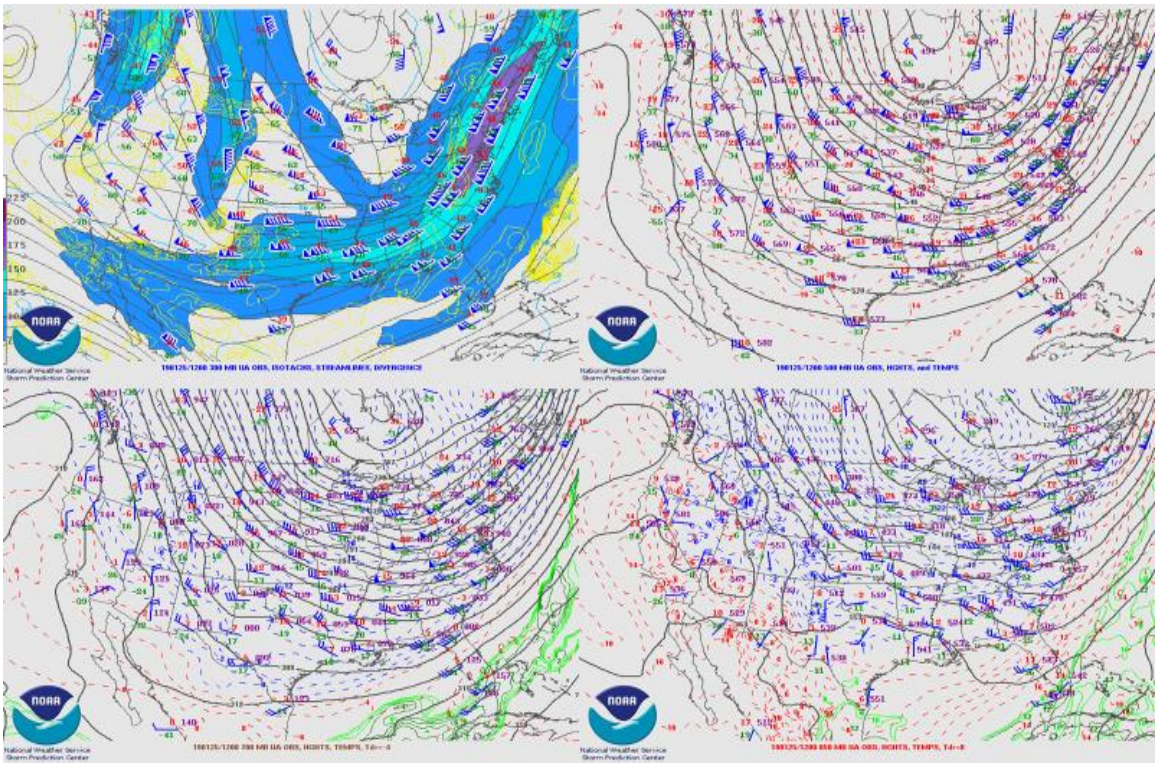

Figure 4.2: 300 hPa analysis (top left), 500 hPa analysis (top right), 700 hPa analysis (bottom left), 850 hPa analysis (bottom right) at 1200 UTC 25 January 2019. Image credits: SPC (2020)

flow remains over the Great Plains. At 6:00 pm LST 25 January 2019 (0000 UTC 26 January 2019) 300 hPa analysis reveals that another jet streak appears to form over Alberta, Canada while 500, 700, and 850 hPa patterns remain fairly consistent (Figure 4.3). This jet streak is rather strong with isotachs reaching at least 150 knots (77.2 m/s). It should be noted that, the left exit region of this streak at this time is located over North Dakota and southern Canada. The left exit region promotes divergence aloft which can aid the development of a low pressure system by enhancing surface convergence. This divergence from this streak in the 300 hPa analysis can be even better seen by 6:00 am LST 26 January 2019 (1200 UTC 26 January 2019) while the 500, 700, and 850 hPa analysis remains fairly consistent through time (Figure 4.4).

Moving to surface analyses, more of a consistent picture can be created. Surface analyses are available at 3 hourly intervals within upper air analysis times. At 6:00 pm LST 24 January 2019 (0000 UTC 25 January 2019) a strong surface high pressure system dominates the Great Plains with a strong low pressure system over New England and a pronounced cold front stretching eastward from Colorado to the Great Lakes region (Figure 4.5). As time progresses the high pressure system over the Great Plains moves southeastward along with a cold front as the strong low pressure system over New England begins to exit into the Canadian Maritimes. Surface analysis reveals that by 9:00 pm LST 24 January 2019 (0300 UTC 25 January 2019) there is an Alberta clipper system over southern Alberta that begins pushing southeastward with time (Figure 4.5). The second surface analysis time, 6:00 am LST 25 January 2019 (1200 UTC 25 January 2019), shows the movement of another, unrelated Alberta clipper system over the Great Plains with a large high pressure system noted to the north of its frontal boundaries by

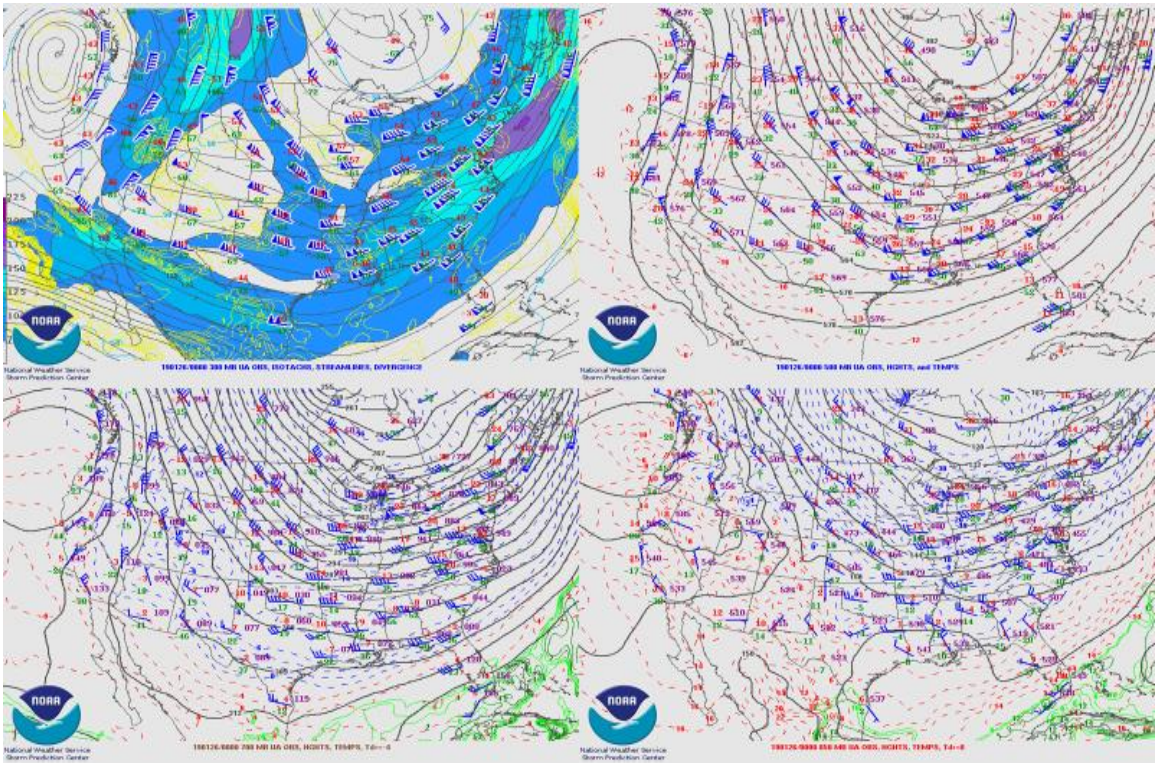

Figure 4.3: 300 hPa analysis (top left), 500 hPa analysis (top right), 700 hPa analysis (bottom left), 850 hPa analysis (bottom right) at 0000 UTC 26 January 2019. Image credits: SPC (2020)

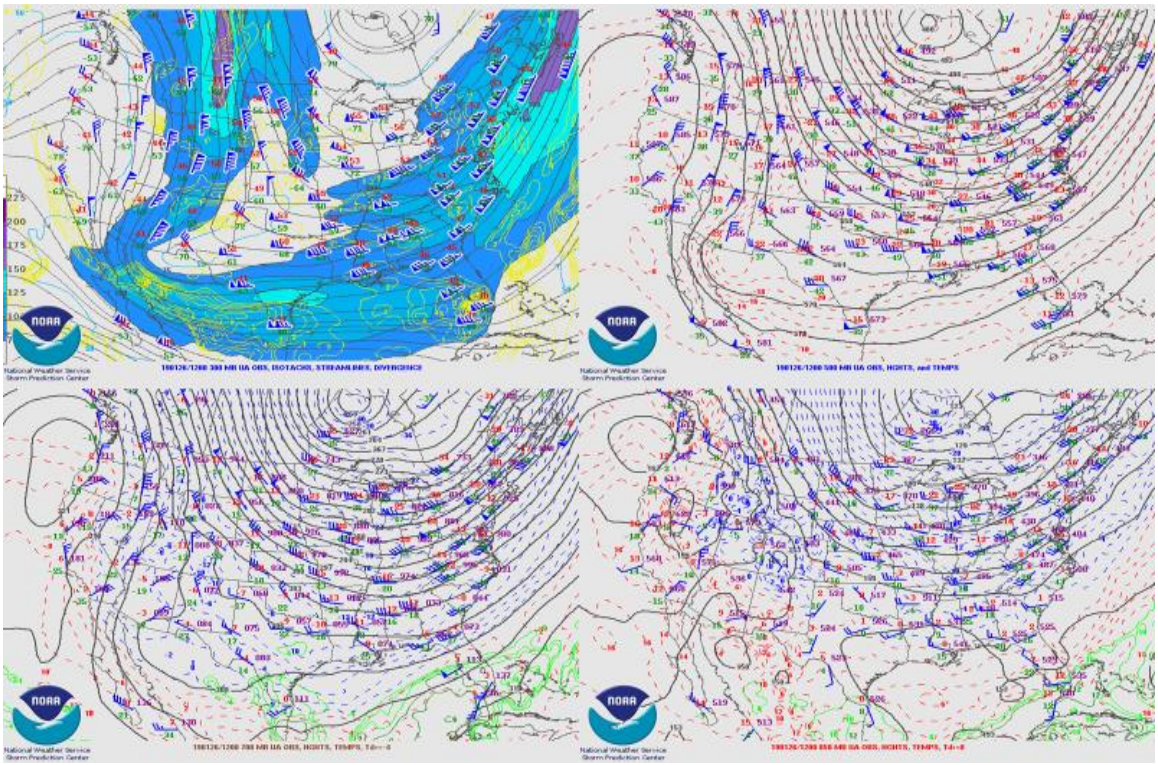

Figure 4.4: 300 hPa analysis (top left), 500 hPa analysis (top right), 700 hPa analysis (bottom left), 850 hPa analysis (bottom right) at 1200 UTC 26 January 2019. Image credits: SPC (2020)

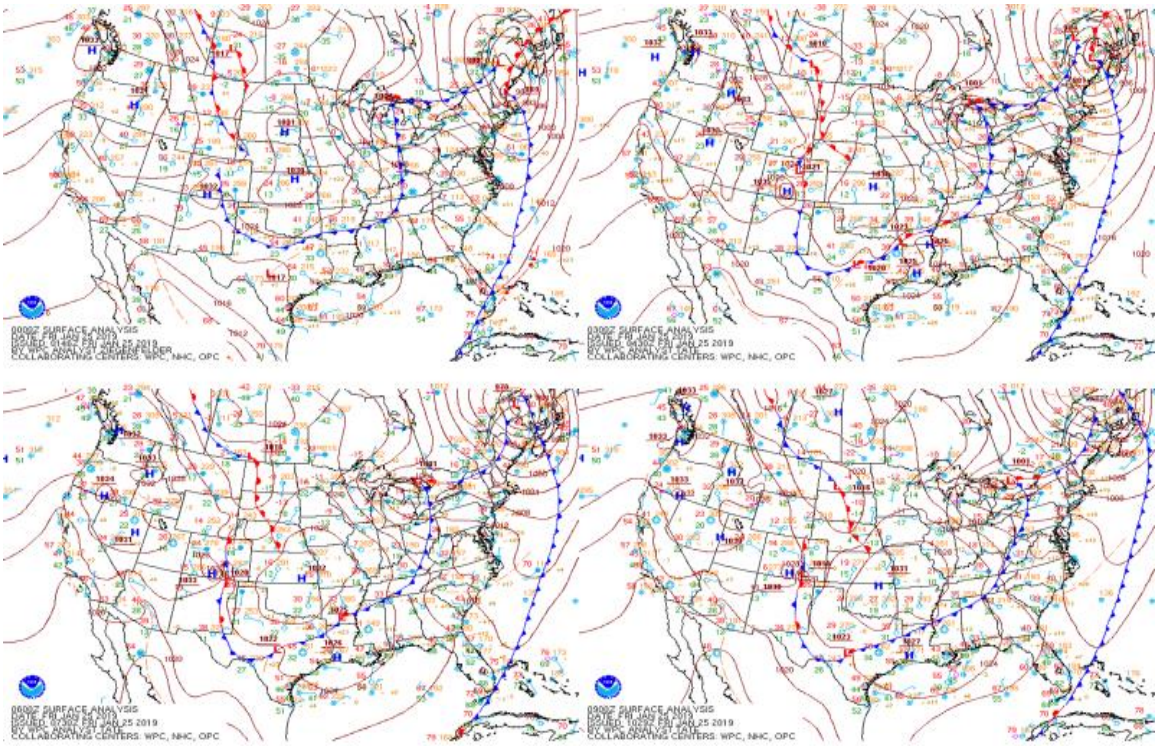

Figure 4.5: Surface analysis at 0000 UTC (top left), 0300 UTC (top right), 0600 UTC (bottom left), 0900 UTC (bottom right) on 25 January 2019. Image credits: WPC (2020)

6:00 am LST 25 January 2019 (1200 UTC 25 January 2019) (Figure 4.6). This weak low pressure system appears to dissipate over time as the high continues to move southward from 9:00 am to 3:00 pm LST 25 January 2019 (1500 to 2100 UTC 25 January 2019). By 6:00 pm LST 25 January 2019 (0000 UTC 26 January 2019) the surface features associated with the Alberta clipper system that cause snowfall for the Omaha region can finally be seen (Figure 4.7). By 12:00 am LST 26 January 2019 (0600 UTC 26 January 2019) an Alberta clipper system is present to the east of Alberta with a long warm front over the Great Plains to the southeast of the cyclone and a stationary front to the cyclone's northwest. The long warm front is likely the mechanism which begins to bring precipitation to the Omaha region at 1:00 am LST 26 January 2019 (0700 UTC 26 January 2019) for the selected segments. By 6:00 am LST 26 January 2019 (1200 UTC 26 January 2019) the Alberta clipper system center can be seen clearly over North Dakota (Figure 4.7). As the system progresses with time, a more familiar frontal structure associated with an Alberta clipper system begins to manifest. A pronounced cold front can be seen trailing the system (Figure 4.8). A warm front to the southeast associated with warm air advecting from the south can be seen on surface analysis. These surface analyses reiterate that Alberta clipper systems are fast moving systems. In this case; however, there is certainly not a strong pressure gradient between the low and trailing anticyclone, which is uncommon for a typical Alberta clipper system.

4.1.2 NDOT-MDSS Analysis:

In order to analyze this case study for the rest of the first objective, the meteorological parameters of temperature, dewpoint temperature, and wind speed, are attempted to be analyzed at 3-, 6-, 9-, and 12-hour prior intervals within NDOT-MDSS

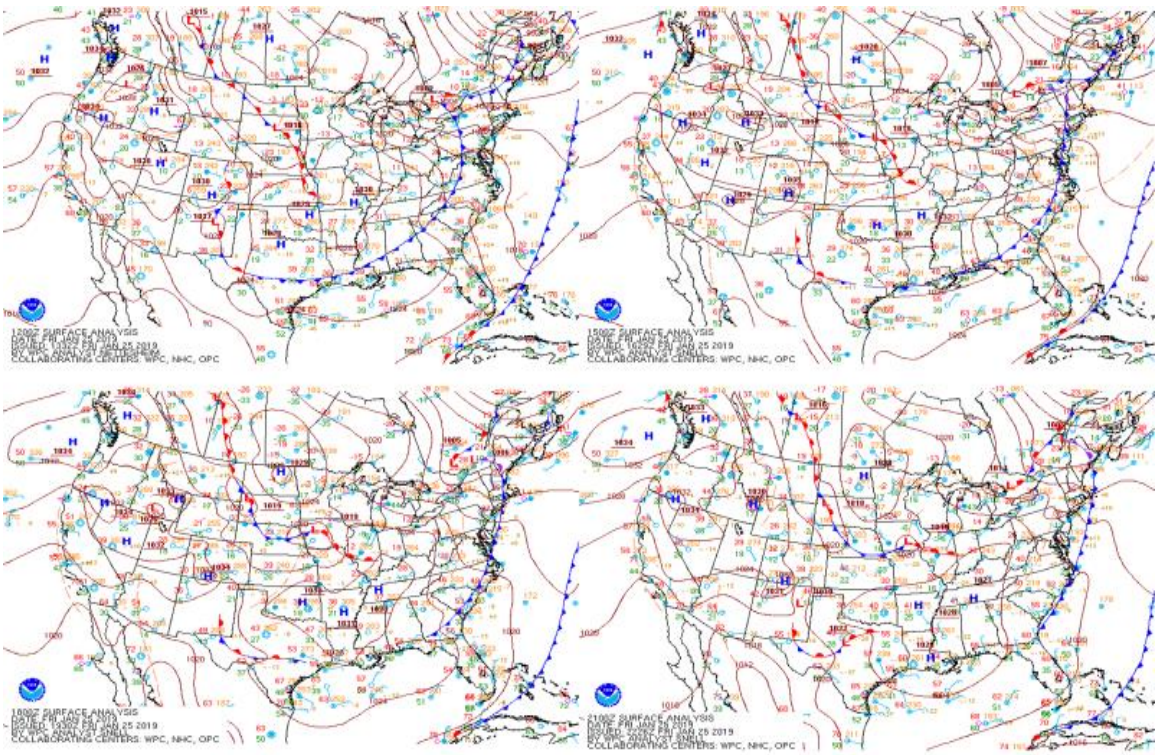

Figure 4.6: Surface analysis at 1200 UTC (top left), 1500 UTC (top right), 1800 UTC (bottom left), 2100 UTC (bottom right) on 25 January 2019. Image credits: WPC (2020)

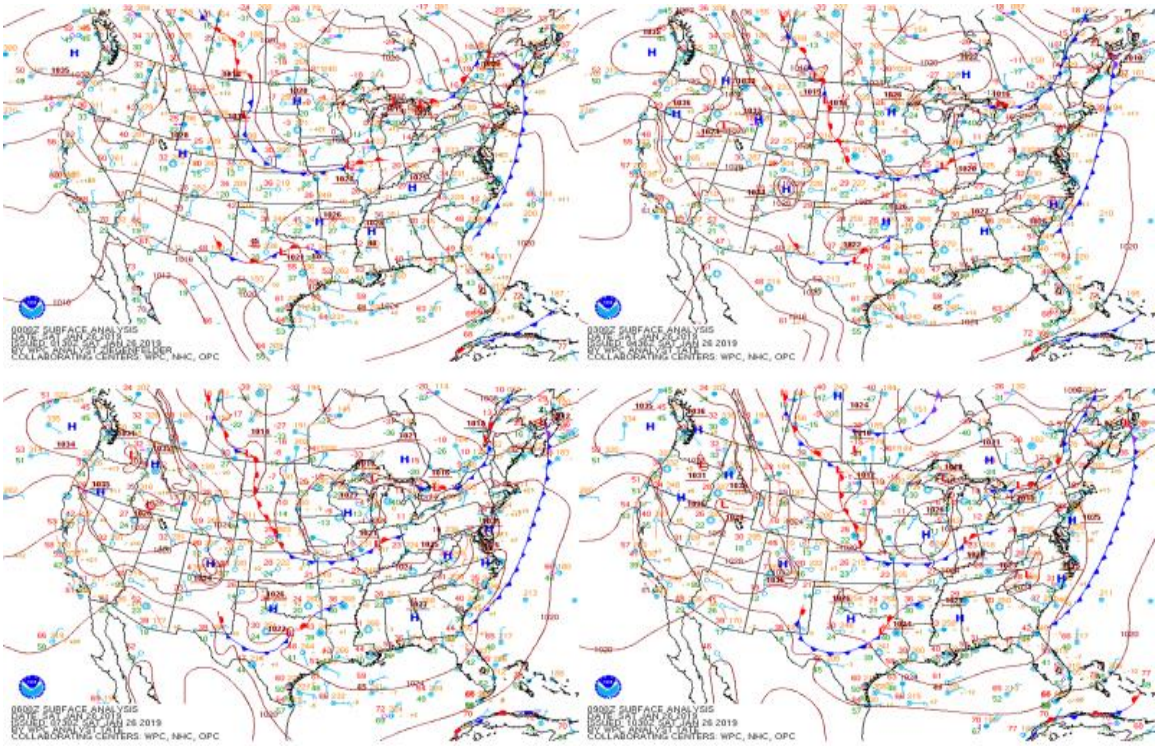

Figure 4.7: Surface analysis at 0000 UTC (top left), 0300 UTC (top right), 0600 UTC (bottom left), 0900 UTC (bottom right) on 26 January 2019. Image credits: WPC (2020)

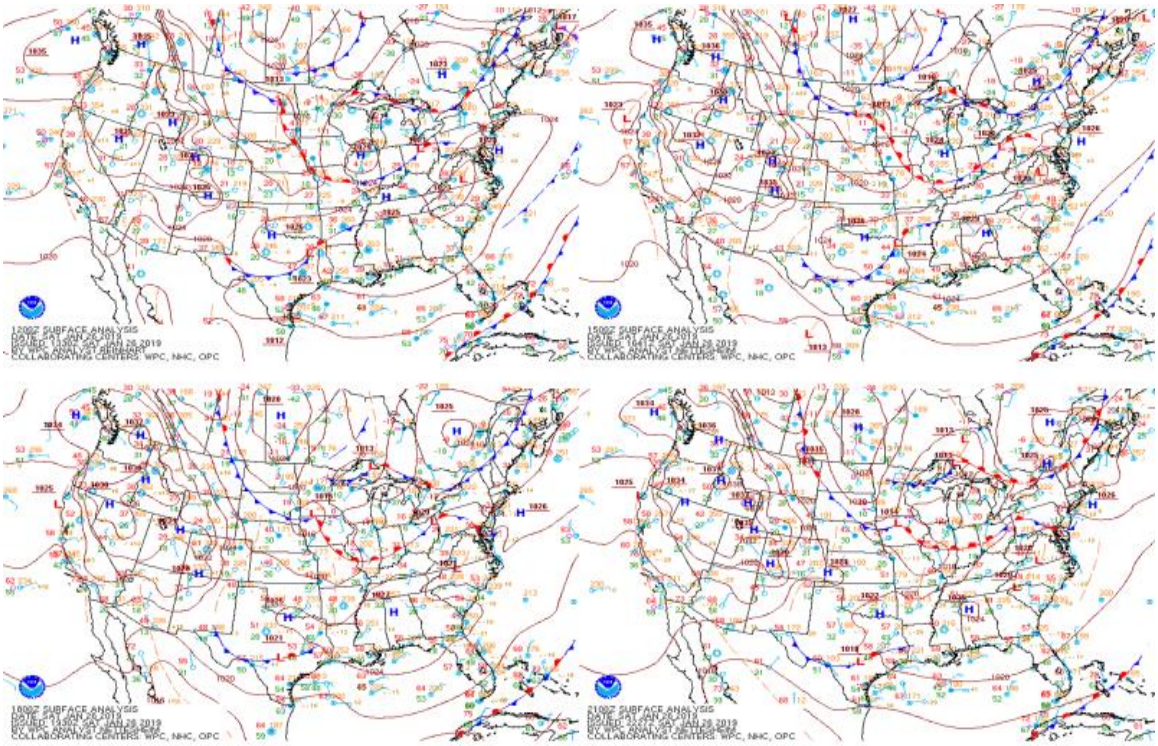

Figure 4.8: Surface analysis at 1200 UTC (top left), 1500 UTC (top right), 1800 UTC (bottom left), 2100 UTC (bottom right) on 26 January 2019. Image credits: WPC (2020)

and compared to the nearest observed values from the ASOS at KOMA. For the second objective hourly forecasts for snow conditions from the NDOT-MDSS are obtained and analyzed for each event. When beginning to conduct this analysis the first limitation of NDOT-MDSS shows up for this saved storm case. Data were only saved in the system from 4:30 pm LST 25 January 2019 (22:30 UTC 25 January 2019) until 5:50 pm LST 27 January 2019 (2350 UTC 25 January 2019), making it not possible to retrieve data for 9 and 12 hours prior to the onset of snowfall upon the selected roadway segments. Analysis had to be completed using what data were available.

Overall air temperature forecasts from the NDOT-MDSS are consistently low compared to ASOS observed values for both 3 and 6 hours prior to the onset of snowfall. (Figure 4.9). NDOT-MDSS forecasts for routes are closer to ASOS observed temperatures 3 hours prior than 6 hours prior. As time approaches the start of snowfall it appears that in every case forecasts for each segment either improve towards observed ASOS values or remain consistent. There are several times in which NDOT-MDSS does predict the observed temperature for the road segments Mahoney, HW1, HW31, and US75 (Figure 4.10). It is only for S72 in which NDOT-MDSS does not predict an observed temperature at any time. For road segments Mahoney, HW1, and HW31, NDOT-MDSS temperature forecasts improve for the start of snowfall hour for the 3-hour forecast but then generally revert back to what was being forecast in the 6-hour forecast. For S72. NDOT-MDSS forecasted temperatures do not vary at all between the 3 and 6 hourly forecasts. The biggest departure difference occurs for US75 and S72 which is 4.0 °F (2.2 °C) with the smallest departure being 0.0 °F (0.0 °C). The minimum and maximum temperature observed by ASOS was 13 °F (-10.6 °C) and 14 °F (-10.0 °C)

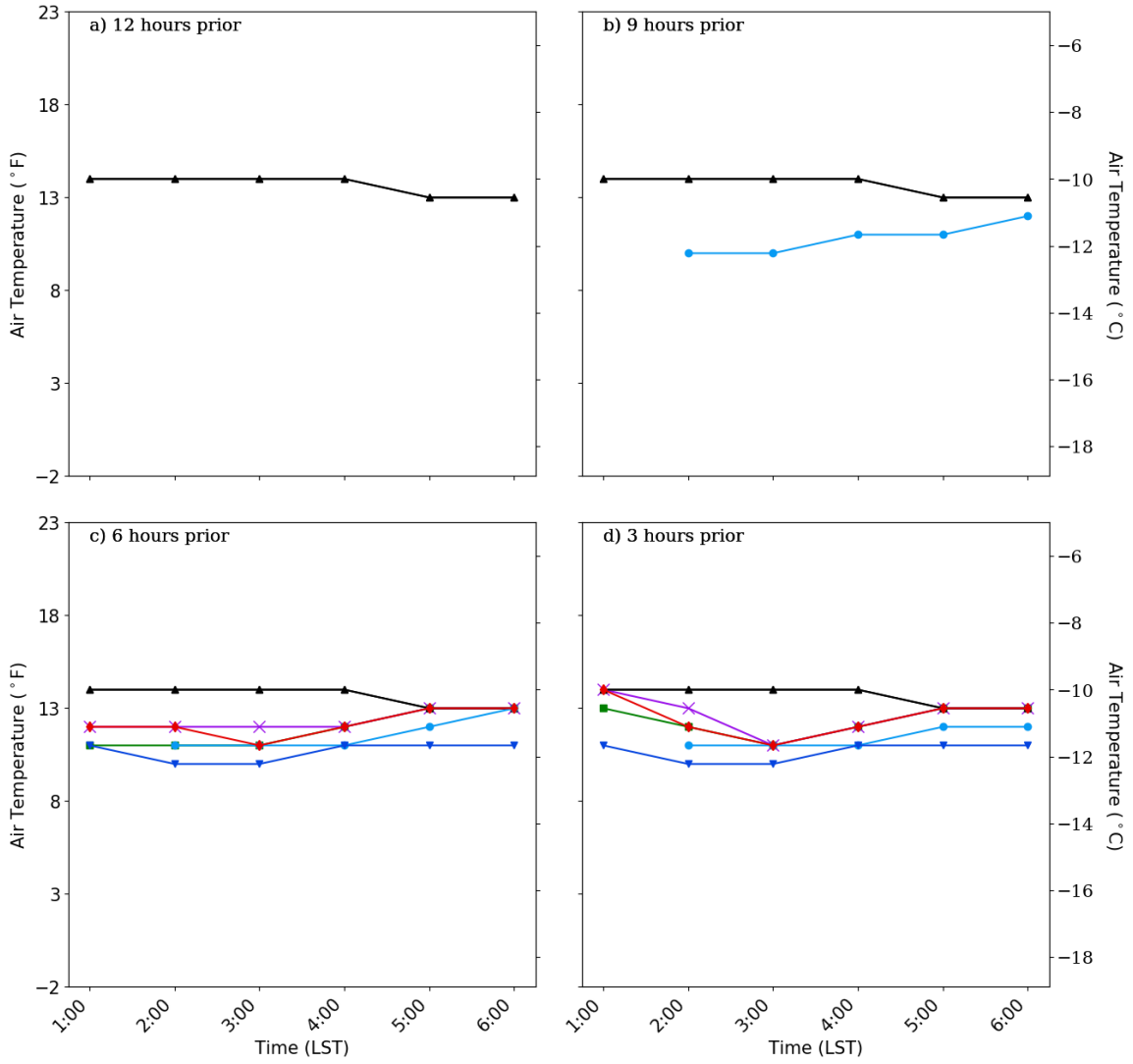

Figure 4.9: 26 January 2019 hourly temperature forecasted by NDOT-MDSS at (a) 1:00 pm LST 25 January 2019 forecast run (12 hours prior to snowfall start (earliest time upon any segment), (b) 4:00 pm LST forecast run (9 hours prior to snowfall start), (c) 7:00 pm LST forecast run (6 hours prior to snowfall start), and (d) 10:00 pm LST forecast run (3 hours prior to snowfall start) for Mahoney (violet), S72 (blue), HW31 (red), HW1 (green), and US75 (light blue) compared to ASOS observed (black). Date and time run from the start of snowfall to the end of snowfall.

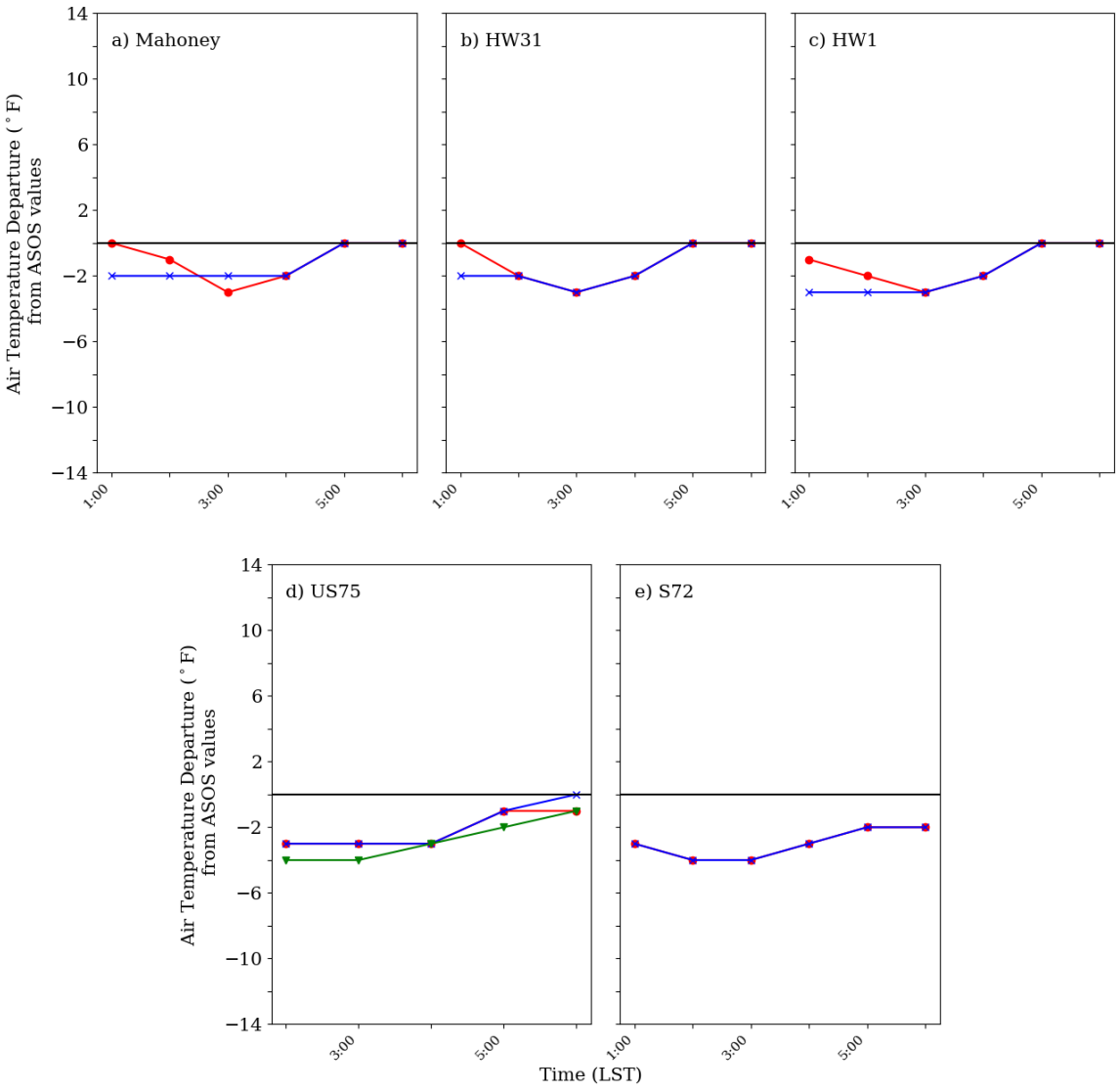

Figure 4.10: NDOT-MDSS forecasted temperature departure for 26 January 2019 from the observed ASOS values at (a) Mahoney, (b) HW31, (c) HW1, (d) US75, and (e) S72 for 3 hours (red), 6 hours (blue), 9 hours (green), 12 hours (black) prior to snowfall onset. The solid horizontal black line denotes zero departure from ASOS.

respectively. The minimum temperature forecasted by NDOT-MDSS for any of the segments was for S72 which was 10 °F (-12.2 °C). The maximum forecasted for any of the segments was for Mahoney which was 14 °F (-10.0 °C). Based on these temperatures and departures NDOT-MDSS forecasts for temperature are well forecasted with no major errors occurring. It appears NDOT-MDSS had a good handle on temperatures during the event but may have had a slight cold bias in this situation.

Dewpoint temperature forecasts from NDOT-MDSS are consistently too low compared to observed values for both 3 and 6 hours prior to the onset of snowfall and are sometimes too high when compared to observed dewpoint temperatures (Figure 4.11). Dewpoint temperatures forecasts remain too high at the start of snow and just near the end of snowfall for HW1. During snowfall dewpoint temperatures remain consistently under-forecasted for all segments. For Mahoney, S72, and HW31, NDOT-MDSS forecasts for dewpoint temperatures are 1 °F (0.7 °C) too warm at the first hour of snowfall. Forecasts for HW1 are also too warm at the start of snowfall and then are too warm again at the last two hours of snowfall by 1 °F (0.7 °C). For all other segments and times in general, the dewpoint temperature is under-forecasted. The biggest dewpoint temperature departure occurs for forecasts made by NDOT-MDSS for Mahoney with a difference of -3 °F (-1.7 °C) at 4:00 am LST 26 January 2019 (1000 UTC 26 January 2019) (Figure 4.12). The minimum and maximum dewpoint temperature observed was 6 °F (-14.4 °C) and 9 °F (-12.8 °C) respectively. The minimum dewpoint temperature forecasted for any of the segments by NDOT-MDSS was for S72 which was 5 °F (-15.0 °C) during the 3-hour forecast. The maximum forecasted dewpoint temperature for any of the segments was for HW1 which was 10 °F (-12.2 °C) which occurred both

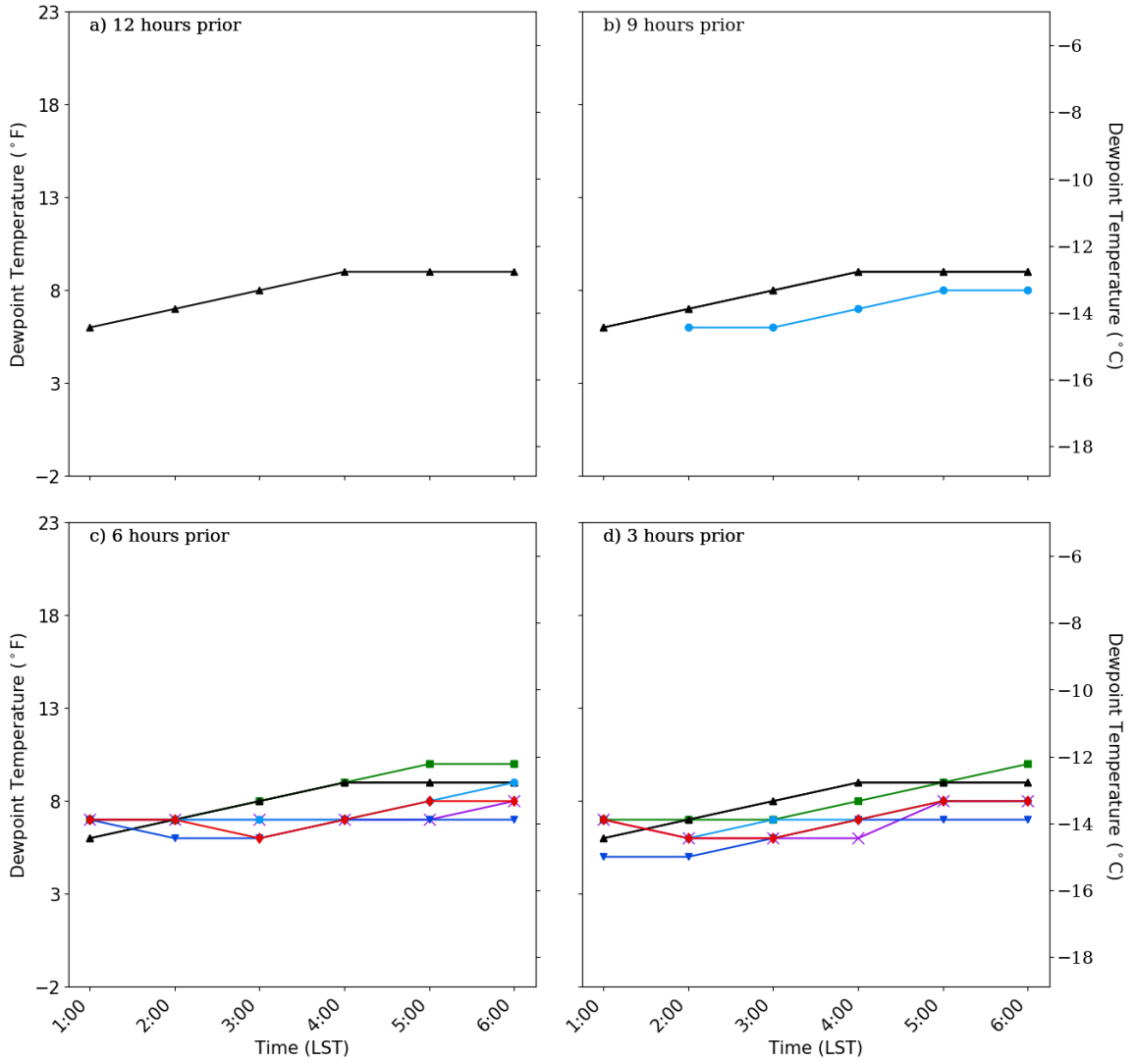

Figure 4.11: 26 January 2019 dewpoint temperature forecasted by NDOT-MDSS at (a) 1:00 pm LST 25 January 2019 forecast run (12 hours prior to snowfall start (earliest time upon any segment), (b) 4:00 pm LST forecast run (9 hours prior to snowfall start), (c) 7:00 pm LST forecast run (6 hours prior to snowfall start), and (d) 10:00 pm LST forecast run (3 hours prior to snowfall start) for Mahoney (violet), S72 (blue), HW31 (red), HW1 (green), and US75 (light blue) compared to ASOS observed (black). Date and time run from the start of snowfall to the end of snowfall.

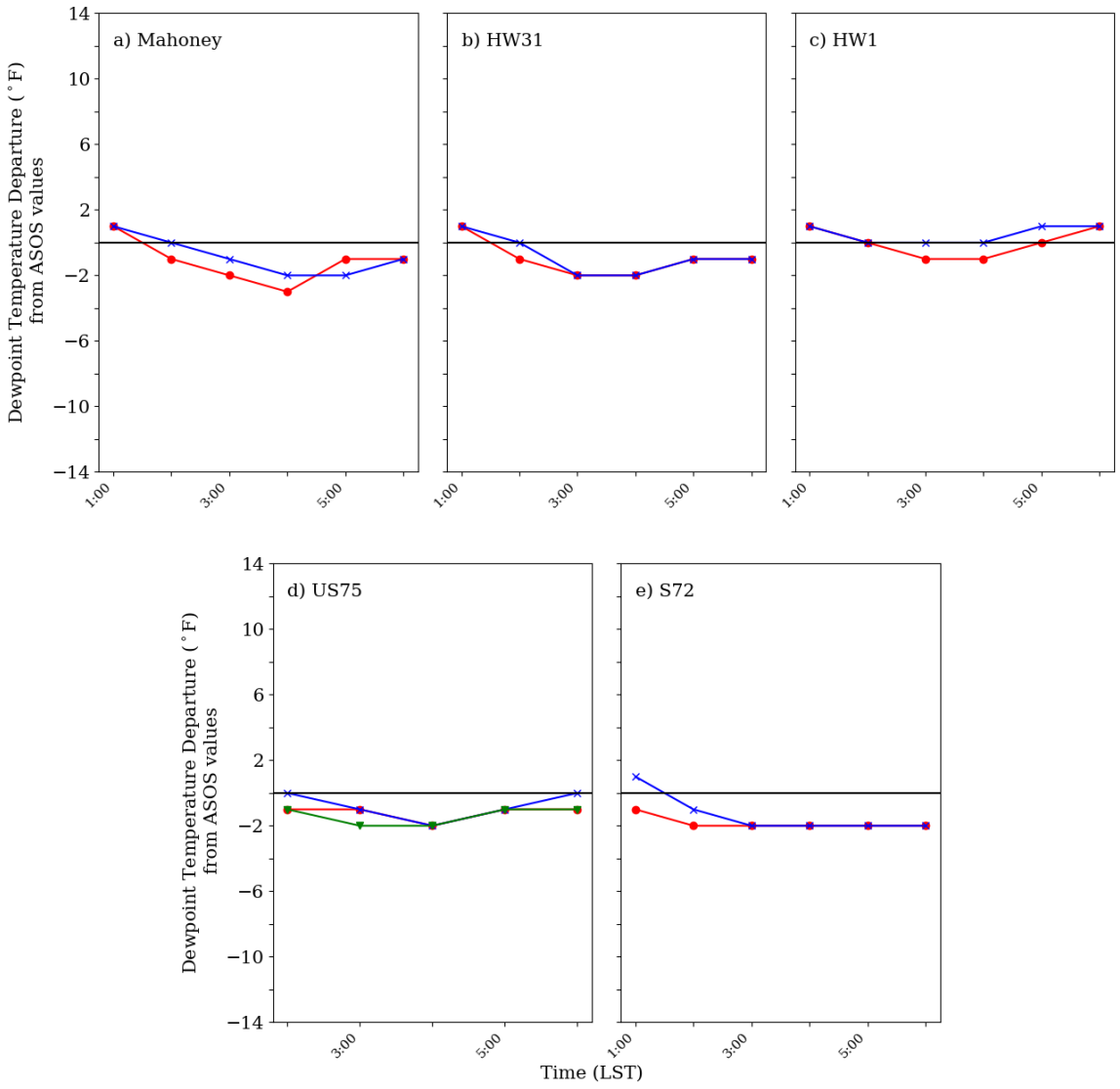

Figure 4.12: NDOT-MDSS forecasted dewpoint temperature departure for 26 January 2019 from the observed ASOS values at (a) Mahoney, (b) HW31, (c) HW1, (d) US75, and (e) S72 for 3 hours (red), 6 hours (blue), 9 hours (green), 12 hours (black) prior to snowfall onset. The solid horizontal black line denotes zero departure from ASOS.

during the 3-hour and 6-hour forecasts towards the end of snowfall. Based on these dewpoint temperatures and departures NDOT-MDSS forecasts for dewpoint temperature are well forecasted with no major errors. It appears NDOT-MDSS had a good handle on dewpoint temperatures during the event.

Throughout snowfall wind speed is consistently under-forecasted from what is observed by ASOS (Figure 4.13). From the 3-hour to 6-hour forecast by NDOT-MDSS, the forecast shows little improvement in regard to wind speed. Little improvement is also shown given what wind speed data are available for 9 hours prior with S72. The greatest wind speed departure from ASOS occurs for forecasts made for Mahoney and HW31 with a difference of 10 mph (4.5 m/s) at 5:00 am LST 26 January 2019 (1100 UTC 26 January 2019) (Figure 4.14). The minimum and maximum wind speed observed by ASOS was 8 mph (3.6 m/s) and 11 mph (4.9 m/s) respectively. The minimum wind speed forecasted by NDOT-MDSS for any of the segments was for Mahoney which was 0 mph (0 m/s) during both the 3-hour and 6-hour forecasts. The maximum wind speed forecasted for any of the segments was 4 mph (1.8 m/s) for several of the routes during both the 3- and 6-hour forecasts. Based on wind speeds and departures, wind speed is the worst parameter forecasted by NDOT-MDSS when compared to the other parameters of temperature and dewpoint. NDOT-MDSS forecasts for wind speed are not forecasted well in this case. NDOT-MDSS may have a calm wind bias in this case.

For the second objective of this study, the NDOT-MDSS analysis includes examining snowfall and forecast ability of the system regarding accumulation and timing of snowfall. Snowfall information is a critical element needed to be known by NDOT and similar agencies when assisting in maintenance practices. KOMA recorded 1.0 inches

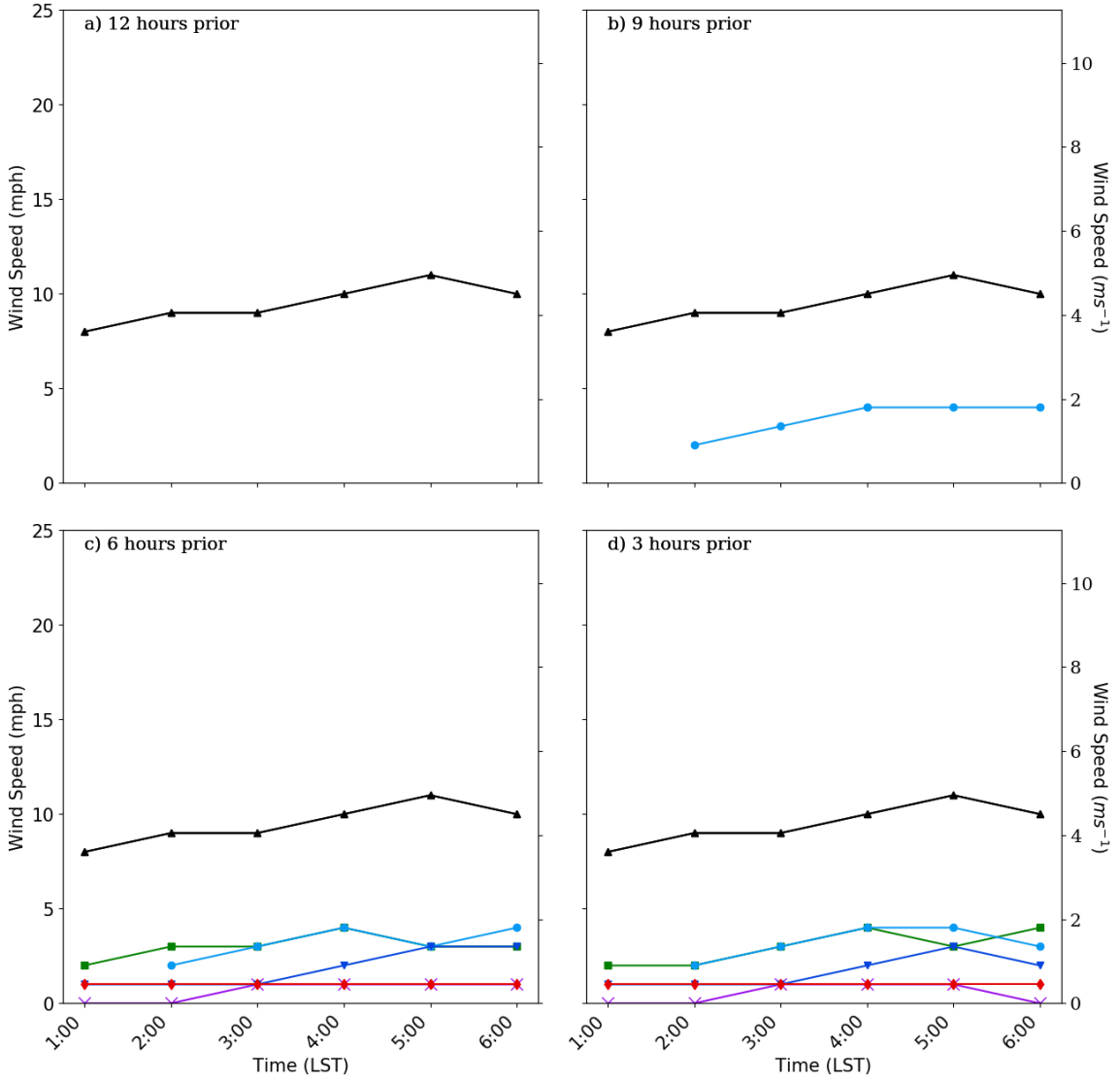

Figure 4.13: 26 January 2019 hourly wind speed forecasted by NDOT-MDSS at (a) 1:00 pm LST 25 January 2019 forecast run (12 hours prior to snowfall start (earliest time upon any segment), (b) 4:00 pm LST forecast run (9 hours prior to snowfall start), (c) 7:00 pm LST forecast run (6 hours prior to snowfall start), and (d) 10:00 pm LST forecast run (3 hours prior to snowfall start) for Mahoney (violet), S72 (blue), HW31 (red), HW1 (green), and US75 (light blue) compared to ASOS observed (black). Date and time run from the start of snowfall to the end of snowfall.

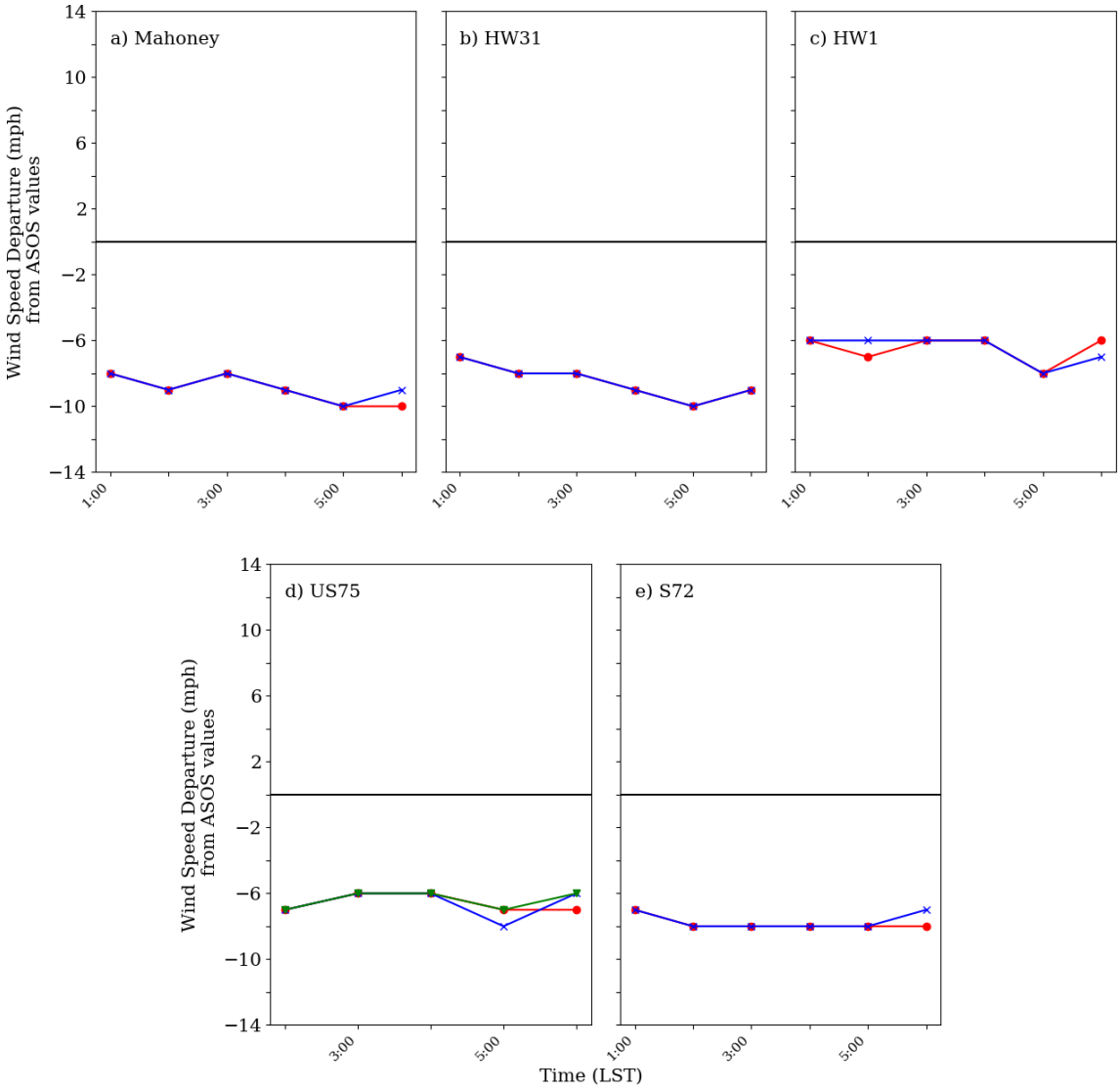

Figure 4.14: NDOT-MDSS forecasted wind speed departure for 26 January 2019 from the observed ASOS values at (a) Mahoney, (b) HW31, (c) HW1, (d) US75, and (e) S72 for 3 hours (red), 6 hours (blue), 9 hours (green), 12 hours (black) prior to snowfall onset. The solid horizontal black line denotes zero departure from ASOS.

(2.5 cm) of snowfall during the event. It is helpful to examine each model forecast run for each segment to see if and how NDOT-MDSS was improving with time. Forecasts runs are examined from the earliest time saved in the NDOT-MDSS system to 24 hours after the start of snowfall (to ensure NDOT-MDSS was not producing additional snow for the event after the event had ended) which was from 5:00 pm LST 25 January to 1:00 am LST 27 January 2019 (2300 UTC 25 January to 0700 UTC 27 January 2019) (Figure 4.15). During the first forecast hour, NDOT-MDSS ranges just below 1.0 inch (2.5 cm) of snowfall. Forecasts for S72 are closest to the observed value while forecasts for HW31 are the furthest off. As forecast time progresses, generally NDOT-MDSS gets worse leading up to the start of snowfall. However, forecasts for road segments get more consistent between each other which can be seen by overlap in Figure 4.15. After snowfall start at 1:00 am LST 26 January 2019 (0700 UTC 26 January 2019), all forecasted amounts for each of the five segments consistently rise. A dramatic rise in snowfall accumulation for each segment can be seen between 4:00 am LST 26 January 2019 (1000 UTC 26 January 2019) and 6:00 am LST 26 January 2019 (1200 UTC 26 January 2019). At 6:00 am LST 26 January 2019 (1200 UTC 26 January 2019), the stop of snowfall, the forecasted accumulation for each segment is furthest off from the observed value. Forecasts for HW31 and Mahoney are the furthest off at this time while forecasts for US75 and S72 are the closest to observed snowfall. By 7:00 am LST 26 January 2019 (1300 UTC 26 January 2019), when snowfall has ended, the accumulation seen by NDOT-MDSS for each segment has shifted downwards and remains fairly constant until 1:00 am LST 27 January 2019 (0700 UTC 27 January 2019). By this time however, the NDOT-MDSS has still not forecasted the observed snowfall accumulation

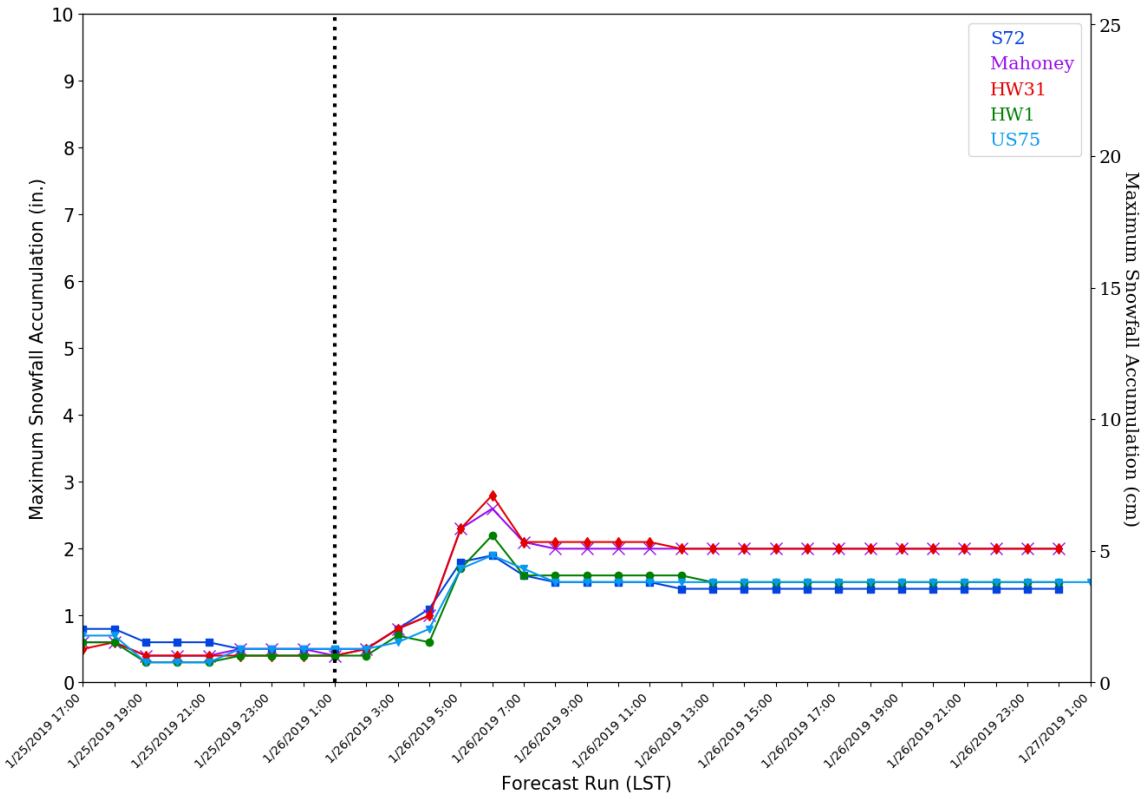

Figure 4.15: Maximum NDOT-MDSS forecasted snowfall accumulation for each selected segment per forecast run. The vertical dotted line denote snowfall start time for all selected road segments.

that occurred at KOMA. Forecasts for Mahoney and HW31 by NDOT-MDSS had the segments receiving 2 inches (5.1 cm) which are the forecasts furthest off from the observed snowfall. The closest accumulation forecasts to observed snowfall are for S72. There are no major errors in the NDOT-MDSS forecasts for each segment before, during, or after the event. Generally, NDOT-MDSS handles the event well regarding forecasted snowfall accumulations. Another important aspect to consider is how well NDOT-MDSS handles the total amount of time it was forecasting snowfall from the start of available forecast runs for all segments, 5:00 pm LST 25 January 2019 (2300 UTC 25 January 2019), to the start of snowfall for each segment. The start of snowfall for the segments was 1:00 am LST 26 January 2019 (0700 UTC 26 January 2019) for HW31, HW1, Mahoney, and S72 and 2:00 am LST 26 January 2019 (0800 UTC 26 January 2019) for US75 (Table 3.1). This amount of time is known as the event length and is defined as the time of snowfall start to the time of snowfall end as output by NDOT-MDSS. For this task, event length for each segment is graphed and compared with each other. S72, Mahoney, and HW31 are grouped together while HW1 and US75 are also grouped together. These segments were grouped together based on the proximity of each segment to each other. For S72, Mahoney, and HW31 the event length seen by each forecast run of the NDOT-MDSS from the beginning of data to the start of snowfall is too long for all road segments (Figure 4.16 and Figure 4.17). The actual observed length of time for snowfall is five hours for all three of these segments. The shortest forecasted event length of snowfall between S72, Mahoney, and HW31 is eight hours while the longest is 11 hours forecasted for S72 and 10 hours for both Mahoney and HW31 at some point. For the HW1 and US75 group the shortest event length forecasted by NDOT-MDSS

Run	2200	2300	0000	0100	0200	0300	0400	0500	0600	0700	0800	0900	1000
1/25/2019 17:00													
1/25/2019 18:00													
1/25/2019 19:00													
1/25/2019 20:00													
1/25/2019 21:00													
1/25/2019 22:00													
1/25/2019 23:00													
1/26/2019 00:00													
1/26/2019 01:00													
Run	2200	2300	0000	0100	0200	0300	0400	0500	0600	0700	0800	0900	1000
1/25/2019 17:00													
1/25/2019 18:00													
1/25/2019 19:00													
1/25/2019 20:00													
1/25/2019 21:00													
1/25/2019 22:00													
1/25/2019 23:00													
1/26/2019 00:00													
1/26/2019 01:00													
Run	2200	2300	0000	0100	0200	0300	0400	0500	0600	0700	0800	0900	1000
1/25/2019 17:00													
1/25/2019 18:00													
1/25/2019 19:00													
1/25/2019 20:00													
1/25/2019 21:00													
1/25/2019 22:00													
1/25/2019 23:00													
1/26/2019 00:00													
1/26/2019 01:00													

Figure 4.16: The NDOT-MDSS forecasted start and end times of snowfall for 25 January to 26 January for each segment; S72 (blue), Mahoney (violet), HW31 (red). The actual event length for segments is highlighted by the orange cells. Time is in LST.

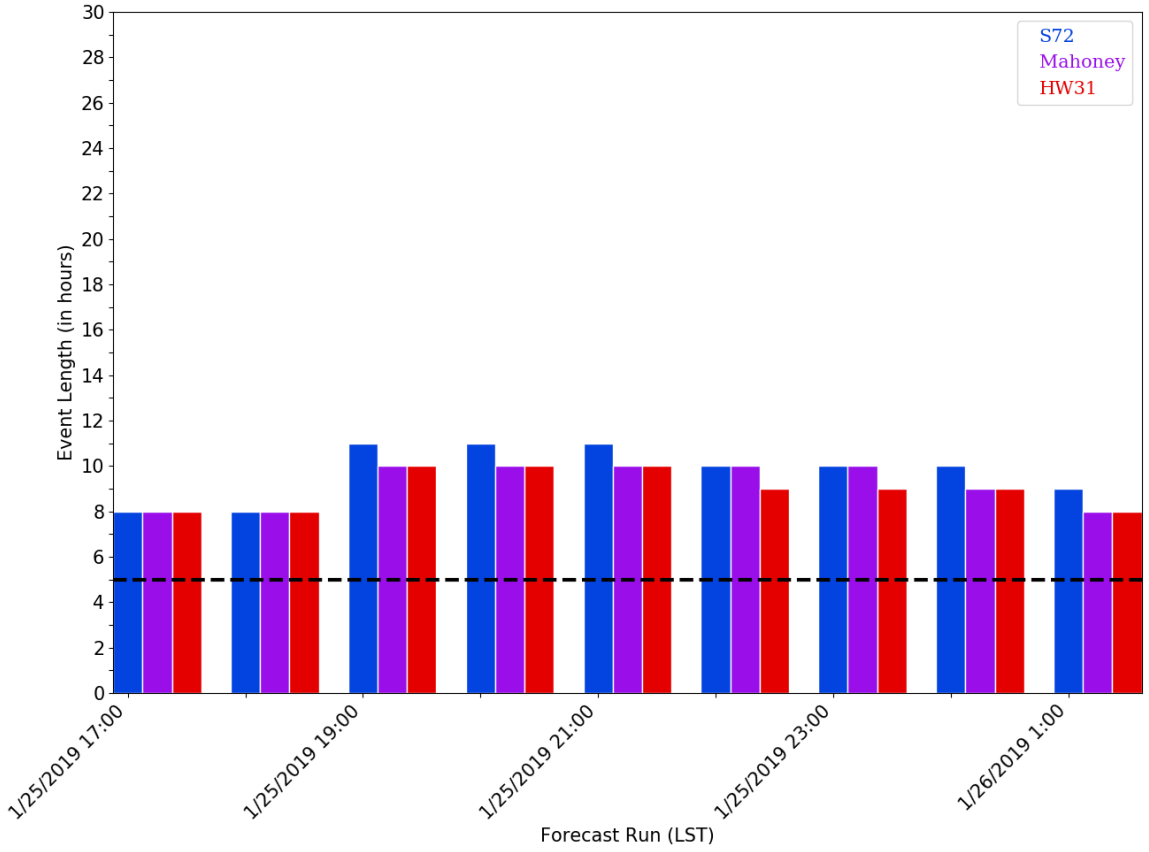

Figure 4.17: NDOT-MDSS forecasted event length for S72 (blue), Mahoney (violet), and HW31 (red) per forecast run. The black horizontal line denotes the observed event length for all three of the segments.

between the two segments seen is 8 hours (Figure 4.18 and Figure 4.19). The longest forecast event duration is 11 hours for both HW1 and US75. NDOT-MDSS makes the worst event length forecasts from 7:00 pm LST 25 January 2019 (0100 UTC 26 January 2019) to 12:00 am LST 26 January 2019 (0600 UTC 26 January 2019) for these segments. Thereafter, a slight improvement occurs as the start of snowfall is approached. It is also important to look at end time differential. The end time differential is defined as the difference between the forecasted and observed snowfall end time. For every segment, NDOT-MDSS over-forecasted not only the amount of snow received but also has snowfall lasting longer than what is observed (Figure 4.20). A negative end time differential shows NDOT-MDSS was predicting snowfall to last longer than what was observed, while a positive end time differential shows NDOT-MDSS predicting snowfall to stop before the observed snowfall end time. In the case of the five segments, every NDOT-MDSS forecast has snowfall lasting after snowfall has already stopped as seen by negative differentials for each forecast run from 5:00 pm LST 25 January 2019 (2300 UTC 25 January 2019) to 6:00 am LST 26 January 2019 (1200 UTC 26 January 2019). The smallest differential is -3 hours while the largest is -4 hours. Forecasts made by NDOT-MDSS for both HW31 and Mahoney have a consistent differential of -3 hours through each forecast run while forecasts for US75 has a consistent result of -4 hours as an end time differential. The worse end time differential is for US75 while the best is for HW31 and Mahoney. End time differentials are consistently between -4 hours and -3 hours over each forecast run for S72 and HW1. Based on event length and end time differential, NDOT-MDSS generally overpredicts how long impacts from this Alberta clipper system will last. In some cases NDOT-MDSS has snowfall lasting or an event

Run	2200	2300	0000	0100	0200	0300	0400	0500	0600	0700	0800	0900	1000
1/25/2019 17:00													
1/25/2019 18:00													
1/25/2019 19:00													
1/25/2019 20:00													
1/25/2019 21:00													
1/25/2019 22:00													
1/25/2019 23:00													
1/26/2019 00:00													
1/26/2019 01:00													
Run	2200	2300	0000	0100	0200	0300	0400	0500	0600	0700	0800	0900	1000
1/25/2019 17:00													
1/25/2019 18:00													
1/25/2019 19:00													
1/25/2019 20:00													
1/25/2019 21:00													
1/25/2019 22:00													
1/25/2019 23:00													
1/26/2019 00:00													
1/26/2019 01:00													
1/26/2019 02:00													

Figure 4.18: The NDOT-MDSS forecasted start and end times of snowfall for 25 January to 26 January for each segment; HW1 (green), US75 (light blue). The actual event length for segments is highlighted by the orange cells. Time is in LST.

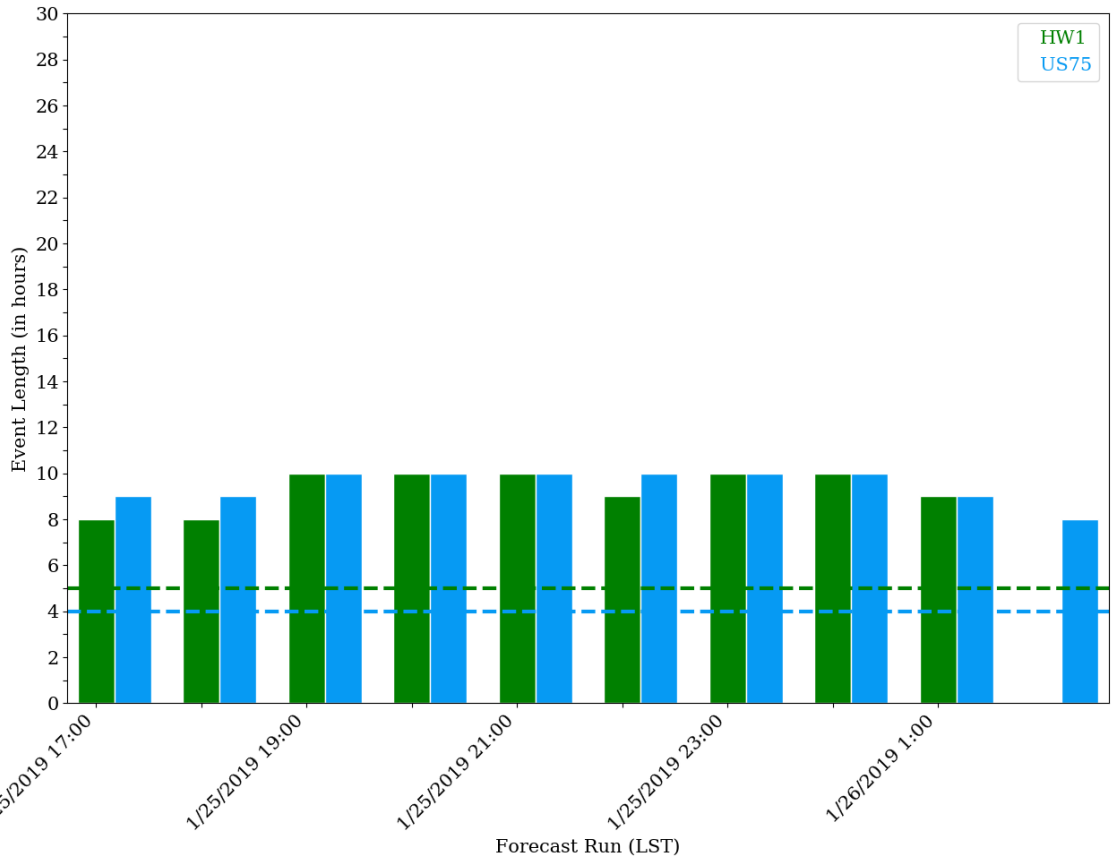

Figure 4.19: NDOT-MDSS forecasted event length for HW1 (green) and US75 (light blue) per forecast run. The green horizontal line denotes the observed event length for HW1 while the light blue horizontal line denotes the observed event length for US75.

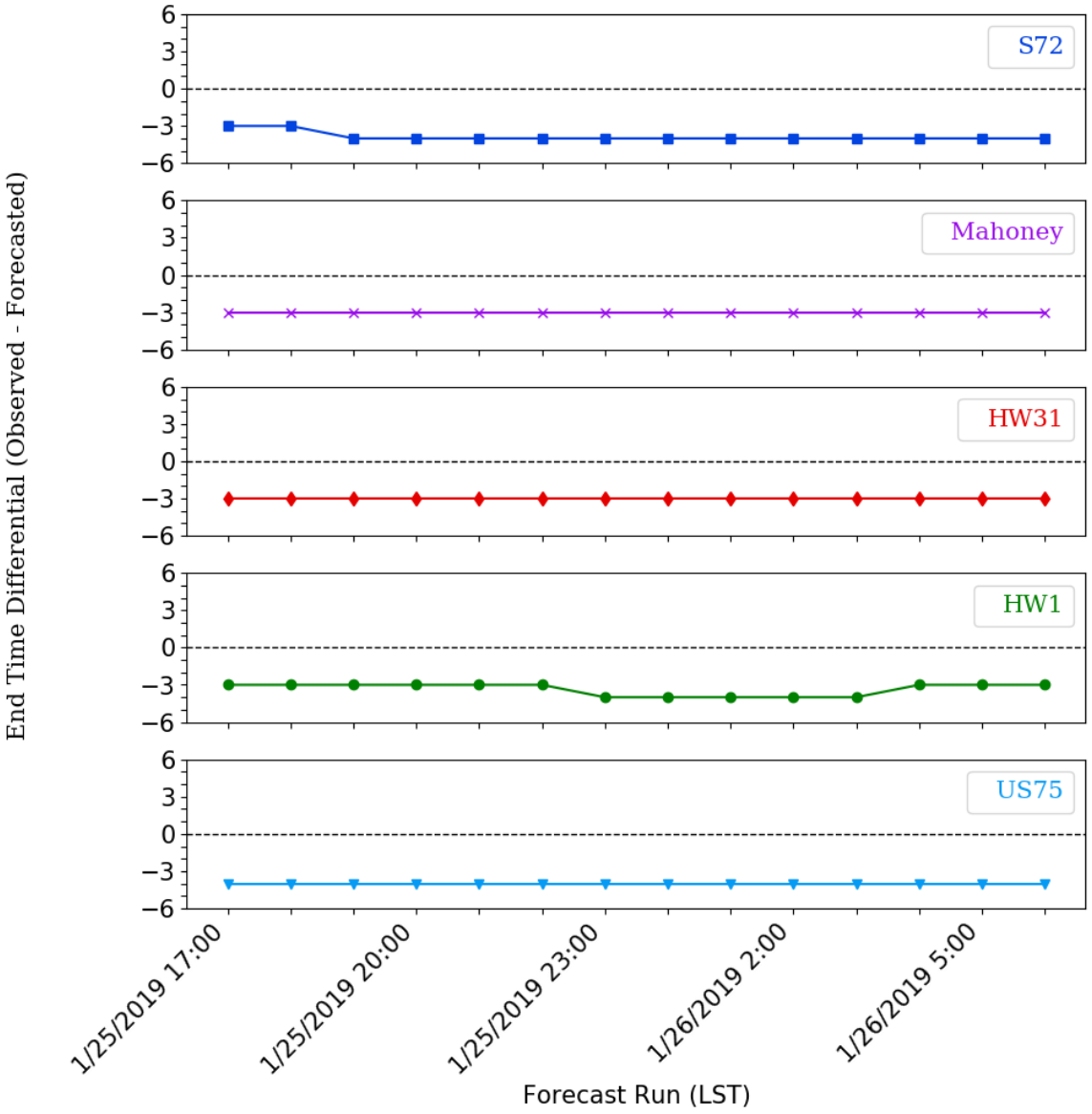

Figure 4.20: 25-26 January 2019 snowfall end time difference graphs for the five selected segments from NDOT-MDSS.

occurring double in length. The overprediction of snowfall end time and event length are major errors that should be watched. These errors are defined as major because presumable they would affect both the planning and the timing of maintenance operations. Users of NDOT-MDSS should watch this overprediction by remaining cautious and careful while planning. Snowfall timing is critical to NDOT maintenance procedures, so planning should be done accordingly.

4.2 Case Study II: 15 February 2019

4.2.1 Synoptic Analysis:

The 15 February 2019 case study event was an Alberta clipper system that impacts the Lincoln region with snow from approximately 6:00 am to 4:00 pm LST 15 February 2019 (1200 to 2200 UTC 15 February 2019). This Alberta clipper system brought light amounts of snow which largely impacted transportation within District 1 (Figure 3.1 and Figure 3.3). Synoptic conditions starting from 6:00 am LST 14 February 2019 (1200 UTC 14 February 2019) through 6:00 pm LST 15 February 2019 (0000 UTC 16 February 2019) are analyzed. This timeframe of analysis is based on a snowfall start time of 6:00 am LST 15 February 2019 (1200 UTC 15 February 2019) for several segments chosen within District 1 for the second event. At 6:00 am LST 14 February 2019 (1200 UTC 14 February 2019), a large jet streak is noted across the CONUS (Figure 4.21). This jet streak is mainly zonal with a particularly strong portion of the jet streak being located over the western part of the CONUS. The 500 hPa analysis shows a broad zonal pattern over the CONUS with some short waves embedded within the flow (Figure 4.21). There is a shortwave trough centered over Montana with a ridge associated with high pressure building over the West Coast. The 850 and 700 hPa analyses mainly

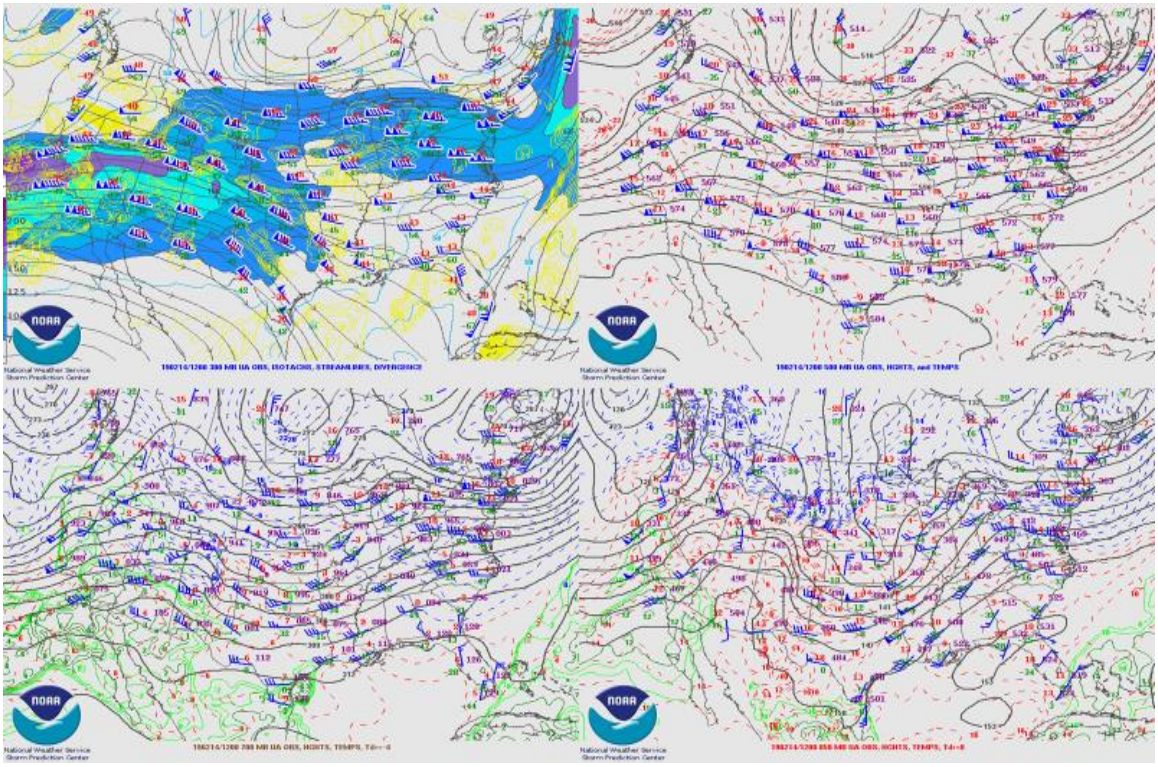

Figure 4.21: 300 hPa analysis (top left), 500 hPa analysis (top right), 700 hPa analysis (bottom left), 850 hPa analysis (bottom right) at 1200 UTC 14 February 2019. Image credits: SPC (2020)

reveal dry, westerly flow from the Intermountain West to the Great Plains (Figure 4.21). Synoptic conditions begin to change by 6:00 pm LST 14 February 2019 (0000 UTC 15 February 2019) as the western ridge continues to build (Figure 4.22). At the 300 hPa level the zonal jet stream pattern remains zonal, while the 500 hPa level shows the shortwave trough centered over Montana has amplified somewhat along with the ridge to its west (Figure 4.22). The shortwave has progressed slightly eastward. The 700 and 850 hPa levels show dry flow that has become more northwesterly with time (Figure 4.22). By 6:00 am LST 15 February 2019 (1200 UTC 15 February 2019), a large stronger zonal jet streak is still in place over the West (Figure 4.23). The left exit region associated with the jet streak is located over northern Colorado/southern Wyoming with an anticyclone to the north. At 500 hPa, a shortwave axis can be seen over northern Colorado/southern Wyoming while another shortwave trough is now located over the Great Lakes region (Figure 4.23). The flow at 700 hPa indicates that winds have shifted from northwesterly to southwesterly over time while 850 hPa flow shows a col-like wind flow situation (Figure 4.23). The overall pattern remains essentially the same by 6:00 pm LST 15 February 2019 (0000 UTC 16 February 2019) with a strong zonal jet streak still to the west (Figure 4.24). The 500 hPa map indicates the weak shortwave trough centered over northern Colorado/southern Wyoming has continued moving eastward (Figure 4.24). This weak trough is likely associated with the system of interest based on timing and location. The 700 hPa analysis shows flow has now switched back to northwesterly flow while 850 hPa continues to show weak flow (Figure 4.24).

Moving to surface analysis, a more consistent picture can be created. Beginning at 6:00 am LST 14 February 2019 (1200 UTC 14 February 2019) an Alberta clipper system

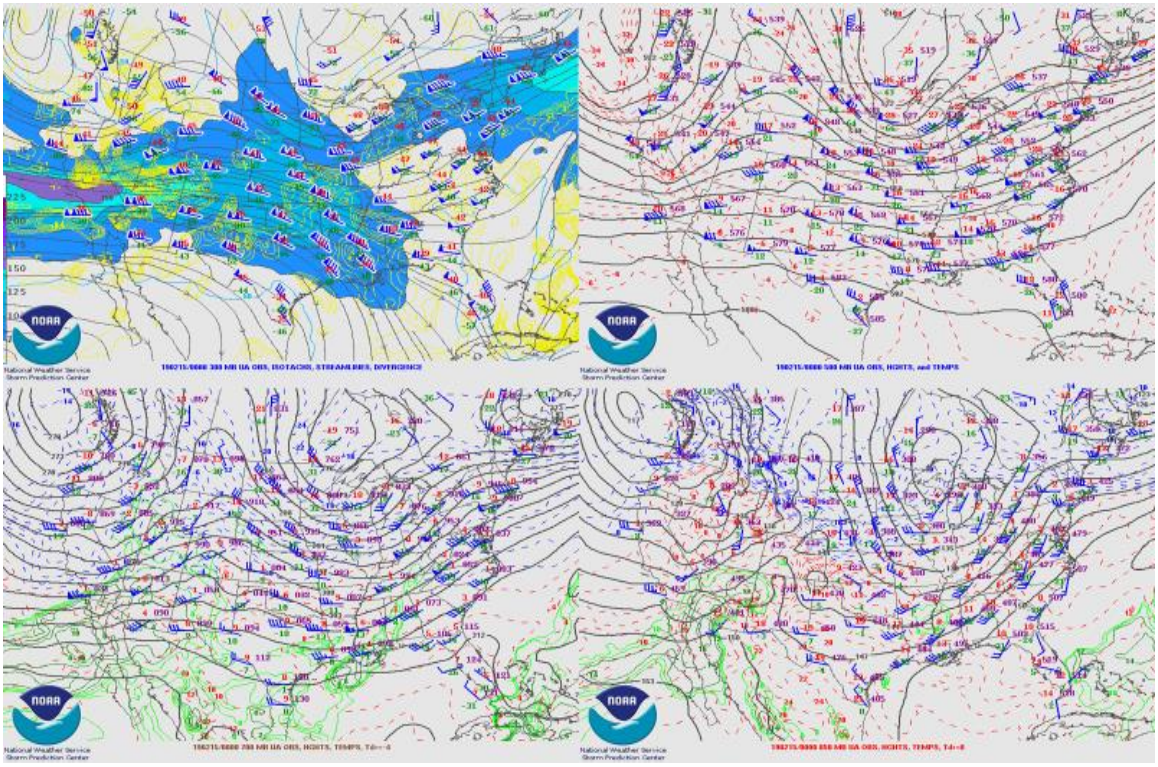

Figure 4.22: 300 hPa analysis (top left), 500 hPa analysis (top right), 700 hPa analysis (bottom left), 850 hPa analysis (bottom right) at 0000 UTC 15 February 2019. Image credits: SPC (2020)

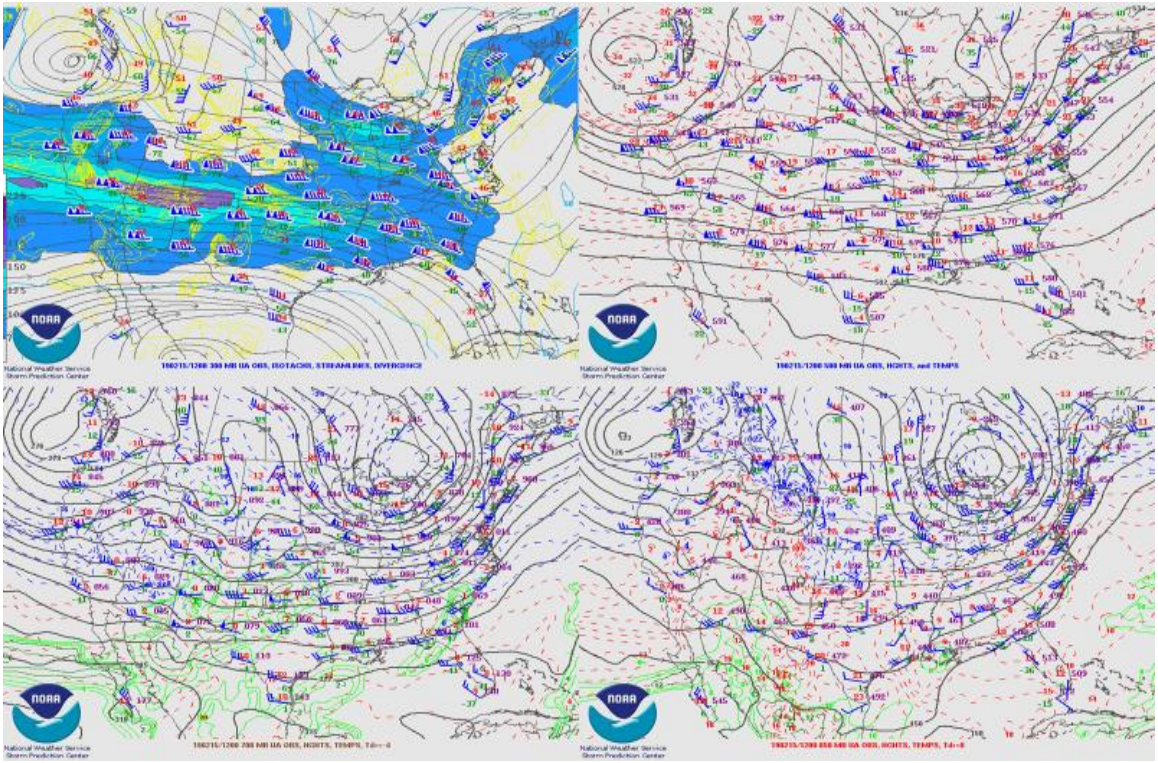

Figure 4.23: 300 hPa analysis (top left), 500 hPa analysis (top right), 700 hPa analysis (bottom left), 850 hPa analysis (bottom right) at 1200 UTC 15 February 2019. Image credits: SPC (2020)

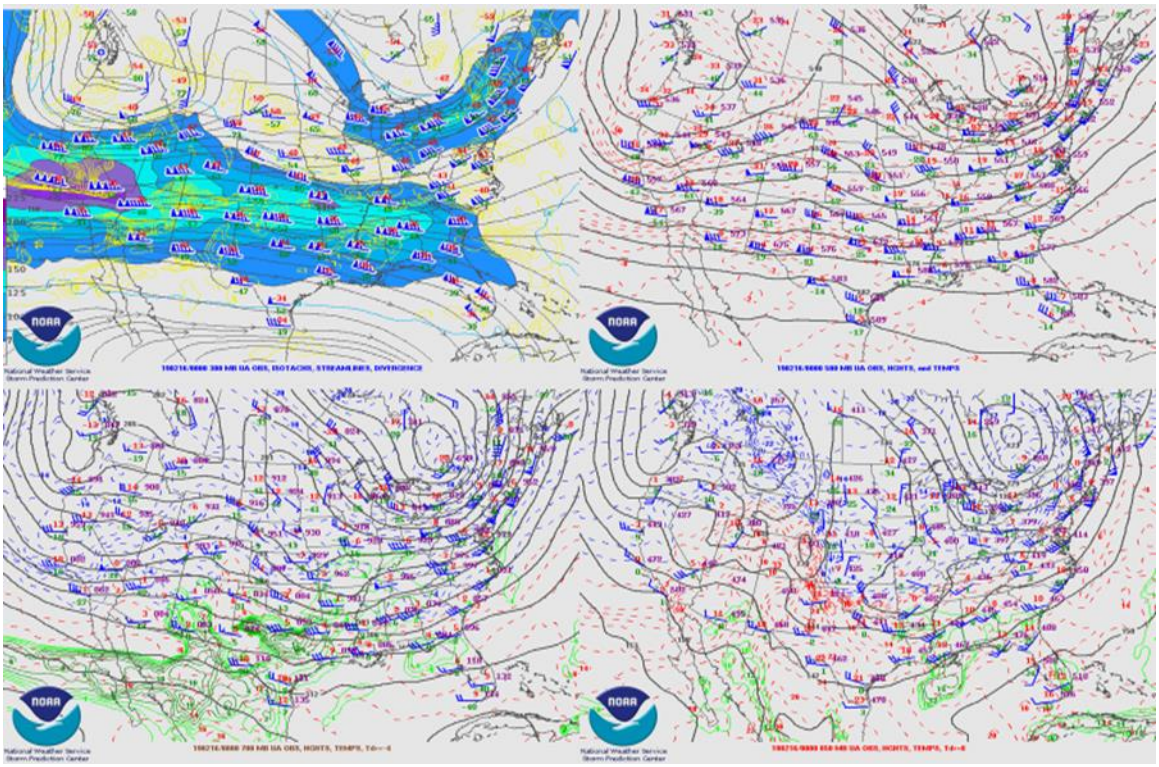

Figure 4.24: 300 hPa analysis (top left), 500 hPa analysis (top right), 700 hPa analysis (bottom left), 850 hPa analysis (bottom right) at 0000 UTC 16 February 2019. Image credits: SPC (2020)

was noted over the Nebraska/Iowa border with associated warm and cold fronts (Figure 4.25). With time this low continues to push eastward, and the trailing anticyclone can be seen over Saskatchewan with a strong pressure gradient trailing the cold front associated with the low (Figure 4.25). However, this is not the Alberta clipper system of interest. From 6:00 pm LST 14 February 2019 to 3:00 am LST 15 February 2019 (0000 to 0900 UTC 15 February 2019) this Alberta clipper system continues to have its cold front push southward along with noted pressure gradients while the cyclone swings northeastward over the Great Lakes (Figure 4.26). The trailing anticyclone associated with the system remains nearly stationary over and just north of North Dakota. It is not until 6:00 am LST 15 February 2019 (1200 UTC 15 February 2019), that a low pressure system can be seen forming over Wyoming (lee side of the Wyoming mountains) with the low pushing southwards with time (Figure 4.27). The anticyclone associated with the previous Alberta clipper system still dominates over the northern Great Plains rather than being associated with this new low. This Wyoming Alberta clipper type low pressure dissipates while the high pressure system associated with the Alberta clipper system before this low remains stationary for the rest of the observed time (Figure 4.28).

4.2.2 NDOT-MDSS Analysis:

The 15 February 2019 case study event is an Alberta clipper system that moves over eastern Nebraska. Although not truly formed in Alberta the system can be thought more of a “Wyoming low” with the same formation and characteristics as a typical Alberta clipper system due to the more southerly and dry formation environment. In order to analyze this case study for the rest of the first objective, the meteorological parameters of temperature, dewpoint, and wind speed, are analyzed at 3-, 6-, 9-, and 12-hour prior

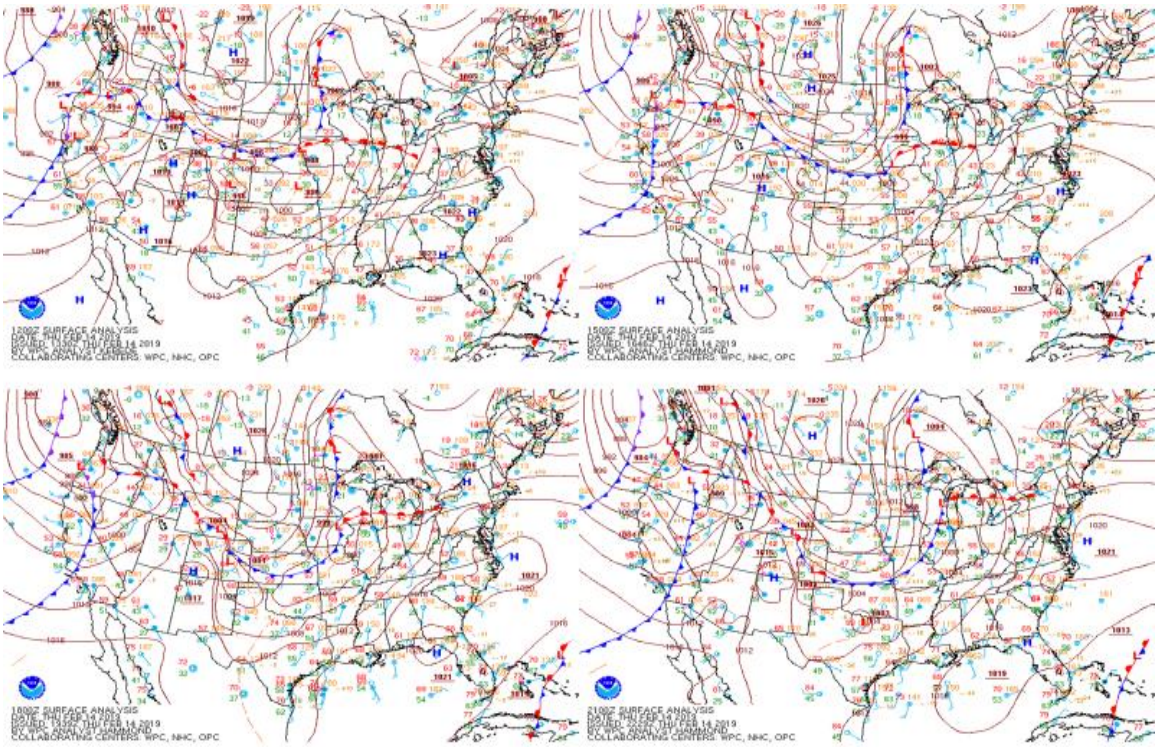

Figure 4.25: Surface analysis at 1200 UTC (top left), 1500 UTC (top right), 1800 UTC (bottom left), 2100 UTC (bottom right) on 14 February 2019. Image credits: WPC (2020)

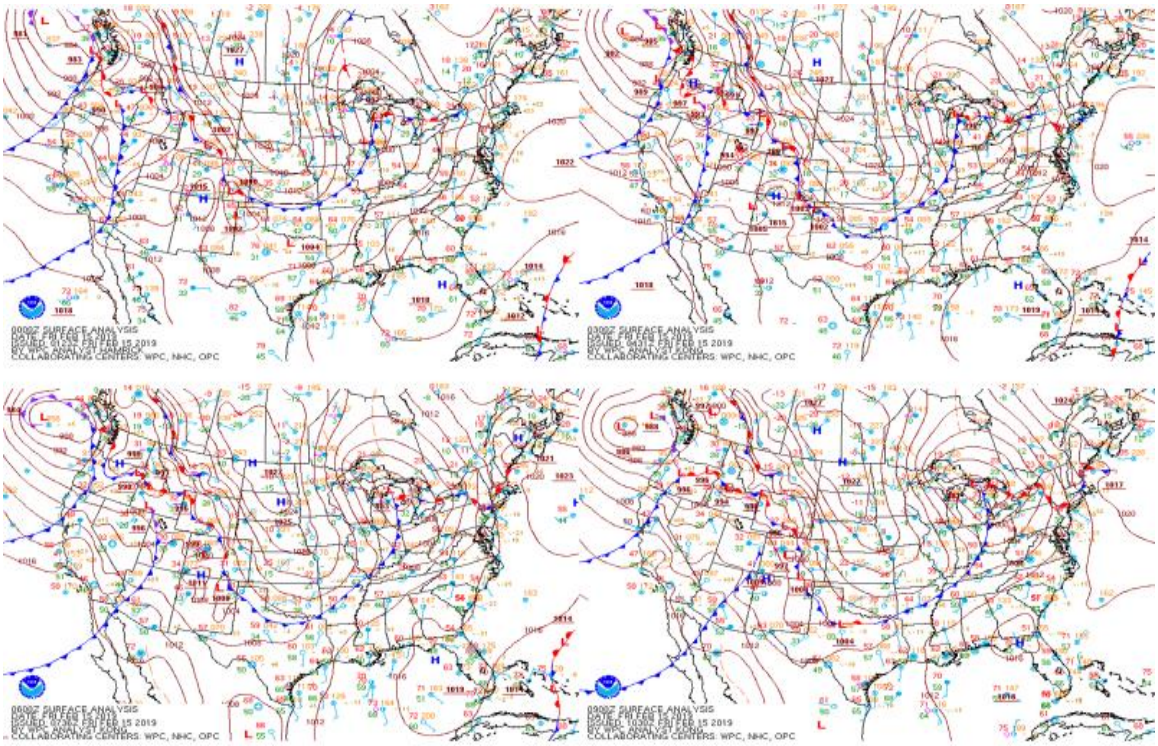

Figure 4.26: Surface analysis at 0000 UTC (top left), 0300 UTC (top right), 0600 UTC (bottom left), 0900 UTC (bottom right) on 15 February 2019. Image credits: WPC (2020)

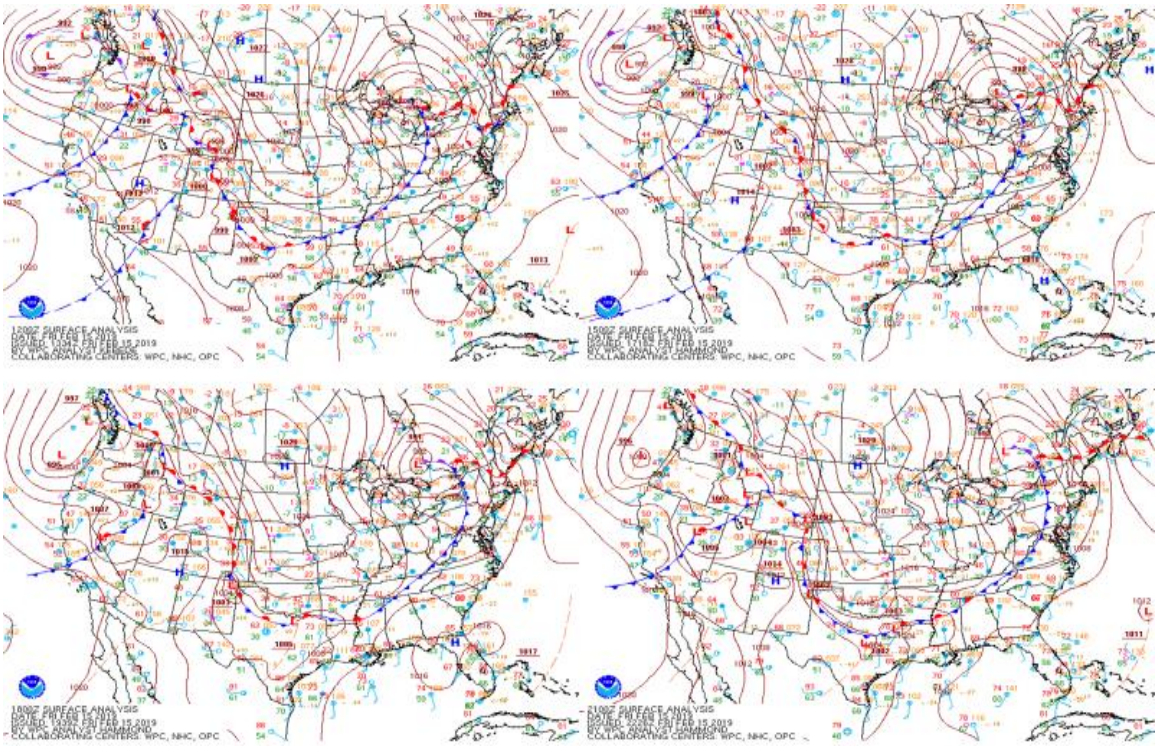

Figure 4.27: Surface analysis at 1200 UTC (top left), 1500 UTC (top right), 1800 UTC (bottom left), 2100 UTC (bottom right) on 15 February 2019. Image credits: WPC (2020)

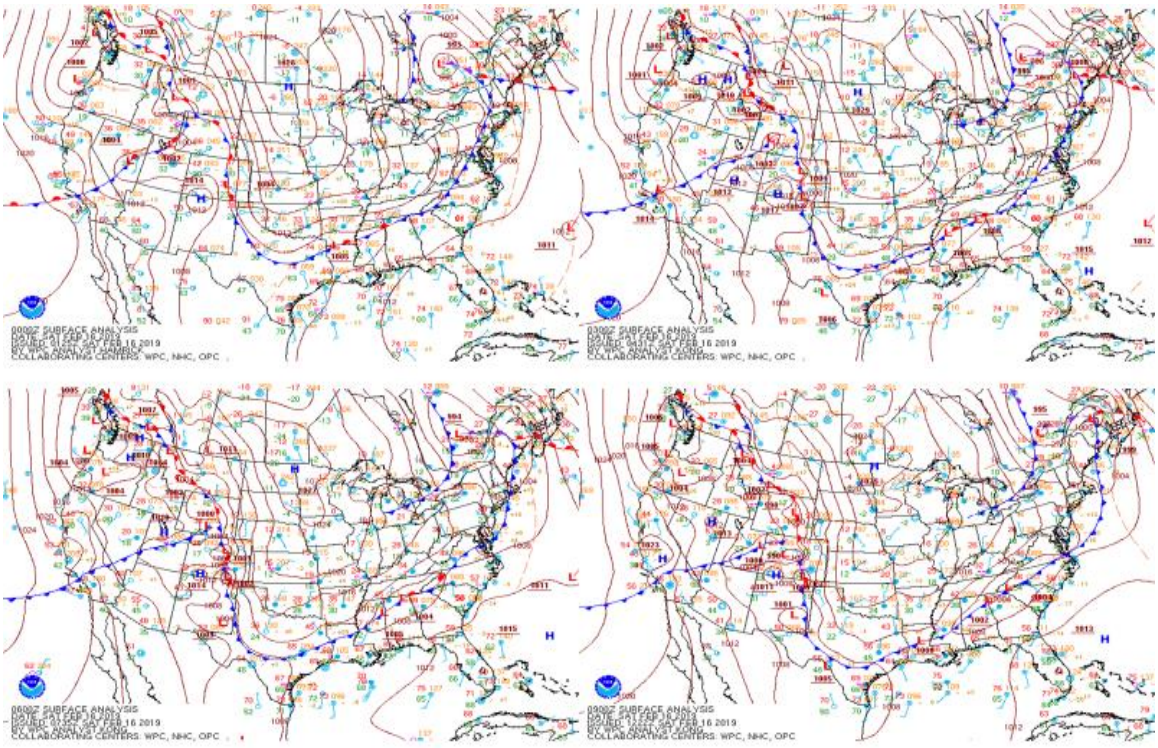

Figure 4.28: Surface analysis at 0000 UTC (top left), 0300 UTC (top right), 0600 UTC (bottom left), 0900 UTC (bottom right) on 16 February 2019. Image credits: WPC (2020)

intervals within NDOT-MDSS and compared to observed values from the nearest ASOS at KLNK. For the second objective, hourly forecasts for snow conditions from the NDOT-MDSS are obtained and analyzed for each event. Data are saved in the system from 6:00 pm LST 14 February 2019 (0000 UTC 15 February 2019) until 11:50 am LST 18 February 2019 (1750 UTC 18 February 2019). This timeframe therefore allowed data to be obtained 3, 6, 9, and 12 hours prior to the onset of snowfall upon the selected segments.

Air temperature forecasts from the NDOT-MDSS are sometimes too low or too high compared to ASOS observed values for all road segments for all forecast runs (Figure 4.29). However, at some hours NDOT-MDSS forecasts match observed temperatures. As the snowfall start time for the five road segments approaches, forecasts for each segment remain generally consistent. Of note, forecasts for W80 are consistently too low and do not show improvement over time. NDOT-MDSS temperature forecasts for P80, HW34, HW33, and HW77 do at some point predict an observed value while forecasts for W80 never do (Figure 4.30). The biggest difference occurs with forecasts for W80 which is 4.0 °F (2.2 °C) with the smallest departure being 0.0 °F (0.0 °C) for all other segments (Figure 4.30). The minimum and maximum temperature observed by the ASOS was 9 °F (-12.8 °C) and 14 °F (-10.0 °C) respectively. The minimum temperature forecasted for any of the segments was for W80 which was 6 °F (-14.4 °C). The maximum temperature forecasted for any of the segments was for both HW34 and P80 which was 16 °F (-8.9 °C). Based on these temperatures and departures NDOT-MDSS forecasts for temperature are forecasted well with no major errors occurring. It appears NDOT-MDSS had a good handle on temperatures during the event.

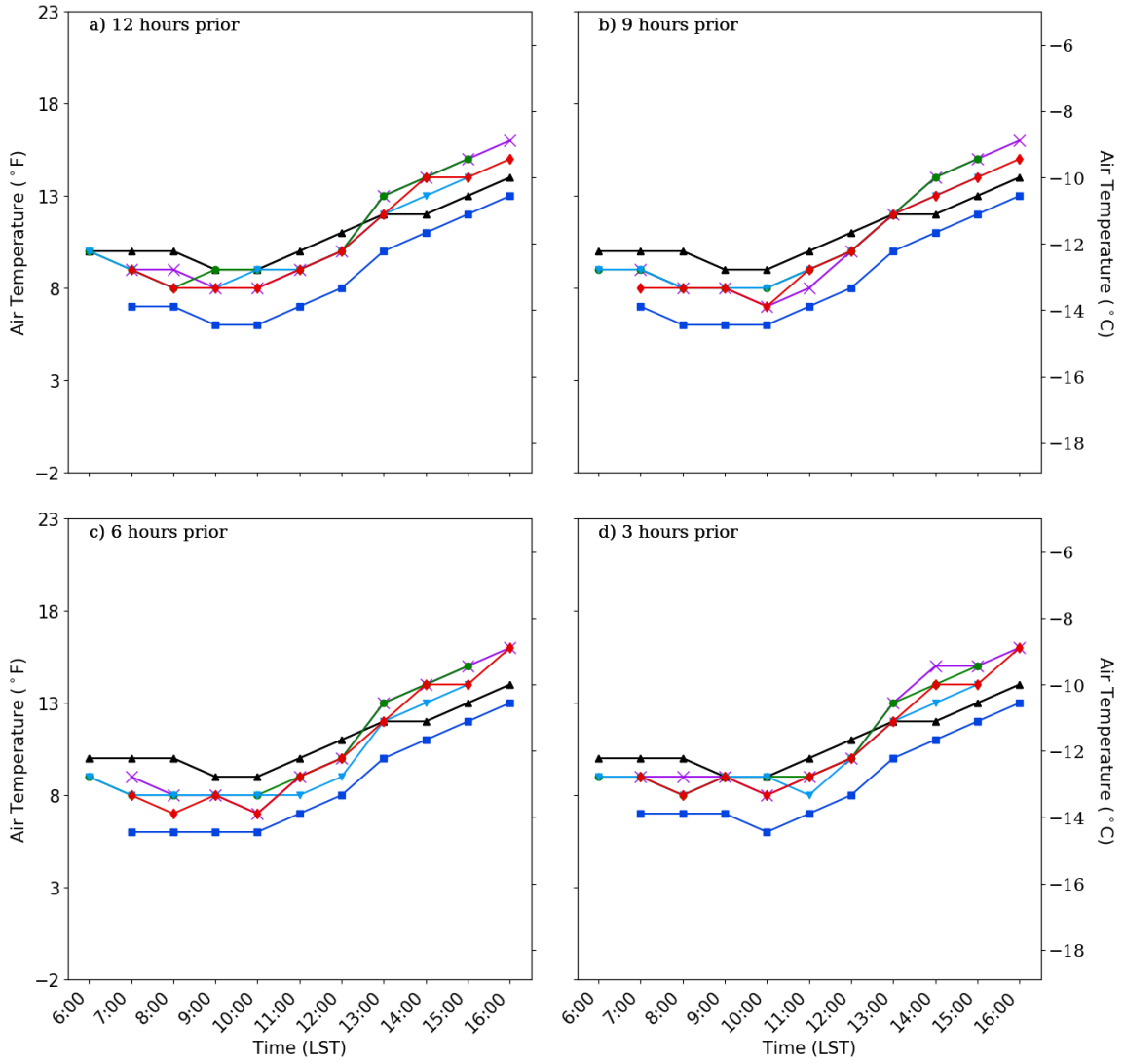

Figure 4.29: 15 February 2019 hourly temperature forecasted by NDOT-MDSS at (a) 6:00 pm LST 14 February 2019 forecast run (12 hours prior to snowfall start), (b) 9:00 pm LST forecast run (9 hours prior to snowfall start), (c) 1200 am LST 15 February 2019 forecast run (6 hours prior to snowfall start), and (d) 3:00 am LST forecast run (3 hours prior to snowfall start) for W80 (blue), P80 (violet), HW34 (red), HW33 (green), and HW77 (light blue) compared to ASOS observed (black). Date and time run from the start of snowfall to the end of snowfall.

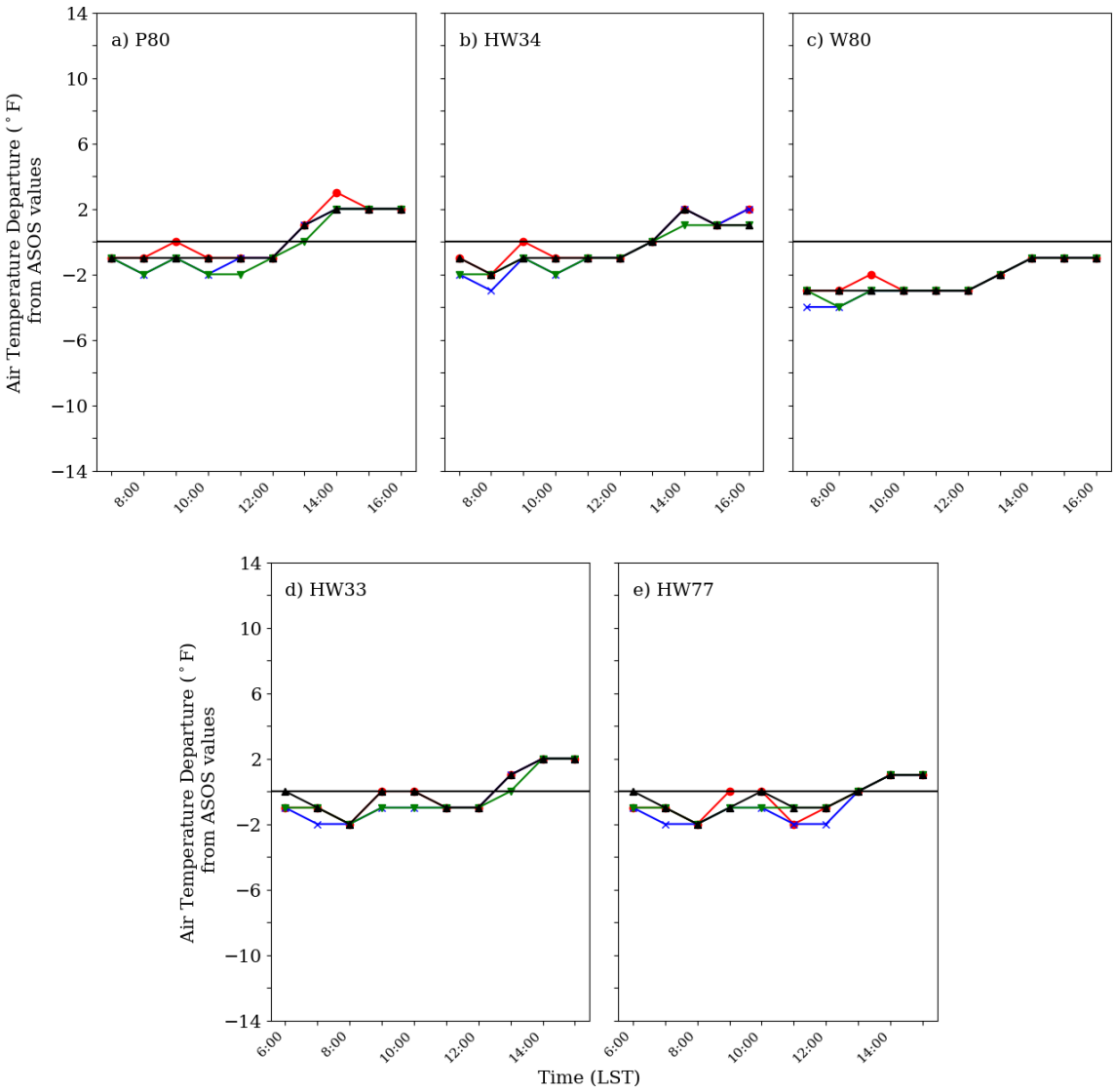

Figure 4.30: NDOT-MDSS forecasted temperature departure for 15 February 2019 from the observed ASOS values at (a) P80, (b) HW34, (c) W80, (d) HW33, and (e) HW77 for 3 hours (red), 6 hours (blue), 9 hours (green), 12 hours (black) prior to snowfall onset. The solid horizontal black line denotes zero departure from ASOS.

Dewpoint temperature forecasts from the NDOT-MDSS are consistently too high compared to observed values from ASOS for all forecasts prior to the onset of snowfall (Figure 4.31). Forecasts for P80, HW33, and HW77 do not at any time predict an observed dewpoint temperature while forecasts for HW34 and W80 do at multiple instances. With the exception of P80, NDOT-MDSS forecasts do show some improvement closer to the start time of snowfall (Figure 4.32). Forecasts for P80, HW33, and HW77 are noticeable warmer than what was observed by the ASOS. The largest dewpoint temperature departure occurs for multiple forecasts for the five segments with a difference of 8 °F (4.4°C) towards the end of snowfall. The minimum and maximum dewpoint temperature observed by the ASOS was 0 °F (-17.8 °C) and 7 °F (-13.9 °C) respectively. The minimum dewpoint temperature forecasted for any of the segments was for HW34 which was -1 °F (-18.3 °C) during the 6-hour and 3-hour forecasts. The maximum forecasted for any of the segments was 14 °F (10.0 °C) which occurred during multiple forecasts for several segments. Based on these dewpoint temperatures and departures NDOT-MDSS forecasts for dewpoint temperature are appropriate with no major errors. It appears, overall, that NDOT-MDSS had a good handle on dewpoint temperatures during the event. However, it appears NDOT-MDSS had a greater handle on dewpoint temperatures during the beginning of the event and a worse handle towards the end of the event.

Throughout snowfall, wind speed is largely under-forecasted for P80, W80, and HW34 while wind speed is mainly over-forecasted for HW33 and HW77 (Figure 4.33). Over time, there does appear to be improved in the forecasts for P80, W80, and HW34 while HW33 and HW77 remain more consistent. The largest wind speed departure

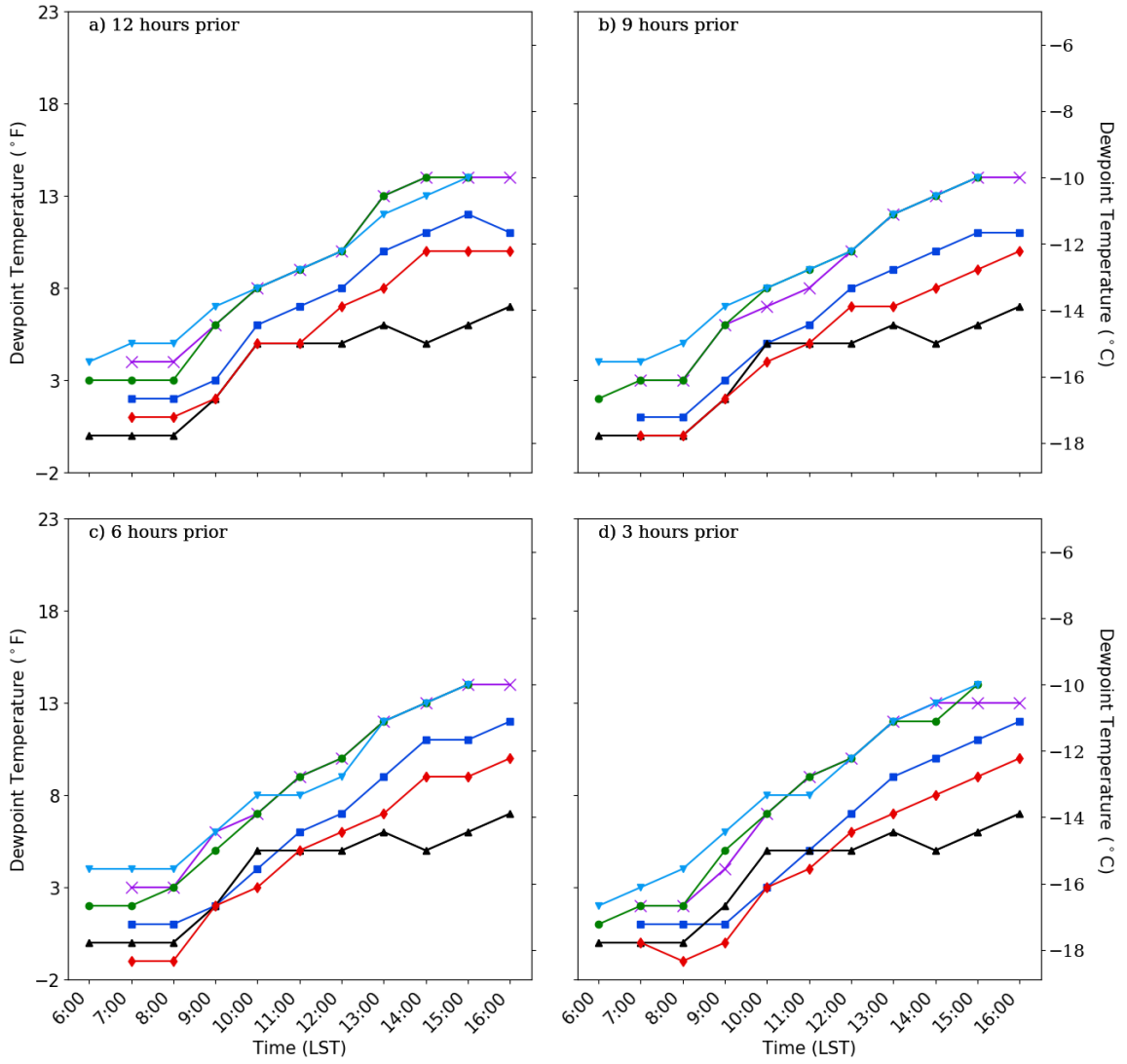

Figure 4.31: 15 February 2019 hourly dewpoint temperature forecasted by NDOT-MDSS at (a) 6:00 pm LST 14 February 2019 forecast run (12 hours prior to snowfall start), (b) 9:00 pm LST forecast run (9 hours prior to snowfall start), (c) 1200 am LST 15 February 2019 forecast run (6 hours prior to snowfall start), and (d) 3:00 am LST forecast run (3 hours prior to snowfall start) for W80 (blue), P80 (violet), HW34 (red), HW33 (green), and HW77 (light blue) compared to ASOS observed (black). Date and time run from the start of snowfall to the end of snowfall.

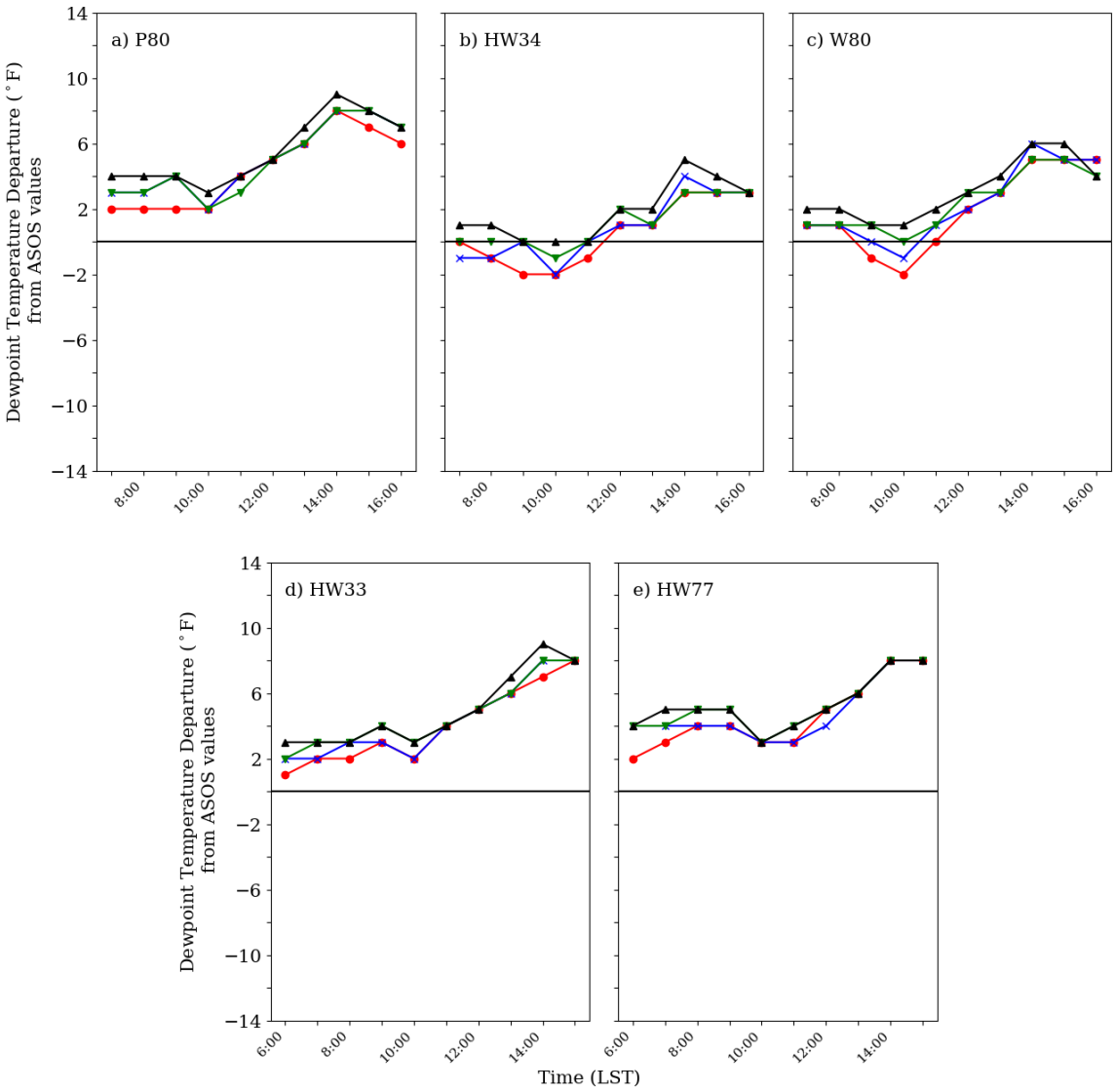

Figure 4.32: NDOT-MDSS forecasted dewpoint temperature departure for 15 February 2019 from the observed ASOS values at (a) P80, (b) HW34, (c) W80, (d) HW33, and (e) HW77 for 3 hours (red), 6 hours (blue), 9 hours (green), 12 hours (black) prior to snowfall onset. The solid horizontal black line denotes zero departure from ASOS.

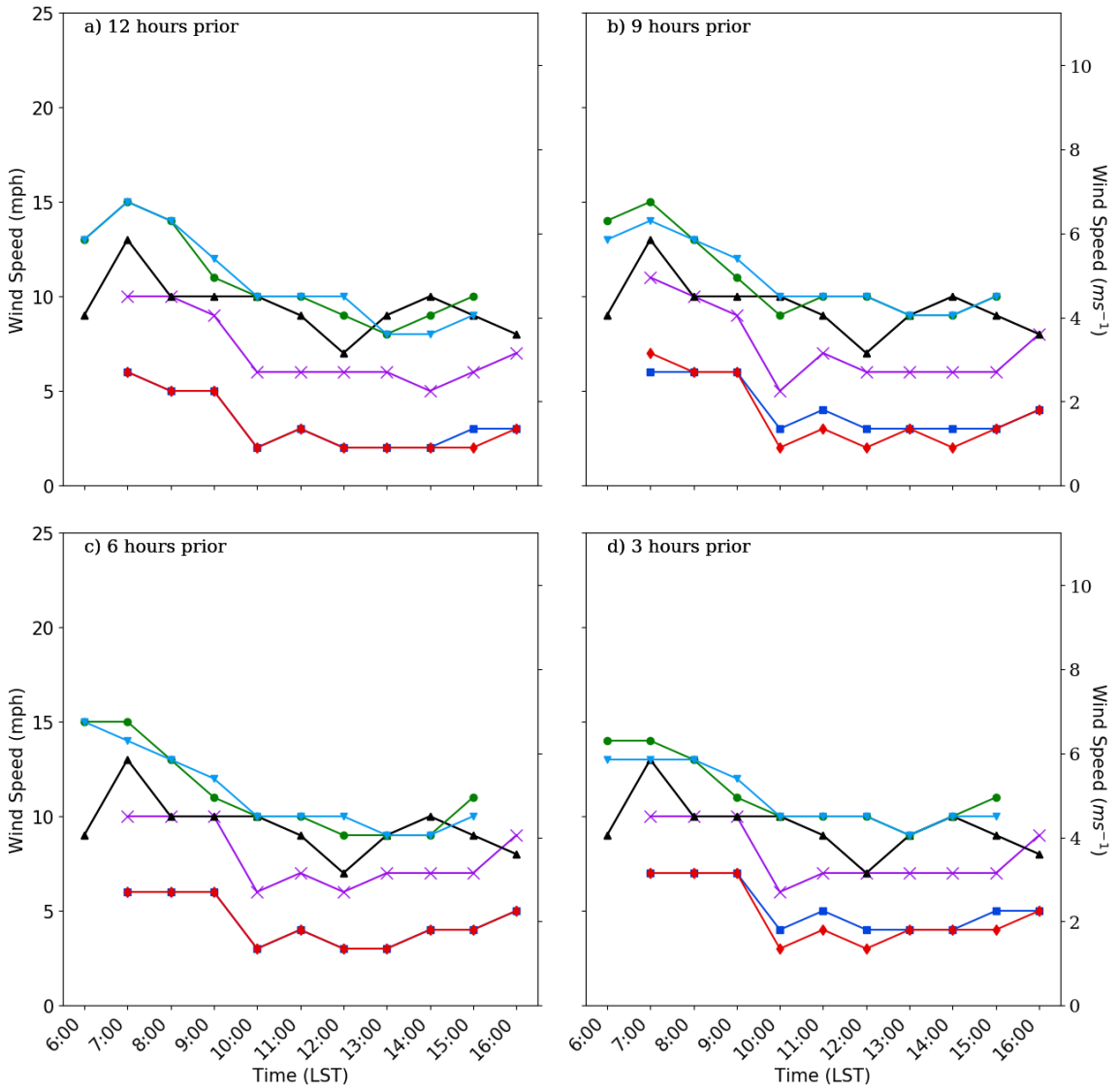

Figure 4.33: 15 February 2019 hourly wind speed forecasted by NDOT-MDSS at (a) 6:00 pm LST 14 February 2019 forecast run (12 hours prior to snowfall start), (b) 9:00 pm LST forecast run (9 hours prior to snowfall start), (c) 1200 am LST 15 February 2019 forecast run (6 hours prior to snowfall start), and (d) 3:00 am LST forecast run (3 hours prior to snowfall start) for W80 (blue), P80 (violet), HW34 (red), HW33 (green), and HW77 (light blue) compared to ASOS observed (black). Date and time run from the start of snowfall to the end of snowfall.

(Figure 4.34) occurs for forecasts made for both HW34 and W80 with a difference of 8 mph (3.6 m/s). The minimum and maximum wind speed observed at KLNK was 7 mph (3.1 m/s) and 13 mph (5.8 m/s) respectively. The minimum wind speed forecasted for any of the segments is for W80 and HW34 which is 2 mph (0.9 m/s). The maximum wind speed forecasted for any of the segments is 15 mph (6.7 m/s) for both HW33 and HW77. Based on observed wind speeds and wind speed departures, wind speeds are forecasted reasonably well by NDOT-MDSS. In this case wind speed appears to be dependent upon segment and NDOT-MDSS forecasts for wind speed appear to improve with time.

KLNK received 2.6 inches (6.6 cm) of snowfall during the event. Forecasts runs were examined from the earliest time saved in the NDOT-MDSS system to 24 hours after the start of snowfall which was from 6:00 pm LST 14 February 2019 (0000 UTC 15 February 2019) to 6:00 am LST 16 February 2019 (1200 UTC 16 February 2019). During the first forecast hour NDOT-MDSS over predicts the 2.6 inches of observed snowfall for all road segments (Figure 4.35). Forecasts for W80 are closest to the observed snowfall while forecasts for HW33 are furthest off. As forecast time progresses, generally NDOT-MDSS forecasts improve for HW33, HW77, and P80 leading up to the start of snowfall while producing more error for both HW34 and W80. In this case, forecasts for road segments begin to get more consistent between each other as seen by overlap (Figure 4.35) and then produce more error as the start time of snowfall occurs. Only forecasts for HW34 and W80 are the exception as a slight overlap can be seen as the start time approaches. After snowfall starts at 6:00 am LST 15 February 2019 (1200 UTC 15 February 2019), all forecasted snowfall accumulation amounts for each of the five segments stay about the same before dropping by 9:00 am LST 15 February 2019

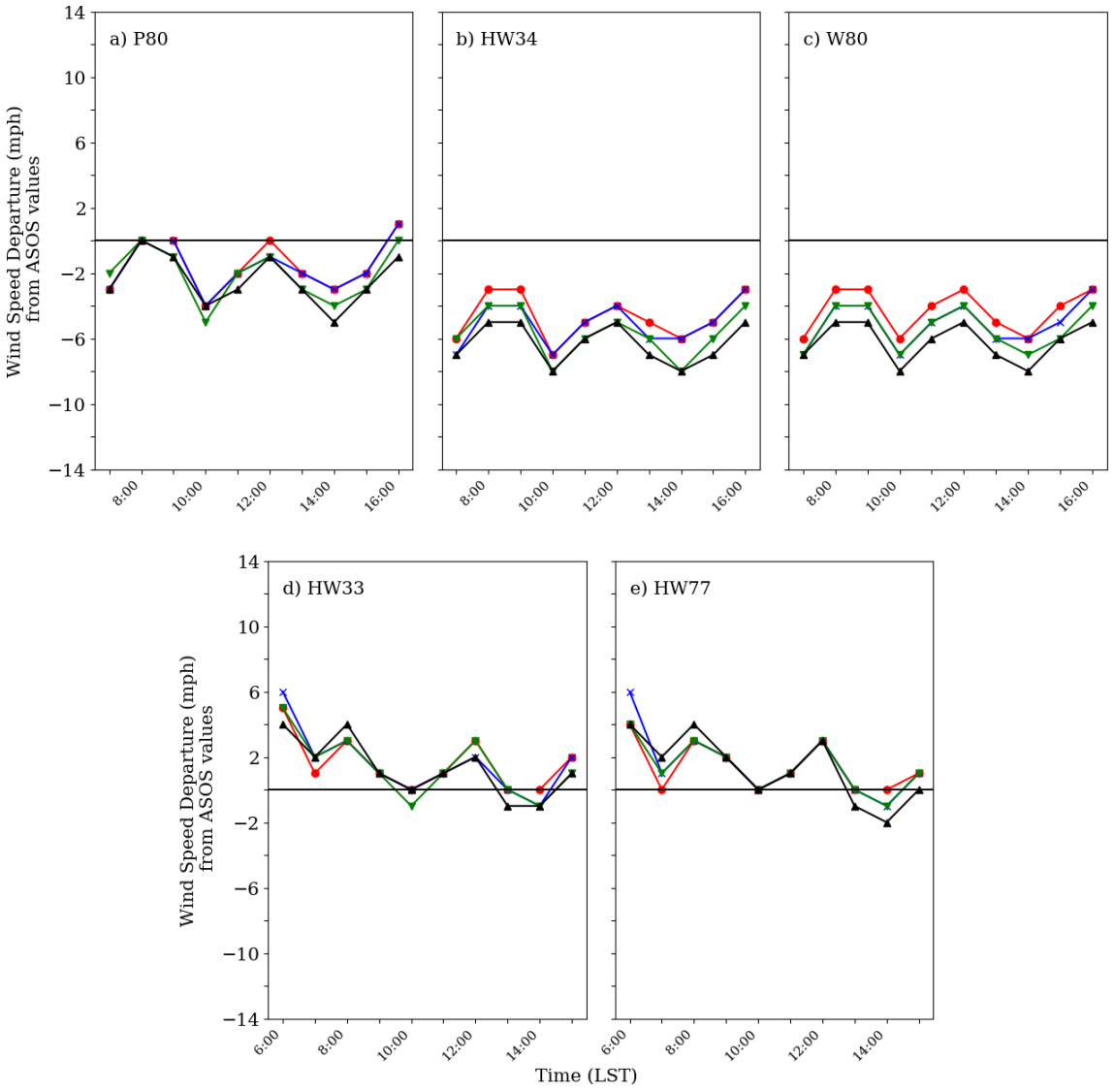

Figure 4.34: NDOT-MDSS forecasted wind speed departure for 15 February 2019 from the observed ASOS values at (a) P80, (b) HW34, (c) W80, (d) HW33, and (e) HW77 for 3 hours (red), 6 hours (blue), 9 hours (green), 12 hours (black) prior to snowfall onset. The solid horizontal black line denotes zero departure from ASOS.

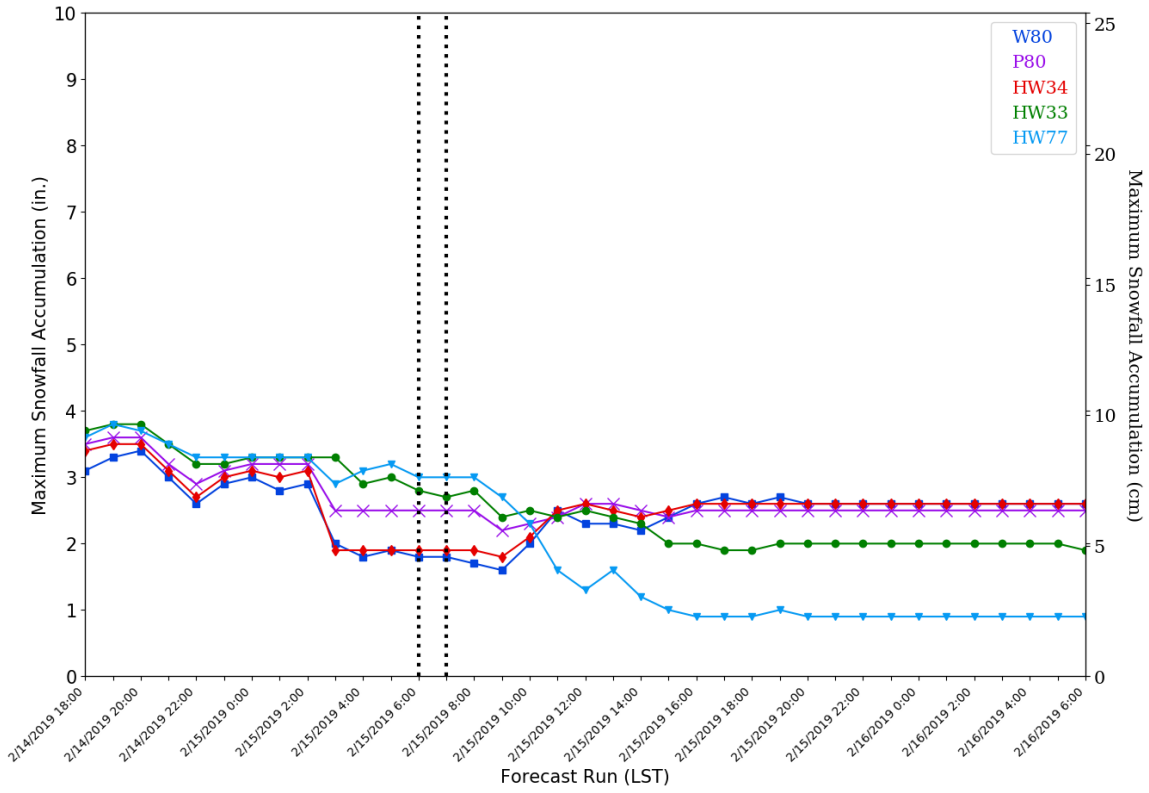

Figure 4.35: Maximum NDOT-MDSS forecasted snowfall accumulation for each selected segment per forecast run. The black vertical dotted lines denote snowfall start time for groups of segments (6:00 LST for HW33 and HW77; 7:00 LST for W80, P80, and HW34).

(1500 UTC 15 February 2019). By the time snowfall ends at 4:00 pm LST 15 February 2019 (2200 UTC 15 February 2019), the forecast accumulation for each segment is closer than before to the observed snowfall at KLNK. Thereafter, forecasted snowfall accumulations remain consistent through the last NDOT-MDSS model run time of 6:00 am LST 16 February 2019 (1200 UTC 16 February 2019). Forecasts for P80, W80, and HW34 are very similar if not the same as the observed value and each other while forecasts for HW33 and HW77 show the most deviation. Post-snowfall forecasts for HW77 have an especially large forecast error with a final accumulation of 0.9 inches (2.3 cm) while post-snowfall forecasts for HW33 has a final accumulation of 2.0 inches (5.1 cm). The forecasted snowfall accumulation for HW77 may be because of the length of HW77, which is longer than the other routes (Barnhardt 2019; Rick 2020). Both W80 and HW34 have a forecast for the exact snowfall total received at KLNK while the forecasts for P80 are only off by 0.1 inch (0.3 cm) of snowfall at 2.5 inches (6.4 cm). Overall, there are no major errors in the NDOT-MDSS snowfall accumulation forecasts for any segment. Another important aspect to look at is how NDOT-MDSS handles the total amount of time it is calling for snowfall from the start of available forecast runs, 6:00 pm LST 14 February 2019 (0000 UTC 15 February 2019), to the start of snowfall for each segment. The start of snowfall was 6:00 am LST 15 February 2019 (1200 UTC 15 February 2019), for HW33, and HW77 and 7:00 am LST 15 February for P80, W80, and HW34. For the second case study, W80, P80, and HW34 were grouped together (Figure 4.36 and Figure 4.37) while HW33 and HW77 were also grouped together (Figure 4.38 and Figure 4.39) due to proximity of the segments to each other. For W80,

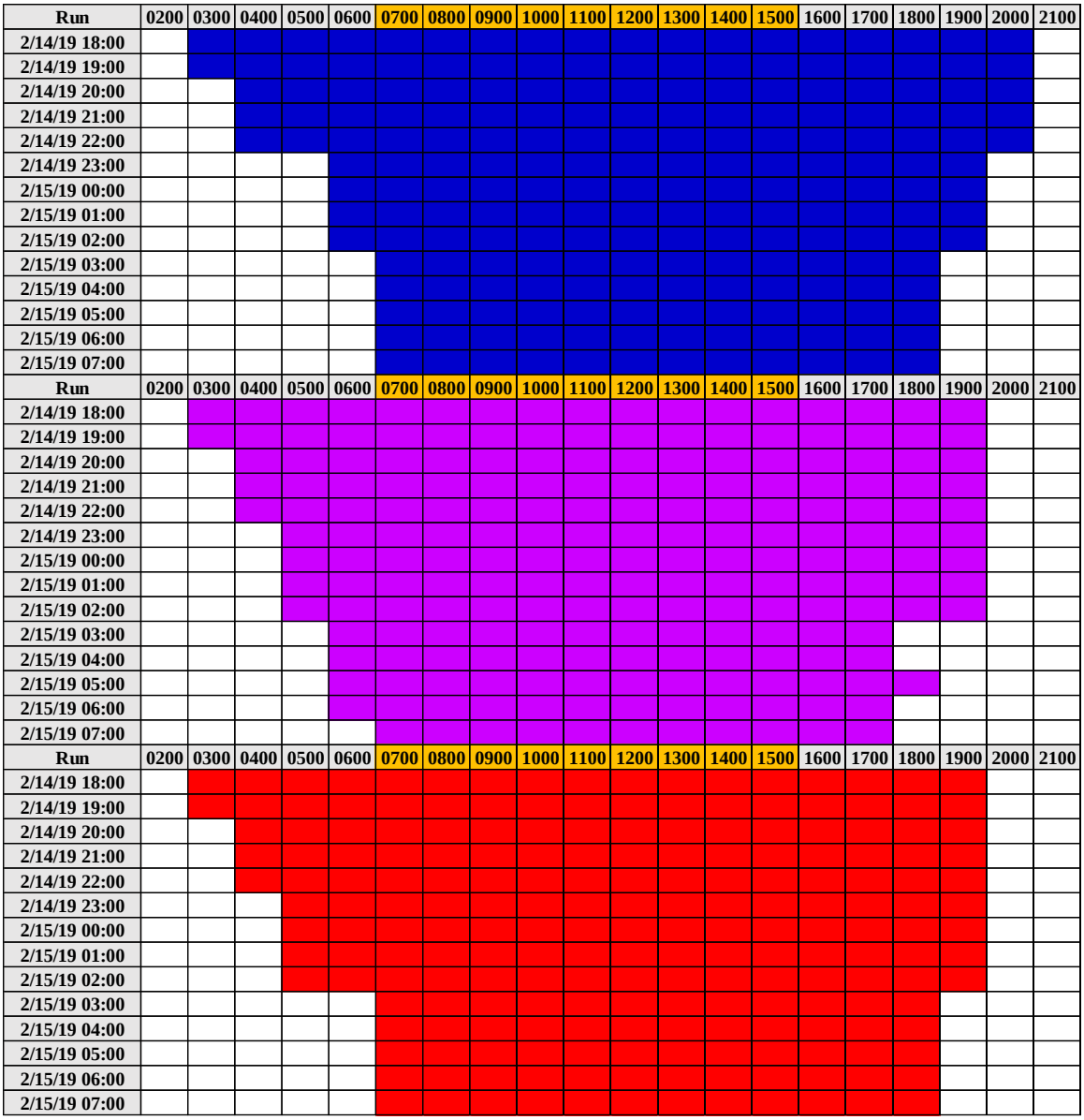

Figure 4.36: The NDOT-MDSS forecasted start and end times of snowfall for 15 February for each segment; W80 (blue), P80 (violet), HW34 (red). The actual event length for segments is highlighted by the orange cells. Time is in LST.

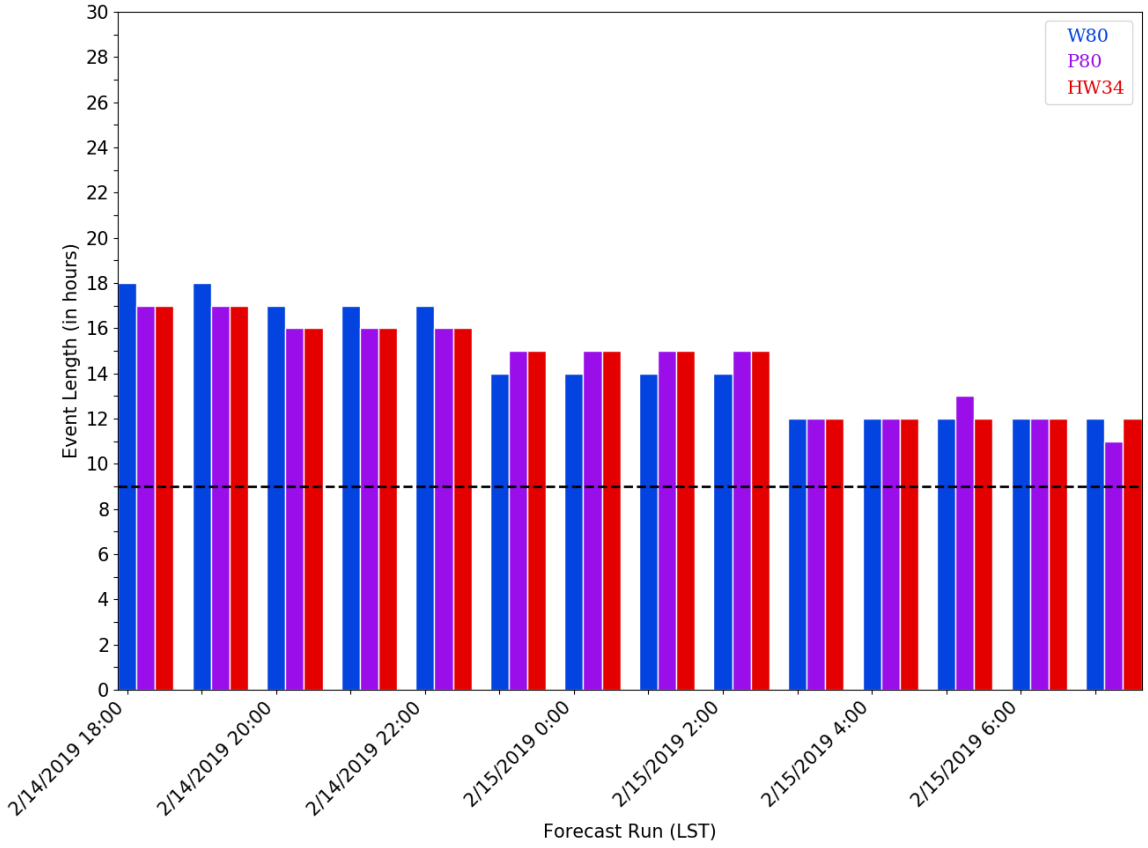

Figure 4.37: NDOT-MDSS forecasted event length for W80 (blue), P80 (violet), and HW34 (red) per forecast run. The black horizontal line denotes the observed event length for all three of the segments.

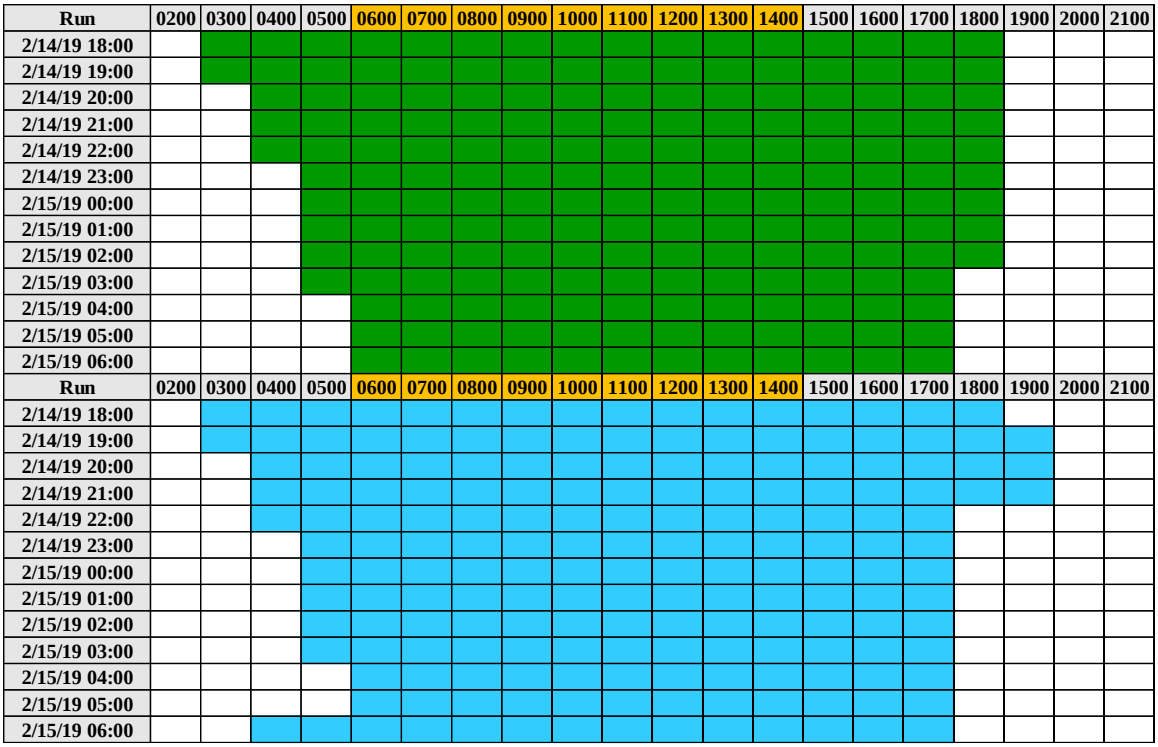

Figure 4.38: The NDOT-MDSS forecasted start and end times of snowfall for 15 February for each segment; HW33 (green), HW77 (light blue). The actual event length for segments is highlighted by the orange cells. Time is in LST.

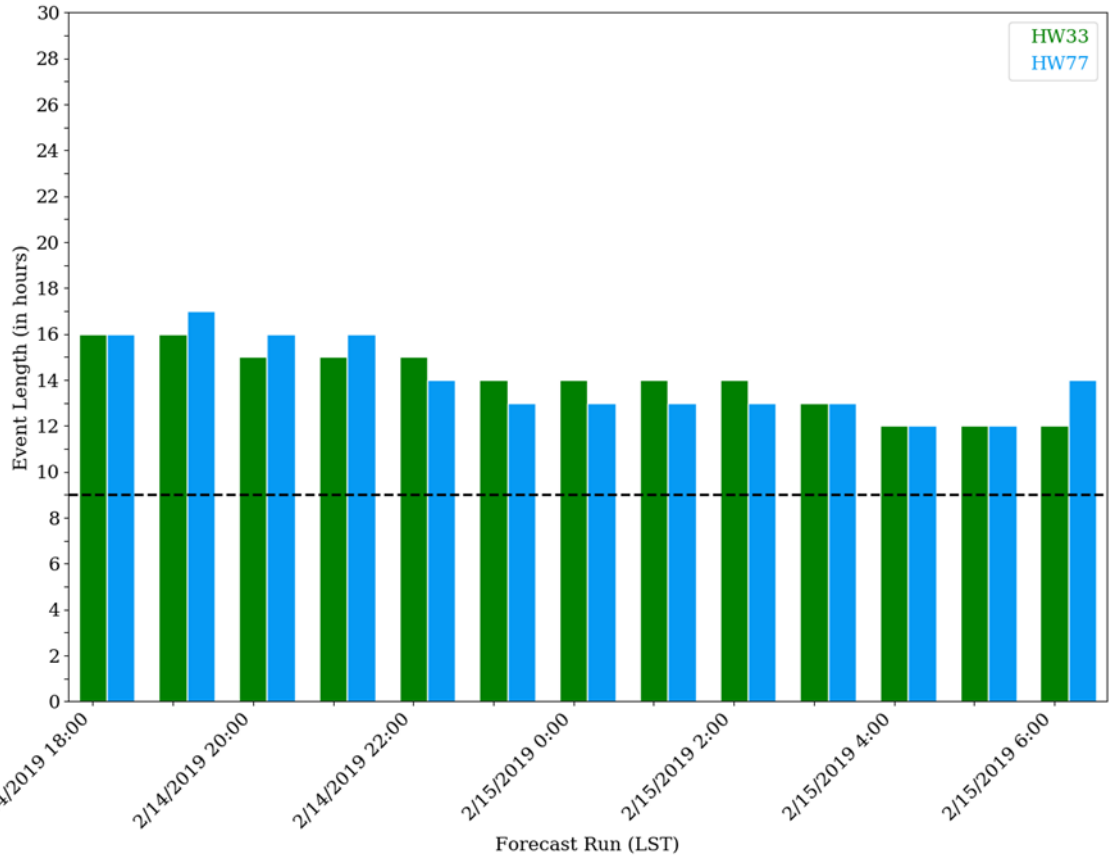

Figure 4.39: NDOT-MDSS forecasted event length for HW33 (green) and HW77 (light blue) per forecast run. The black horizontal line denotes the observed event length for the two segments.

P80, and HW34 the event length seen by each run of the NDOT-MDSS from the beginning of data to the start of snowfall is too long for all road segments. The actual observed length of snowfall is nine hours for all segments. The lowest event length between W80, P80, and HW34 is 11 hours forecasted for P80. The largest event length is 18 hours forecasted for W80 at the beginning of forecast runs. Despite these errors, progression towards the end of snowfall shows event length improvement. For HW33 and HW77, observed event length is nine hours for both segments. The shortest event length forecasted is 12 hours for both segments at the towards the end of snowfall. The longest event length forecasted is 17 hours for HW77 at the start of available forecasts. Despite these errors, as the event progresses towards the end of snowfall the forecasted event length generally improves. With regard to end time differential for this case study, forecasts for every segment have snowfall lasting longer than what is observed as seen by negative differentials (Figure 4.40). The smallest differential observed is -2 hours while the largest is -5 hours. Forecasts for both HW33 and HW34 have a range of -3 hours to -4 hours. The largest differential of -5 hours occurs for both forecasts for W80 and HW77. NDOT-MDSS has the lowest forecast error with a differential of -2 hours for P80. For all road segments, forecasts only improve slightly over time while then in some cases becoming worse towards 4:00 pm LST 15 February 2019 (2200 UTC 15 February 2019). Based on event length and end time differential, NDOT-MDSS generally overpredicts how long Alberta clipper system impacts will last in this case. In some cases NDOT-MDSS has an event occurring that is double in length then observed. The overprediction of snowfall end time and event length are major errors that should be

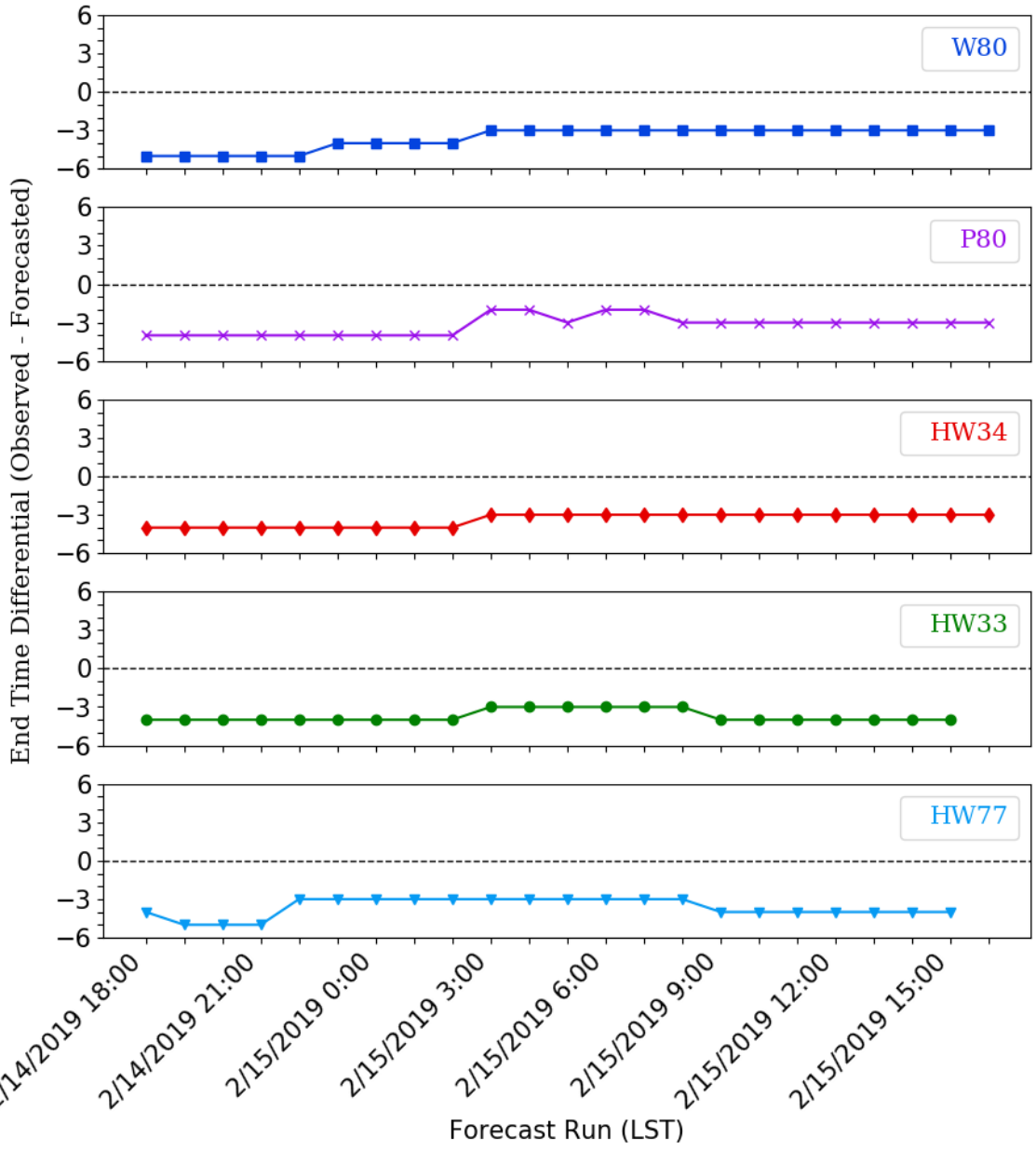

Figure 4.40: 14-15 February 2019 Snowfall end time difference graphs for the five observed routes from the NDOT-MDSS.

watched. These errors are defined as major because presumable they would affect both the planning and the timing of maintenance operations. Users of NDOT-MDSS should watch this overprediction by remaining cautious and careful while planning. Although the impacts from an Alberta clipper system such as strong winds and freezing temperatures may last this long, snowfall from a typical Alberta clipper system will not last 17-18 hours.

4.3 Snowfall Forecast Analysis and Comparison:

An additional snowfall analysis and comparison of each event was carried out to gauge how NDOT-MDSS stacked up against other numerical weather prediction models and the NWS. The first event saw a recorded snowfall total of 1.0 inch (2.5 cm) at KOMA. When examining numerical model output starting at the first forecast time data were available within the NDOT-MDSS storm data, 5:00 pm LST 25 January 2019 (2300 UTC 25 January 2019), and ending at the start of snowfall for which snow fell upon all road segments, 2:00 am LST 26 January 2019 (0800 UTC 26 January 2019), all numerical models did not at any point forecast the observed snowfall total and consistently under-forecast the observed snowfall total (Figure 4.41a). The RAP (2300 UTC 25 January 2019 to 0800 UTC 26 January runs), NAM (1200 UTC 25 January and 0000 UTC 26 January runs), NAM 4km (1200 UTC 25 January and 0000 UTC 26 January runs), GFS (1200 UTC 25 January and 0000 UTC 26 January runs), and average of all these models are generally consistent; however, up to the start of snowfall the RAP was the closest numerical model to the observed total. Numerical model errors are mirrored with looking at NDOT-MDSS for each road segment

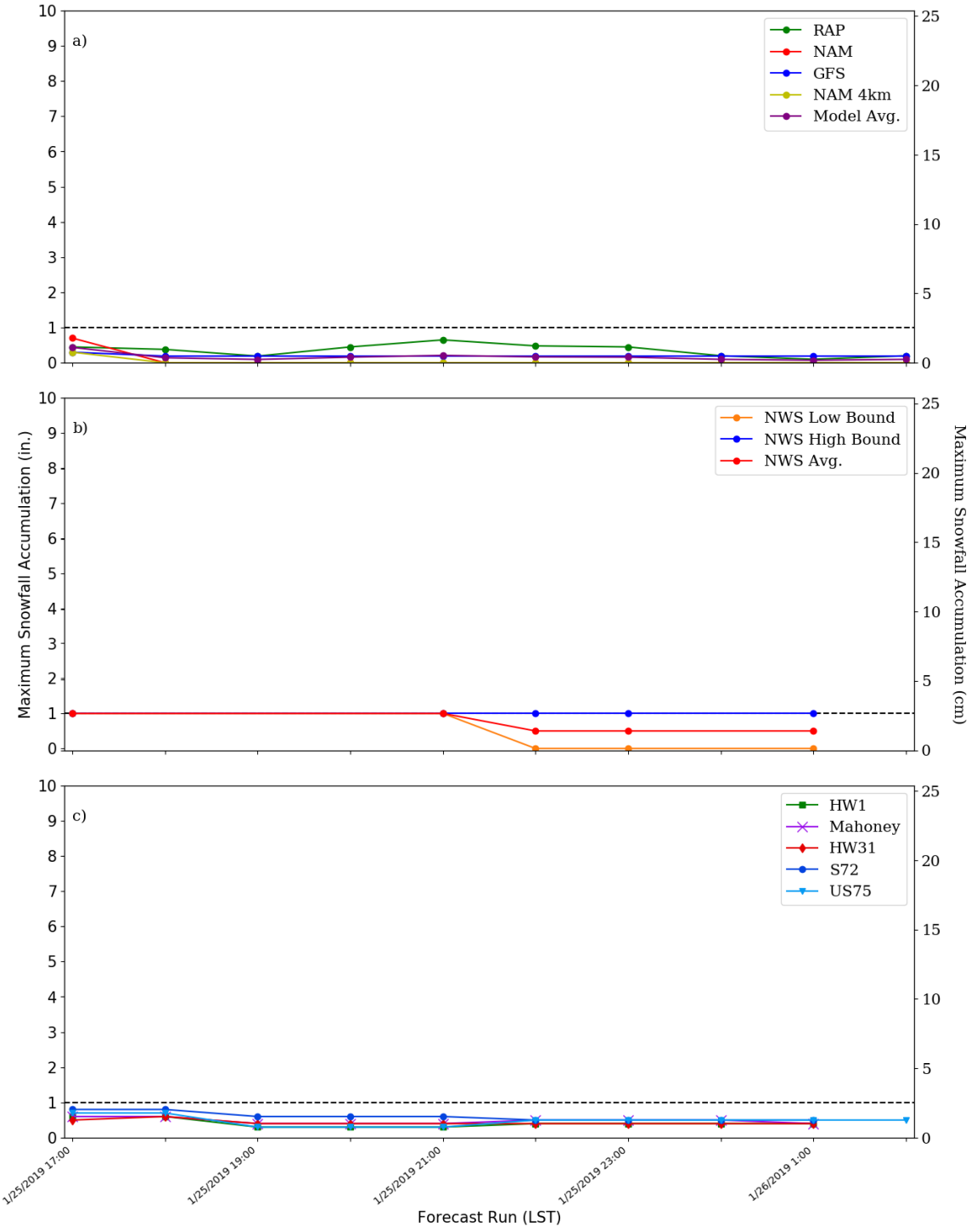

Figure 4.41: 25-26 January case study forecasted snowfall accumulation composite for: a) weather models (RAP, NAM, GFS, NAM 4km), b) National Weather Service zone forecast product, c) NDOT-MDSS.

(Figure 4.41c). Each snowfall accumulation forecast for each road segment is consistently under-forecasted, with the forecasts for HW1, Mahoney, HW31, S72, and US75 remaining close to each other. The numerical models do not improve over time and NDOT-MDSS becomes slightly worse over time leading up to the onset of snowfall. The NWS correctly calls the observed snowfall total within its forecast low, high, and average snowfall accumulation range up until 9:00 pm LST 25 January 2019 (0300 UTC 26 January 2019) (Figure 4.41b). Thereafter, the NWS is generally correct as it called for the observed snowfall total within accumulation range. It is interesting to note the similarities of the numerical weather models and NDOT-MDSS forecasts for each segment. Both remain consistent over time and both under-forecast the observed amount of snow. This may be because some of the numerical model data are feed in NDOT-MDSS to generate forecasts. Regardless, in this case, NDOT-MDSS does slightly better than the numerical weather models. However, this is regarding less than an inch of snow. Overall, this analysis shows NDOT-MDSS handled snowfall totals well.

For the second event, the KLNK recorded 2.6 inches (6.6 cm) inches of snowfall for the event. When examining numerical model output starting at the first forecast time data available within the NDOT-MDSS storm data, 6:00 pm LST 14 February (0000 UTC 15 February 2019), and ending at the start of snowfall for all road segments, 7:00 am LST 15 February (1300 UTC 15 February 2019), all numerical models under-forecast snowfall (Figure 4.42a). Only the RAP forecasts the exact amount of snowfall towards the start of snowfall. For many of the forecasts runs, the NAM does the best at predicting the total accumulation while the NAM 4km does most poorly. In the second case, the models have a larger spread in snowfall accumulation totals then the first

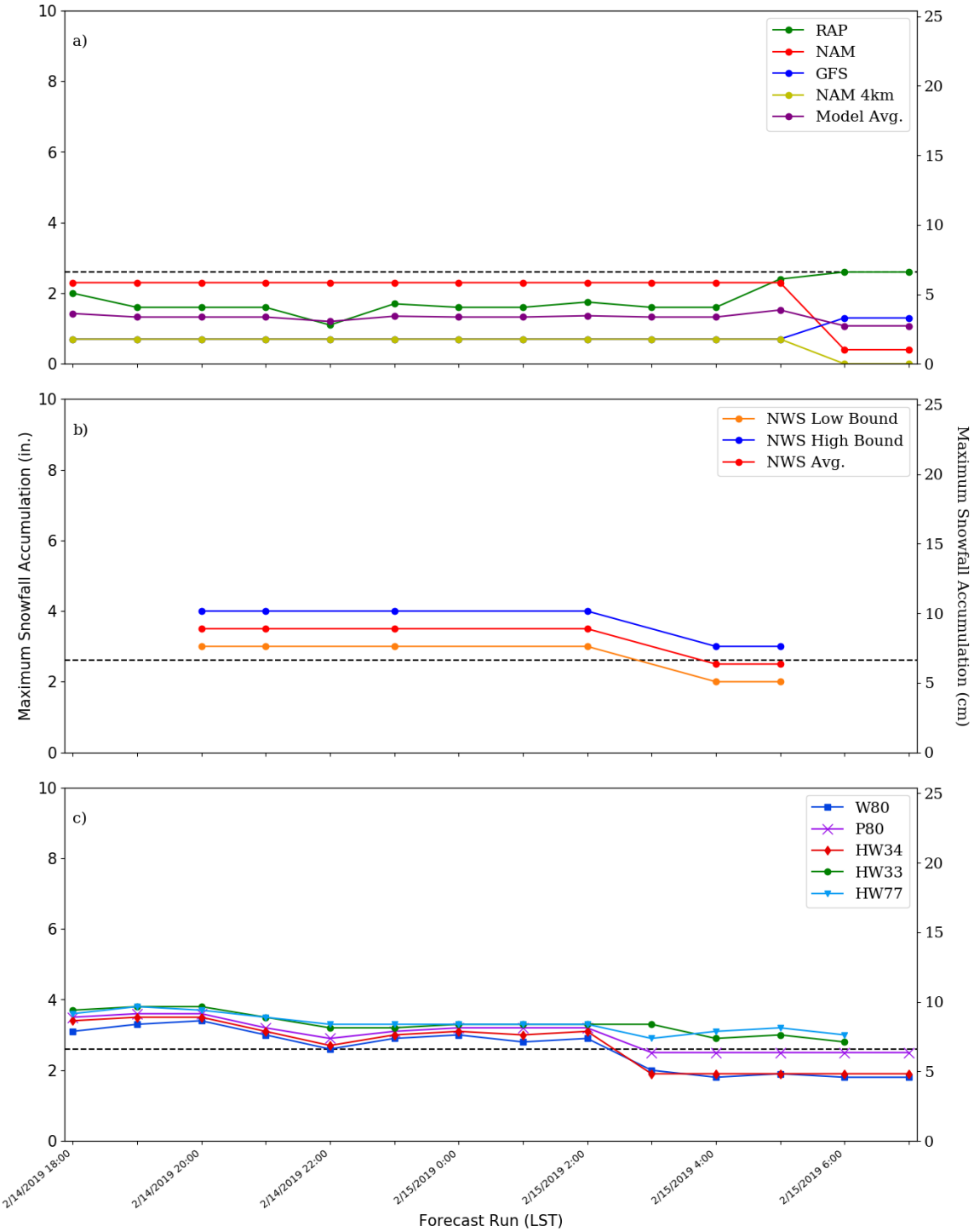

Figure 4.42: 14-15 February 2019 case study forecasted snowfall accumulation composite for: a) weather models (RAP, NAM, GFS, NAM 4km), b) National Weather Service zone forecast product, c) NDOT-MDSS.

case. By 6:00 am LST 15 February 2019, the NAM, NAM 4km, and model average get worse while the GFS and RAP improve. NDOT-MDSS in this case generally over-forecasts the amount of snow, possibly because of more low pressure systems that move into the area after this Alberta clipper system (Figure 4.42c). However, there is some slight improvement with time and at some instances some forecasts for a segment do predict the observed amount of snowfall, 10:00 pm LST 14 February 2019 (0400 UTC 15 February 2019) for W80. After 2:00 am LST 15 February 2019 (0800 UTC 15 February 2019), the forecasts for segments begin to lose consistency with each other. By 3:00 am LST 15 February 2019 (0900 UTC 15 February 2019), NDOT-MDSS is under-forecasting for W80, HW34, and P80 and over-forecasting total snowfall accumulation for HW33 and HW77. Forecasts for P80 predict the most similar total snowfall to KLNK in this case compared to forecasts for other segments. Forecasts for HW33 and HW77 predict a similar total upon the segments as do forecasts for HW34 and W80 in this case. This may be because the segments are close to each other or because of the segment length. Regarding the NWS forecast, the NWS starts off by over-forecasting the observed total in both their average and range (Figure 4.42b). By 4:00 am LST 15 February 2019 (1000 UTC 15 February 2019) their range includes the observed snowfall total with the average between the high and low bound given being very close to the observed total. In this case NDOT-MDSS is more in line with the NWS than the other numerical models regarding over-forecast of snowfall. Overall, this analysis shows NDOT-MDSS handled snowfall totals well.

When comparing these two different Alberta clipper systems analyzed in this study there are several similarities and several differences which are important to

recognize. The first is regarding the synoptic environment which allow them to form. The synoptic background which allowed the first case to form is more typical of what is seen with Alberta clipper systems. The synoptic environment which allowed the system observed in the second case to form is more of an atypical case. This can be seen by the zonal jet stream and trough and ridge patterns in the upper air analysis. In addition, the low pressure center associated with the system forms over the Rocky Mountains in Wyoming rather than in Alberta. However, this system is essentially an Alberta clipper system based on the dry air that is associated with it and the similar formation environment, located just slightly farther south for the formation location. Both cases have similar features of true Alberta clipper systems including formation on the lee side of the Northern Rockies, dry, cold air associated with the system; low pressure centers which are relatively weak.

NDOT-MDSS overall does a good job at handling both cases and their impact. NDOT-MDSS road segment forecasts in both cases do not have large forecast errors in any snowfall amounts. In fact, in both cases, all segments are close to the total amount of accumulated snow observed by the respective observations. A notable similarity between each of the cases is that NDOT-MDSS over-forecasts the length of observed events. The over-forecast of event length is a bias that needs to be watched when using NDOT-MDSS. NDOT personnel should consider this when developing maintenance plans for events. This bias may be related to the formation of other low pressure systems which occurred directly after both events. In both events, NDOT-MDSS forecasts snowfall to last longer than what was observed, typically by 3 to 4 hours. NDOT-MDSS for both cases does poorer with dewpoint temperatures and wind speeds then

temperatures and snowfall. Compared to other numerical weather prediction models NDOT-MDSS is more in line with model guidance during the first case than the second. In both cases, NDOT-MDSS is similar to forecast ranges made by the NWS. Since in both cases, the NWS correctly predicts the observed snowfall total, NDOT-MDSS being closer to NWS prediction rather than the other numerical weather prediction models may be a strength of the system. NDOT-MDSS overall seems to have handled both Alberta clipper system cases well with few major errors occurring in several forecast parameters. The only major errors made by NDOT-MDSS is those regarding event length and end snowfall stop time in both case studies. NDOT-MDSS may be able to be relied on in the future for events and Alberta clipper systems similar to these; however, the lasting of snowfall longer then observed should be keep in mind.

CHAPTER 5: CONCLUSIONS

This study investigated how the recent MDSS system adopted by NDOT (NDOT-MDSS), forecasted and represented two different winter storms during the 2018-2019 winter season. The first case occurred on 26 January 2019 for which the Omaha region was examined. The second case occurred on 15 February 2019 for which the Lincoln region was examined. Alberta clipper systems are a type of extratropical cyclone which impact the Great Plains and Nebraska. Due to their formation location and evolution, they bring a different set of conditions and impacts to regions they cross than do other types of extratropical systems, such as the Colorado low system. The Alberta clipper system typically brings light snowfalls before and after passage, and strong winds and freezing temperatures after passage. Alberta Clipper systems and often cross over a region very quickly. These winter weather impacts brought by Alberta clipper systems have a notable impact on road transportation in North American and the Great Plains. This has led society to develop and put into practice mitigation efforts to minimize the impacts. NDOT-MDSS is an example of how a modern information system can assist in the potential mitigation of winter weather impacts. The MDSS system has a long and complex history dating back to the 1990s and has undergone considerable evolution and change.

Both of the case studies encompassed Alberta clipper systems impacting different road segments in two different NDOT districts. The upper air environment which leads to the development of the Alberta clipper system in the first case was very different from the upper air environment which leads to development in the second. However, the impacts, such as little but quickly falling snowfall accumulations upon road segments are

fairly similar in both case studies, most likely because the systems are similar in characteristics of formation and evolution (dry cold air and minimal pressure gradient). In both cases NDOT-MDSS does a fairly good job representing the systems and the impacts brought to each segment. For both cases NDOT-MDSS did not forecast any large or substantial snowfall accumulation errors. In both cases NDOT-MDSS generally improves with time leading up to start of an event. One thing to note from this study is that it seems when NDOT-MDSS is forecasting for Alberta clipper systems it over-forecasts the event length of the snowfall and the end time of snowfall. This may because Alberta clipper systems are fast moving and the model does not account for this, or because the model is detecting another low pressure system impacting the segments with snowfall after passage of each Alberta clipper system studied here (in both cases low pressure systems impacted the region directly after as seen in saved storm data). The overprediction of event length and snowfall end time are biases and major errors that needs to be watched with NDOT-MDSS. Presumable these errors would affect both the planning and the timing of maintenance operations. NDOT or another entity using NDOT-MDSS should be cautious when planning for the timing of snowfall impacts. Besides event length and snowfall end time, NDOT-MDSS did not at any point make any major errors during the events and handled meteorological conditions well. NDOT-MDSS may be able to be relied on for future winter weather events similar to the two case studies analyzed while keeping in mind the event length bias.

It is important to recall that there were several limitations in this study. Overall, these limitations mainly arise due to the closed source nature of the proprietary NDOT-MDSS system. The proprietary architecture of the system makes NDOT-MDSS

resemble a “black box” where it is unknown how the system is working. It is unknown what the criteria were or the reason behind the saved storm data creation for each event, however, it appears the storms were saved based on snowfall impact. Compared to Colorado low systems which also impacts Nebraska, Alberta clipper systems impact the region far less frequently. In addition, the Colorado low system is more likely to bring significant snowfall and impacts to transportation. There was a limited number of Alberta clipper systems to be analyzed for this study and the saved storm data function of the system was itself a limitation. There is no way to verify why NDOT-MDSS was forecasting what it was or if the treatment guidance it was suggesting was accurate, given model input without a copy of the source code. In addition, reliance on nearest ASOS data and observations at nearest airports for verification may not be best for each road segment. Road segments are different lengths (snowfall may be spread over model grid points leading to different totals for different segments), are different distances from the airports, and have different directional orientations. Overall, while there may be many benefits to a closed source proprietary environment in some cases, and NDOT-MDSS being proprietary in nature was an original goal during the evolution and development of MDSS, this study would have benefited if the system was open source in order to conduct a more thorough analysis of how the system was working internally.

The study was ultimately limited to two Alberta clipper systems. Future work will include a larger sample of Alberta clipper systems to increase the validity of the analysis. Overall, NDOT-MDSS did a good job at representing and forecasting both events in this study. However, it is important to note that NDOT-MDSS relies on numerical model data fed into the system to generate forecasts. NDOT-MDSS will hence only be as accurate as

the data that are input to the system. The system will also only be as accurate as the theory that defines the system.

REFERENCES

Ahrens, C. D., 2012: Air masses, fronts, and middle-latitude cyclones. *Essentials of Meteorology: An Invitation to the Atmosphere, Sixth Edition.* Brooks/Cole, Cengage Learning, 212-243.

Angel, J. R., and S. A. Isard, 1997: An observational study of the influence of the Great Lakes on the speed and intensity of passing cyclones. *Mon. Wea. Rev.,* **125,** 2228–2237, https://doi.org/10.1175/1520-0493(1997)125<2228:AOSOTI>2.0.CO;2.

Andrey, J., B. Mills, M. Leahy, and J. Suggett, 2003: Weather as a chronic hazard for road transportation in Canadian cities. *Nat. Hazards,* **28,** 319–343.

Barnhardt, N., 2019: A case study analysis of two heavy snowfall events and road weather implications in 2018 for Nebraska. M.S. thesis, Dept. of Earth & Atmospheric Sciences, University of Nebraska-Lincoln, 147 pp.

Beckman, S. K., 1987: Use of enhanced IR/visible satellite imagery to determine heavy snow areas. *Mon. Wea. Rev.,* **115,** 2060–2087, https://doi.org/10.1175/1520-0493(1987)115<2060:UOEISI>2.0.CO;2.

Bjerknes, J., and H. Solberg, 1922: Life cycle of cyclones and the polar front theory of atmospheric circulation. *Geofys. Publ.,* **12,** 1–61.

Black, A. W., and T. L. Mote, 2015a: Characteristics of winter-precipitation-related transportation fatalities in the United States. *Wea. Climate Soc*., **7,** 133–145, https://doi.org/10.1175/WCAS-D-14-00011.1

——, and ——, 2015b: Effects of winter precipitation on automobile collisions, injuries, and fatalities in the United States. *J. Transport Geography,* **48,** 165-175.

Carmichael, C. G., W. A. Gallus Jr., B. R. Temeyer, and M. K. Bryden, 2004: A winter weather index for estimating winter roadway maintenance costs in the Midwest. *J. Appl. Meteor.,* **43,** 1783–1790, https://doi.org/10.1175/JAM2167.1

Cayan, D. R., 1996: Interannual climate variability and snowpack in the western United States. *J. Climate*, **9,** 928–948, https://doi.org/10.1175/1520-0442(1996)009<0928:ICVASI>2.0.CO;2.

Changnon, D., T. B. McKee, and N. J. Doesken, 1993: Annual snowpack patterns across the Rockies: Long-term trends and associated 500-mb synoptic patterns. *Mon. Wea. Rev.,* **121,** 633–647, https://doi.org/10.1175/1520-0493(1993)121<0633:ASPATR>2.0.CO;2.

Davis, C. A., 1997: The modification of baroclinic waves by the Rocky Mountains. *J. Atmos. Sci.*, **54,** 848–868, https://doi.org/10.1175/1520 0469(1997)054<0848:TMOBWB>2.0.CO;2.

DTN, 2019: WebMDSS. Accessed 1 April 2019, https://www.webmdss.com

Eisenberg, D., and K. E. Warner, 2005: Effects of snowfalls on motor vehicle collisions, injuries, and fatalities. *Amer. J. Public Health,* **95,** 120–125.

Gallus, W. A., and J. F. Bresch, 1997: An intense small-scale wintertime vortex in the midwest United States. *Mon. Wea. Rev.,* **125,** 2787-2807, https://doi.org/10.1175/1520-0493(1997)125<2787:AISSWV>2.0.CO;2.

Glickman, T. S., 2000: *Glossary of Meteorology.* 2nd ed. Amer. Meteor. Soc., 855 pp.

Harms, R. W., 1973: Snow forecasting for southwestern Wisconsin. *Weatherwise,* **26** (12), 250–255.

Hobbs, P. V., J. D. Locatelli, and J. E. Martin, 1996: A new conceptual model for cyclones generated in the lee of the Rocky Mountains. *Bull. Amer. Meteor. Soc.,* **77,** 1169–1178, https://doi.org/10.1175/1520-0477(1996)077<1169:ANCMFC>2.0.CO;2.

Hoskins, B. J., and K. I. Hodges, 2002: New perspectives on the Northern Hemisphere winter storm tracks. *J. Atmos. Sci.,* **59,** 1041–1061, https://doi.org/10.1175/1520-0469(2002)059<1041:NPOTNH>2.0.CO;2.

Hutchinson, T. A., 1995: An analysis of NMC's nested grid model forecasts of Alberta clippers. *Wea. Forecasting,* **10,** 632–641, https://doi.org/10.1175/1520-0434(1995)010<0632:AAONNG>2.0.CO;2.

Iowa State University (ISU), 2020a: Meteogram Generator. Accessed 1 February 2020, https://meteor.geol.iastate.edu/~ckarsten/bufkit/image_loader.phtml

——, 2020b: NWS Text Products by Issuing Center by Date. Accessed 1 February 2020, https://mesonet.agron.iastate.edu/wx/afos/list.phtml

Kapela, A. F., P. W. Leftwich, and R. Van Ess, 1995: Forecasting the impacts of strong wintertime post-cold front winds in the northern Plains. *Wea. Forecasting,* **10,** 229–244, https://doi.org/10.1175/1520-0434(1995)010<0229:FTIOSW>2.0.CO;2.

Lareau, N. P., and J. D. Horel, 2012: The climatology of synoptic-scale ascent over western North America: A Perspective on Storm Tracks. *Mon. Wea. Rev.,* **140,** 1761–1778, https://doi.org/10.1175/MWR-D-11-00203.1.

Mahoney, W. P., III, and W. Myers, 2003: Predicting weather and road conditions: Integrated decision-support tool for winter road-maintenance operations. *Transp. Res. Rec.,* **1824,** 98–105, https://doi.org/10.3141/1824-11.

Moore, J. T., and K. F. Smith, 1989: Diagnosis of anafronts and katafronts, *Wea. Forecasting,* **4** (1), 61-72, https://doi.org/10.1175/1520-0434(1989)004<0061:DOAAK>2.0.CO;2

National Centers for Environmental Information (NCEI), 2019: Climate Data Online. National Oceanic and Atmospheric Administration (NOAA), Accessed 16 April 2019, https://www.ncdc.noaa.gov/cdo-web/

National Weather Service (NWS), 2020: Winter Infographics. Accessed 19 January 2020, https://www.weather.gov/wrn/winter_hazard_infographics

Nebraska Department of Transportation (NDOT), 2020: Divisions and Districts. Accessed 1 August 2020, https://dot.nebraska.gov/about/divisions-districts/

Nielsen, J. W., and R. M. Dole, 1992: A survey of extratropical cyclone characteristics during GALE. *Mon. Wea. Rev.*, **120,** 1156–1168, https://doi.org/10.1175/1520-0493(1992)120<1156:ASOECC>2.0.CO;2.

Newton, C. W., 1956: Mechanisms of circulation change in a lee cyclogenesis. *J. Meteor.*, **13,** 528–539.https://doi.org/10.1175/1520-0469(1956)013<0528:MOCCDA>2.0.CO;2.

Oard, M. J., 1993: A method for predicting chinook winds east of the Montana Rockies. *Wea. Forecasting*, **8,** 166–180, https://doi.org/10.1175/1520-0434(1993)008<0166:AMFPCW>2.0.CO;2.

Petterssen, S., 1956: *Weather Analysis and Forecasting.* Vol. I. McGraw-Hill, 428 pp.

Petty, K. R., and W. P. Mahoney, 2008: The U.S. Federal Highway Administration winter road maintenance decision support system (MDSS): Recent enhancements and refinements. *Proc. 14th Int. Road Weather Conf*., Prague, Czech Republic, Standing International Road Weather Commission, 29.

Pierrehumbert, R. T., 1986: Lee cyclogenesis. *Mesoscale Meteorology and Forecasting*, P. S. Ray, Ed., Amer. Meteor. Soc., 493–515.

Pisano, P. A., A. D. Stern, and W. P. Mahoney III, 2005: The U.S. Federal Highway Administration winter road maintenance decision support system (MDSS) project: Overview and results. Preprints, *21st Int. Conf. on Interactive Information Processing Systems (IIPS) for Meteorology, Oceanography, and Hydrology*, San Diego, CA, Amer. Meteor. Soc., 6.5. [Available online at http://ams.confex.com/ams/pdfpapers/83959.pdf.]

Price, W. B., 1971: Wind and weather regimes at Great Falls, Montana. Western Region Tech. Memo. 64, 35 pp. [Available from National Weather Service Western Region, P.O. Box 11188, Salt Lake City, UT 84147-0188.]

Reitan, C. H., 1974: Frequencies of cyclones and cyclogenesis for North America, 1951–1970. *Mon. Wea. Rev.,* **102,** 861–868, https://doi.org/10.1175/1520-0493(1974)102<0861:FOCACF>2.0.CO;2.

Rick, N., 2020: Case studies of Colorado lows and the impacts on winter weather maintenance. M.S. thesis, Dept. of Earth & Atmospheric Sciences, University of Nebraska-Lincoln, 136 pp.

Schultz, D. M., and C. A. Doswell, 2000: Analyzing and forecasting Rocky Mountain lee cyclogenesis often associated with strong winds. *Wea. Forecasting,* **15,** 152–173, https://doi.org/10.1175/1520-0434(2000)015<0152:AAFRML>2.0.CO;2.

Schwartz, R. M., and T. W. Schmidlin, 2002: Climatology of blizzards in the conterminous United States, 1959–2000. *J. Climate,* **15,** 1765–1772, https://doi.org/10.1175/1520-0442(2002)015<1765:COBITC>2.0.CO;2.

Serreze, M. C., M. P. Clark, R. L. Armstrong, D. A. McGinnis, and R. S. Puwarty, 1996: Characteristics of the western U.S. snowpack from SNOTEL data. *Water Resour. Res.*, **35,** 2145–2160

Silberberg, S. R., 1990: The role of mesoscale features in a wintertime Great Lakes cyclone. *Wea. Forecasting,* **5,** 89–114, https://doi.org/10.1175/1520-0434(1990)005<0089:TROMFI>2.0.CO;2.

Smart, J. R., and F. H. Carr, 1986: Observations and analysis of a polar low over the Great Lakes region. Preprints, *11th Conf. on Weather Analysis and Forecasting,* Kansas City, MO, Amer. Meteor. Soc., 188–193.

Steenburgh, W. J., and C. F. Mass, 1994: The structure and evolution of a simulated Rocky Mountain lee trough. *Mon. Wea. Rev.,* **122,** 2740–2761, https://doi.org/10.1175/1520-0493(1994)122<2740:TSAEOA>2.0.CO;2.

Stewart, R. E., and Coauthors, 1995: Winter storms over Canada. *Atmos.–Ocean,* **33,** 223–247.

Storm Prediction Center (SPC), 2020: Surface and Upper Air Maps. National Weather Service (NWS), Accessed 1 August 2020, https://www.spc.noaa.gov/obswx/maps/

Thomas, B. C., and J. E. Martin, 2007: A synoptic climatology and composite analysis of the Alberta clipper. *Wea. Forecasting,* **22,** 315–333, https://doi.org/10.1175/WAF982.1.

Tibaldi, S., A. Buzzi, and A. Speranza, 1990: Orographic cyclogenesis. *Extratropical Cyclones, The Erik Palmén Memorial Volume,* C. W. Newton and E. O. Holopainen, Eds., Amer. Meteor. Soc., 107–127.

Tobin, D. M., M. R. Kumjian, and A. W. Black, 2019: Characteristics of recent vehicle-related fatalities during active precipitation in the United States. *Wea. Climate Soc.*, **11,** 935–952, https://doi.org/10.1175/WCAS-D-18-0110.1

University Corporation for Atmospheric Research (UCAR), 2010: Alberta Clipper Case Exercise. UCAR MetEd Module, https://www.meted.ucar.edu/norlat/snow/alberta_clipper/

Vinzani, P. G., and S. A. Changnon Jr., 1981: A case study: 1980's surprise long-track snowstorm. *Weatherwise*, **34** (4), 74–76.

Weather Prediction Center (WPC), 2020: WPC's Surface Analysis Archive. National Weather Service (NWS), Accessed 1 August 2020, https://www.wpc.ncep.noaa.gov/archives/web_pages/sfc/sfc_archive.php

Whittaker, L. M., and L. H. Horn, 1981: Geographical and seasonal distribution of North American cyclogenesis, 1958–1977. *Mon. Wea. Rev.*, **109,** 2312–2322, https://doi.org/10.1175/1520-0493(1981)109<2312:GASDON>2.0.CO;2.

Zishka, K. M., and P. J. Smith, 1980: The climatology of cyclones and anticyclones over North America and surrounding ocean environs for January and July, 1950–77. *Mon. Wea. Rev.*, **108,** 387–401, https://doi.org/10.1175/1520-0493(1980)108<0387:TCOCAA>2.0.CO;2.